

UNIVERSIDADE DE LISBOA  
FACULDADE DE CIÊNCIAS  
DEPARTAMENTO DE ENGENHARIA GEOGRÁFICA, GEOFÍSICA E ENERGIA



## **Multi-Parametric Risk Assessment of the Sea Level Rise: the case study of Ria Formosa (Algarve)**

Sílvia Alexandra da Silva Mourão

**Mestrado em Engenharia Geoespacial**

Dissertação orientada por:

Professor Doutor Carlos Manuel Correia Antunes  
Professora Doutora Cristina Maria Sousa Catita



*“I wish it need not have happened in my time,” said Frodo.*

*“So do I,” said Gandalf, “and so do all who live to see such times.  
But that is not for them to decide.  
All we have to decide is what to do with the time that is given us.”*

- J. R. R. Tolkien



## Acknowledgments

This section is dedicated to expressing my heartfelt gratitude to all those who have supported me throughout the duration of this project. Their contributions were crucial in making this dissertation possible.

First and foremost, I would like to extend my deepest thanks to my supervisors, Professor Carlos Antunes and Professor Cristina Catita. Their unwavering support, guidance, and expertise were essential in accompanying me through this journey. They went above and beyond whenever I needed help, always provided important feedback (even to my crazier ideas) and were always available to support me. Their dedication helped me gain valuable professional experience and ensured the success of this dissertation. Additionally, I am grateful to all the professors in the Geospatial Engineering Master's course for imparting the knowledge and skills necessary to achieve this milestone

I would also like extend my gratitude to Carolina, without whose pioneering work my research would not have been possible. I would also like to thank Miguel and Vanessa, whose projects formed the basis for my work. Their help, support, and companionship during my time working at the University have been invaluable.

To my colleagues, Sofia, Tiago, Gonçalo, and Renato, thank you for taking me in and making me feel part of the group. The time we spent together will always be special to me, and I doubt I would have made it without your support. I am also grateful to all the friends who have listened and encouraged me on this journey, and to my gaming buddies for helping to provide a well needed distraction from time to time.

To my siblings, Diogo and Patricia, whose job has been to get on my nerves for a very long time, and yet despite this I'm still glad I'm not an only child. And to my kitties, because when you're down, there's nothing like a cat hug to raise your spirits. Or a scratch if you try to touch Viennetta.

To my partner Valerio, for being the driving force and motivation behind all this. He knows how much this degree means to me and how perfectly it aligns with my amazing sense of orientation and navigation.

*Por fim, mas certamente não menos importante, estou eternamente grata aos meus pais, Cristina e António, por sempre terem acreditado em mim e me terem dado todas as ferramentas para ter sucesso.*

To all of you who have been by my side, sharing in the struggle and the success, my heartfelt thanks for being a part of it all.

## **Abstract**

The accelerating rise in sea levels due to global warming poses significant threats, particularly to low-lying coastal regions. Effective management of these risks requires a comprehensive understanding of how sea level rise impacts the affected areas. Traditional coastal risk assessments evolved to incorporate a broader range of factors, yet a gap remains in methodologies that simultaneously consider physical, socioeconomic, and ecological vulnerabilities.

This dissertation presents a new methodology for comprehensive coastal risk assessment, integrating physical and socioeconomic factors alongside environmental considerations. The Ria Formosa in Algarve, a natural reserve lagoon protected by a barrier island system, serves as the case study. The reserve is under urban pressure from human occupation on the barrier islands and large inland cities such as Faro and Olhão, combining a multitude of factors into one region.

The methodology involves determining the hazard using the IPCC RCP 8.5 sea level rise model and assessing physical vulnerability through regional erosion and accretion rates, factoring in the exacerbation due to rise of the mean sea-level. Socioeconomic vulnerability is evaluated based on population density, infrastructure presence, and potential damage costs, among other indicators. Environmental vulnerability is assessed through the lens of ecosystem services, based on results derived from expert surveys.

Data from these assessments are normalised and integrated, culminating in a multi-parametric risk map. The results underscore that the risk to the ecosystem is significantly higher than the risk levels derived solely from socioeconomic and physical factors. This aligns with expected outcomes and demonstrates the flexibility and adaptability of this methodology for further case studies.

The findings advocate for a broader study into the valuation of ecosystems to standardise practices at a national level, emphasising the critical need to incorporate ecological considerations into coastal risk assessments to ensure comprehensive risk management in the face of accelerating sea level rise.

**Keywords:** Sea-level rise; Coastal hazard; Socioeconomic vulnerability; Environmental vulnerability; Coastal risk.

## Resumo

A aceleração da subida do nível médio do mar, impulsionada pelo aquecimento global, representa uma ameaça crescente e significativa para as regiões costeiras de baixa altitude em todo o mundo. Como consequência, a inundação de zonas costeiras tornar-se-á mais comum, podendo em alguns locais ficar permanentemente ou frequentemente submersos.

Atualmente, grande parte da população mundial habita em zonas costeiras. A subida do nível médio do mar representa uma ameaça significativa para estas áreas, colocando em risco residentes, habitações, infraestruturas, redes de transporte e atividades económicas.

Os ecossistemas costeiros, como mangais e sapais, estão intimamente ligados à dinâmica atual das áreas costeiras, que será profundamente alterada pela subida do nível médio do mar. Esta mudança ameaça causar danos severos aos habitats naturais e à biodiversidade, comprometendo a sua capacidade de sustentar a flora e fauna atual. Além disso, esses ecossistemas desempenham um papel crucial na proteção contra tempestades, absorvendo a energia das ondas e reduzindo os seus impactos nas comunidades e na infraestrutura costeira.

A gestão eficaz destes riscos requer uma compreensão abrangente de como a subida do nível médio do mar irá impactar as áreas afetadas. Gornitz et al. (1994) introduziu o índice de vulnerabilidade costeira como forma de avaliar esse impacto. Atualmente, o conceito evoluiu para a avaliação de risco costeiro, continuando a considerar a vulnerabilidade, mas acrescentando-lhe outros fatores relevantes para cada tipo de estudo. No entanto, persiste uma lacuna crítica nas metodologias existentes: a necessidade de abordagens integradas que considerem a vulnerabilidade ambiental. A falta dessa abordagem holística pode comprometer a capacidade de responder de forma resiliente aos desafios crescentes decorrentes das mudanças climáticas e da subida do nível médio do mar.

Esta dissertação introduz uma metodologia inovadora para a avaliação abrangente do risco costeiro, que integra fatores físicos, socioeconómicos e ambientais. A região de estudo escolhida para este projeto é a Ria Formosa, localizada no Algarve. A Ria Formosa é uma extensa reserva natural que abrange áreas de sapal e é protegida por um sistema dunar de ilhas barreira. No entanto, enfrenta pressão urbana devido à ocupação humana das ilhas barreira e à proximidade de grandes cidades como Faro e Olhão. Esta combinação de características faz da Ria Formosa um cenário ideal para o desenvolvimento de um índice de risco que incorpore todos os seus elementos distintos.

A metodologia envolve, em primeiro lugar, a determinação do perigo utilizando o cenário IPCC RCP 8.5 de subida do nível médio do mar, considerando também fatores como a agitação marítima e a sobrelevação meteorológica. Em seguida, a vulnerabilidade física foi avaliada através da criação de dois modelos digitais de terreno (MDT): um representativo da situação atual e uma simulação da sua evolução para o ano 2100. A criação do modelo digital de terreno foi feita com base em pontos de estereorrestituição fotogramétrica e dados de levantamento LiDAR aéreo, disponibilizados pela Direção Geral do Território (DGT), combinados com informação batimétrica do Instituto Hidrográfico (IH) para o Canal de Faro e do EMODnet para o Oceano Atlântico.

Inicialmente, a região de estudo foi dividida em duas áreas distintas: o sistema de ilhas barreira, sujeito à agitação marítima de elevada energia e a correntes oceânicas, predominantemente afetado pela

erosão (exceto em algumas áreas), e a Ria, onde a sedimentação é o fator dominante. Para as ilhas barreira, o terreno para o ano de 2100 foi simulado utilizando um algoritmo de recuo adaptado de Antunes (2017) e validado por Santo (2022), com taxas de erosão baseadas em Lira et al. (2016). Já para a lagoa, o assoreamento foi determinado através de um algoritmo adaptado de Ferreira (2022).

Os valores de subida do nível médio do mar obtidos foram aplicados ao modelo digital de terreno resultante e normalizados, resultando num índice de vulnerabilidade física.

A avaliação da componente socioeconómica seguiu a metodologia previamente utilizada por Antunes et al. (2019a). Os dados foram obtidos através de camadas de informação do Open Street Maps, dos Censos 2021 (INE) e da Carta de Uso e Ocupação do Solo (DGT). Os dados que representam as características da região, como densidade populacional, redes de transporte, infraestruturas e uso do solo, foram normalizadas e integradas num índice de suscetibilidade. O potencial de dano na região foi também avaliado, utilizando o nível de vulnerabilidade física como fator de ponderação. A combinação destes elementos resultou na determinação do índice de vulnerabilidade socioeconómica.

A componente ambiental foi considerada e desenvolvida especificamente para esta dissertação. A designação das áreas correspondentes a cada ecossistema foi feita através do regime de marés da região, com base no tempo de submersão que caracteriza cada ecossistema. A avaliação do impacto nos ecossistemas envolveu a realização de um inquérito a biólogos especialistas em serviços de ecossistemas, cujos conhecimentos foram fundamentais para atribuir um valor comparativo a cada ecossistema na região. Utilizando a simulação do modelo digital de terreno efetuada para o ano de 2100, foi possível classificar cada pixel do MDT em diferentes épocas, permitindo quantificar o dano aos ecossistemas entre as épocas de 2010 e 2100. A suscetibilidade dos ecossistemas às pressões da subida do nível médio do mar foi classificada e normalizada. Da combinação destes indicadores resulta a determinação do índice de vulnerabilidade ambiental na região.

Os dados provenientes de cada uma destas avaliações são normalizados e integrados, possibilitando a criação de vários índices complementares que culminam na elaboração de um mapa de risco multi-paramétrico.

Os resultados obtidos durante a avaliação da vulnerabilidade física revelam um aumento de 5 km<sup>2</sup> na área submersa, acompanhado de um recuo da linha costeira entre 20-70 m na maior parte da região. Esta expansão da área submersa indica uma alteração significativa nas características físicas da Ria Formosa.

No estudo de vulnerabilidade socioeconómica, Olhão destaca-se como a freguesia mais afetada, devido à proximidade da zona costeira e à elevada ocupação humana. Olhão tem os níveis mais elevados de edifícios e residentes afetados, apresentando mais de 55% da sua área vulnerável à subida do nível médio do mar. Outras freguesias onde a vulnerabilidade socioeconómica é elevada são Faro, Santa Luzia e Conceição e Cabanas de Tavira.

Os resultados ambientais destacam uma perda de mais de metade da área ocupada por alto sapal alto, à medida que este se transforma em baixo sapal ou raso de maré. Danos severos na barreira de dunas, que culminarão com o colapso desta estrutura protetora em algumas regiões, aumentarão a pressão sobre os ecossistemas dentro da lagoa.

A integração dos vários componentes num índice multi-paramétrico revela que o risco para a região é significativamente maior quando a componente ambiental é incluída, em comparação com os níveis de risco derivados apenas de fatores socioeconómicos e físicos.

Nesta dissertação, demonstrou-se a viabilidade de uma metodologia que integra estas três componentes – física, socioeconómica e ambiental, e cujos resultados estão em conformidade com as expectativas. Este processo pode ser facilmente replicado ou adaptado para estudos de caso futuros, permitindo a integração de outros fatores específicos conforme as particularidades de diferentes regiões de estudo.

As conclusões desta dissertação defendem um estudo mais abrangente sobre a valoração dos ecossistemas, com o objetivo de uniformizar práticas a nível nacional e internacional, sublinhando a necessidade crítica de incorporar considerações ecológicas nas avaliações de risco costeiro para garantir uma gestão completa face ao crescente risco da subida do nível médio do mar. A metodologia aqui apresentada proporciona uma compreensão detalhada das mudanças esperadas nas ilhas barreira e na Ria, podendo servir como um modelo para outras regiões costeiras semelhantes, constituindo-se como uma ferramenta crucial para a gestão de riscos futuros.

**Palavras-chave:** Subida do nível médio do mar; Perigo costeiro; Vulnerabilidade socioeconómica; Vulnerabilidade ambiental; Risco costeiro

# Table of Contents

<b>Acknowledgments.....</b>	V
<b>Abstract.....</b>	VI
<b>Resumo .....</b>	VII
Table of Contents .....	X
Table of Figures .....	XIII
Table of Tables.....	XVII
Acronyms .....	XIX
<b>1. Introduction .....</b>	1
<b>1.1 Contextualising the Problem.....</b>	1
<b>1.2 Objectives.....</b>	2
<b>1.3 Motivation.....</b>	2
<b>1.4 Scientific Contribution .....</b>	3
<b>1.5 Structure of the Dissertation.....</b>	3
<b>2. State-of-the-Art.....</b>	3
<b>2.1 Coastal Risk .....</b>	3
<b>2.2 Physical Vulnerability.....</b>	6
2.2.1 Coastal Hazard Processes .....	6
2.2.1.1 Mean Sea Level.....	7
2.2.1.2 Tides .....	8
2.2.1.3 Storm Surge .....	9
2.2.1.4 Sea Swell .....	10
2.2.2 Physical Susceptibility .....	12
2.2.2.1 Erosion, Sedimentation and Coastal Evolution .....	12
2.2.2.2 Coastal Protection Measures .....	14
<b>2.3 Socioeconomic Vulnerability .....</b>	14
2.3.1 Socioeconomic Susceptibility .....	15
2.3.1.1 Population.....	16
2.3.1.2 Infrastructure .....	16
2.3.1.3 Transportation Network.....	16
2.3.1.4 Land Use.....	17
2.3.1.5 Ecological Areas.....	17
2.3.2 Socioeconomic Damage .....	17
<b>2.4 Environmental Vulnerability .....</b>	18
2.4.1 Environmental Susceptibility and Intertidal Ecosystems .....	19
2.4.1.1 Intertidal Mudflats .....	20

2.4.1.2 Saltmarshes.....	21
2.4.1.3 Dunes.....	22
2.4.2 Ecosystem Services .....	23
2.4.3 Environmental Damage .....	25
<b>2.5 Exposure.....</b>	<b>27</b>
<b>2.6 Other Concepts.....</b>	<b>28</b>
2.6.1 Vertical Reference Systems in Portugal .....	28
2.6.1.1 Altimetric Datum Cascais.....	28
2.6.1.2 Chart Datum .....	28
2.6.2. Digital Terrain Models .....	29
<b>3. Methodology and Data.....</b>	<b>30</b>
<b>3.1 Area of Study .....</b>	<b>30</b>
3.1.1 Physical and Geographical Description.....	30
3.1.2 Socioeconomic Characterisation .....	32
3.1.3 Biological Characterisation .....	34
3.2 Methodology .....	35
3.3 Data .....	37
3.4 Physical Vulnerability .....	37
3.4.1 Hazard .....	37
3.4.1.1 Tide.....	38
3.4.1.2 Storm Surge .....	39
3.4.1.3 Sea Swell and Wind Setup.....	39
3.4.1.4 SLR Models.....	39
3.4.2 Physical Susceptibility .....	41
3.4.2.1 Reference Digital Terrain Model .....	41
3.4.2.2 Geological Processes .....	43
3.4.2.3 Digital Terrain Model for 2100 .....	47
3.4.3 Physical Vulnerability Index (PVI).....	48
3.4.3.1 Tide Corrections .....	48
3.4.3.2 Physical Vulnerability Index Cartography .....	49
3.5 Socioeconomic Vulnerability .....	50
3.5.1 Socioeconomic Susceptibility Index (SSI).....	50
3.5.1.1 Population Density .....	51
3.5.1.2 Infrastructures.....	51
3.5.1.3 Transport Network.....	52
3.5.1.4 Soil Use .....	52
3.5.1.5 Ecological Area .....	52

3.5.1.6 Socioeconomic Susceptibility Index .....	53
3.5.2 Socioeconomic Damage Index (SDI) .....	55
3.5.3 Socioeconomic Vulnerability Index (SVI).....	59
<b>3.6 Environmental Vulnerability .....</b>	<b>60</b>
3.6.1 Environmental Susceptibility Index (ESI).....	60
3.6.2 Environmental Damage Index (EDI).....	63
3.6.3 Environmental Vulnerability Index (EVI).....	66
<b>3.7 Composed Indices and Parameter Sensitivity Analysis .....</b>	<b>67</b>
<b>3.8 Coastal Risk .....</b>	<b>67</b>
3.8.1 Socioeconomic Risk Index (SRI) .....	67
3.8.2 Environmental Risk Index (ERI).....	68
3.8.3 Multi-parametric Vulnerability Index (MVI) .....	69
3.8.4 Multi-parametric Coastal Risk Index (MCRI).....	70
<b>4. Discussion.....</b>	<b>71</b>
<b>4.1. Physical Vulnerability .....</b>	<b>71</b>
<b>4.2. Socioeconomic Vulnerability .....</b>	<b>73</b>
<b>4.3. Environmental Vulnerability .....</b>	<b>75</b>
<b>4.4 Multi-parametric Coastal Risk .....</b>	<b>77</b>
<b>5. Conclusions .....</b>	<b>78</b>
<b>5.1 Conclusions .....</b>	<b>78</b>
<b>5.2 Future Recommendations.....</b>	<b>80</b>
Bibliography.....	81
<b>Annexes .....</b>	<b>105</b>
A.     Classification of Socioeconomic Parameters .....	105
i.     Population Density Reclassification .....	105
ii.    Infrastructure Reclassification .....	106
iii.   Transport Network Reclassification.....	107
iv.   Soil Use Reclassification .....	108
v.    Ecological Areas Reclassification.....	109
B.     Survey Results .....	110
i.    Raw Data and Averages per Ecosystem per Service .....	110
ii.   Averages per Ecosystem .....	110
C.     MCRI – Results with Different MVI Methodologies .....	111
i.    MCRI using the EVI or SVI Methodology for MVI.....	111
ii.   MCRI using the Weighted Methodology for MVI .....	112

## Table of Figures

Figure 2.1 - Relationship between the different concepts associated with risk and the different indices that can be calculated. Each index in the first row is independent and can be used in conjunction with any others to obtain the combined indices of the three bottom rows [Source: Rocha et al. (2023)].....	5
Figure 2.2 - Schematization of the concepts of run-up, set-up, surf zone and breaker depth [Source: Sistema Nacional de Informação de Recursos Hídricos (2022)].....	11
Figure 2.3 – Definitions of static and dynamic wave setup components [Source:(Dean et al., 2005)]..	11
Figure 2.4 - Long-term coastline rates of change for the southeastern region of Portugal. Notable rates of coastline advance are seen in the Barreta Island and on the western end of the Armona Island. Coastine retreat is especially significant in the stretch between Cabanas Island and Cacela and on the western end of Culatra Island. [Source:Lira et al. (2016)] .....	13
Figure 2.5 - Segmentation of the intertidal zone. As elevation rises and time inundated diminishes, subtidal environments give way to tidal flats, low marsh, high marsh and finally an upland region. Transition zones have mixed characteristics, with dunes being an example of such areas [adapted from: <a href="https://www.chesapeakequarterly.net/">https://www.chesapeakequarterly.net/</a> ] .....	20
Figure 2.6 - Differences between DSM (surface model that includes structures and vegetation) and DTM (terrain model, represents relief at ground level) [Source: <a href="https://3dmetrica.it/">https://3dmetrica.it/</a> ] .....	29
Figure 3.1 - The Ria Formosa barrier island system, located in the south of Portugal. The barrier system is composed of, from west to east, the Ancão Peninsula, the Barreta Island, the Culatra Island, the Armona Island, the Tavira Island, the Cabanas Island and the Cacela Peninsula. They are divided by six inlets, from west to east, Ancão Inlet, Faro-Olhão Inlet, Armona Inlet, Fuzeta Inlet, Tavira Inlet and Lacém Inlet. [Source: Ceia et al.(2010)] .....	31
Figure 3.2 – Area occupied by the twelve civil parishes that encompass the area of the Ria Formosa	32
Figure 3.3 - Workflow of the methodology applied in this dissertation to reach the Multi-Parametric Coastal Risk Index Cartography. The compete process is divided into three main stages from where the first three products of this dissertation are obtained: First, the determination of the Physical Vulnerability Index (PVI) on the left, which includes the determination of the hazard and the inclusion of erosion and accretion algorithms to simulate a terrain model for 2100. On the right, the Multi-parametric Vulnerability Index (MVI) results from the Socioeconomic Vulnerability Index (SVI), which is based on the reclassification of layers of information and the determination of the potential damage to the region, and the Environmental Vulnerability Index (EVI), a new index developed for this thesis using ecosystem reclassification by using historical tide data and the results of a survey of experts in the field. ....	36
Figure 3.4 – NOAA global mean sea level scenarios for 2100. The graphic highlights the uncertainty of the RCP 8.5 model, considering it an Intermediate-Low to Intermediate-High scenario. [Adapted from: NOAA (2017)].....	38
Figure 3.5 – Workflow for Chapter 3.4.1. The objective of this chapter was the determination of a table of hazard levels, which can then be used to determine the elevation of coastal floods and the overwash that can hit the barrier island system. This data is also critical for the erosion mode used in chapter 3.4.2. The items on the left are the coastal forcing parameters that are used to determine the hazard..	38
Figure 3.6 – Model statistics representing the probability distribution of global mean sea level (in meters, on the left) per year for the IPCC RCP 8.5 scenario.....	40
Figure 3.7 - Workflow for Chapter 3.4.2. The focus of this chapter was the determination of two DTMs for 2100, the Barrier Islands and the Lagoon, using the erosion and accretion algorithms, respectively. Before reaching this step, it was necessary to create a reference DTM, here called DTM 2010, using the data sources on the left of the diagram. ....	41

Figure 3.8 - Reference Digital Terrain Model for the Ria Formosa in 2010, overlayed with the civil parish boundaries shown in chapter 3.1.1. With the exception of the western side of the Almancil civil parish, the whole area has a coastline which is mostly flat and at low elevation.....	42
Figure 3.9 - Location and residuals of levelling benchmarks used for DTM validation. Most of the benchmarks for RNGAP are located along main roads or in urbanised areas, so there is a lack of validation data in the lagoon area.....	43
Figure 3.10 – Sectioning of the areas where each algorithm will be applied. The division of the areas was made along the northern side of the barrier islands, with a slight overlapping area to ensure a smooth transition in the resulting DTM. ....	44
Figure 3.11 - Sectioning of the Barrier Island System Coastline. Stretches were separated according to erosion tendencies and orientation of the coastline, with a slight overlap to prevent any gaps in the model.....	45
Figure 3.12 - Sedimentation rates across ecosystem elevation boundaries, in % relative to the base value of 0.5 mm/yr. The sedimentation increases from the subtidal area until the low saltmarsh, rapidly dropping to as it transitions into the high saltmarsh and reaching zero at the higher limit of the intertidal zone.....	47
Figure 3.13 - Digital Terrain Model for 2100 – this DTM is the composition of the Barrier Island DTM resulting from the erosion algorithm, the Wetland DTM resulting from the accretion algorithm and the remaining area where no change algorithms were implemented.....	48
Figure 3.14 - Workflow for Chapter 3.4.3. The objective of this chapter is to obtain the Physical Vulnerability Index (PVI). This is accomplished by applying the hazard level values in Table 3.3 to their respective area of influence. For the Lagoon, an anomalous tidal surface was also introduced to account for the inland waters' tidal variations.....	48
Figure 3.15 – Anomalous tidal plane for the Ria Formosa and the location of the secondary ports from Table 3.7. This region has a very slight variation in tidal heights, ranging from +0.06 to -0.11, with the area surrounding Faro (Cais Comercial) having the largest difference to the tide observed at the Faro-Olhão tide gauge.....	49
Figure 3.16 - Physical Vulnerability Index Cartography. Each class represents the hazard levels from table 3.3. Most of the region exhibits an extreme PVI level, diminishing as it reaches the upper boundary of the lagoon. Top: Overview of the study area. Bottom Left: City of Faro and surroundings. Bottom Right: City of Olhão and surroundings. ....	50
Figure 3.17 - Workflow for chapter 3.5.1. The objective of this chapter was the calculation of the Socioeconomic Susceptibility Index (SSI). The five variables chosen for this index were Population Density, Infrastructures, Transport Network, Ecological Areas and Soil Use. This data was obtained from various sources, most notably OSM, and normalised or reclassified in ArcGIS Pro. ....	51
Figure 3.18 - Classification for each Socioeconomic Variable (Faro). Top Left: Population Density. Top Right: Ecological Area. Middle Left: Infrastructure. Middle Right: Transport Network. Bottom Left: Soil Use. The city is classified as an urban area with high population density. There is also a high density of roads and some critical infrastructure. The city is surrounded by the Ria Formosa nature reserve. ....	53
Figure 3.19 - The Socioeconomic Susceptibility Index (SSI). Top Left: City of Faro and surroundings. Top Right: City of Olhão and surroundings Bottom: Overview of the study area. With most of the region of the Ria Formosa being unpopulated, this area presents a Very Low SSI. In the population centres the SSI reaches the Moderate, High and Very High classes.....	54
Figure 3.20 - Workflow for chapter 3.5.2. The objective of this chapter was the determination of the Socioeconomic Damage Index (SDI). Initially the Absolute Damage was calculated, based on data obtained from CIMI, Census 2021 and AT. The PVI was used to weigh this damage in a realistic flood scenario, and this was then normalised to reach the SDI. ....	55

Figure 3.21 - Zoning coefficients available on the AT website, for the Ria Formosa region.....	57
Figure 3.22 - Maximum Socioeconomic Damage. Top Left: City of Faro and Surroundings. Top Right: City of Olhão and Surroundings Bottom: Overview of the Area of Study. Areas with the highest levels of damage are found in the urban centres.....	58
Figure 3.23 - Weighted Socioeconomic Damage. Top Left: City of Faro and surroundings. Top Right: City of Olhão and surroundings Bottom: Overview of the study area. Using the PVI to weigh the data shows the areas which will be most damaged by SLR. Olhão in particular has a high concentration of BGRIIs in class 4 and 5 damage estimations.....	59
Figure 3.24 - Workflow for chapter 3.5.3. The objective of this chapter was the creation of the Socioeconomic Vulnerability Index (SVI), by combining the SSI and SDI obtained in chapters 3.5.1 and 3.5.2, respectively.....	60
Figure 3.25 - The Socioeconomic Vulnerability Index (SVI). Top Left: City of Faro and surroundings. Top Right: City of Olhão and surroundings Bottom: Overview of the study area.....	60
Figure 3.26 - Methodology for Chapter 3.6.1. The objective of this chapter was to obtain the Environmental Susceptibility Index (ESI). This was accomplished by using the ecosystem tide limits. Aerial photography and the DTM 2010 to identify the ecosystems and classify them according to their susceptibility to SLR.....	61
Figure 3.27 - Ria Formosa Ecosystem Classification for 2010. Top Left: Faro-Olhão inlet and the Ilha do Farol urban area. Top Right: Armona inlet and the Armona island urban area. Bottom: Overview of the study area.....	62
Figure 3.28 - Environmental Susceptibility Index (ESI). Top Left: Faro-Olhão inlet and the Ilha do Farol urban area. Top Right: Armona inlet and the Armona island urban area. Bottom: Overview of the study area.....	63
Figure 3.29 - Workflow for chapter 3.6.2. The objective of this chapter was the calculation of the Environmental Damage Index (EDI). This was achieved using the results of a survey of experts and the ecosystem mapping done in chapter 3.6.1.....	63
Figure 3.30 - Mapping of the expert valuation of ecosystems. Top Left: Faro-Olhão inlet and the Ilha do Farol urban area. Top Right: Armona inlet and the Armona island urban area. Bottom: Overview of the study area.....	65
Figure 3.31 - Environmental Damage Index (EDI) of the Area of Study. Top Left: Faro-Olhão inlet and the Ilha do Farol urban area. Top Right: Armona inlet and the Armona island urban area. Bottom: Overview of the study area. The loss areas mostly correspond to areas where the intertidal mudflats became subtidal.....	65
Figure 3.32 - Workflow for chapter 3.6.3. The Environmental Vulnerability Index (EVI) resulted from the combination of the ESI and EDI calculated in chapters 3.6.1 and 3.6.2, respectively.....	66
Figure 3.33 - The Environmental Vulnerability Index (EVI). Top Left: Faro-Olhão inlet and the Ilha do Farol urban area. Top Right: Armona inlet and the Armona island urban area. Bottom: Overview of the study area.....	66
Figure 3.34 - Comparison of aggregation methodology, results of joining two different indices.....	67
Figure 3.35 - The Socioeconomic Risk Index (SRI). Top: Overview of the study area. Bottom Left: City of Faro and surroundings. Bottom Right: City of Olhão and surroundings. Most of the high and extreme socioeconomic risk is concentrated in the urban areas, notably the inhabited regions of the barrier islands.....	68
Figure 3.36 – The Environmental Risk Index (ERI). Top Left: Faro-Olhão inlet and the Ilha do Farol urban area. Top Right: Armona inlet and the Armona island urban area. Bottom: Overview of the study area. The whole wetland area is mostly at a high or extreme environmental risk.....	69
Figure 3.37 - Comparison between the results of MVI methodologies applied to the urban area of Culatra Island.....	70

Figure 3.38 - Multi-parametric Coastal Risk Index (MCRI). Top Left: Faro-Olhão inlet and the Ilha do Farol urban area. Top Right: Armona inlet and the Armona island urban area. Bottom: Overview of the study area.....	71
Figure 4.1 - Shoreline difference between 2010 and 2100. Left: Armona Inlet. Right: Lagoon area, south of Olhão. ....	72
Figure 4.2 - Coastline Retreat by 10 m Segment. Negative Values Represent Shoreline Advance while Positive Values Represent Shoreline Retreat.....	72
Figure 4.3 - Demographic Vulnerability Statistics. Classes have been divided by quintiles. Olhão is the only civil parish with the highest level of vulnerability on every category.....	73
Figure 4.4 - Infrastructure affected by the RCP 8.5 SLR scenario. The Faro airport is the largest infrastructure at risk in this scenario, but many other ferry terminals and piers used mostly for fishing or recreation can also be damaged.....	75
Figure 4.5 - Comparison between the classified damage to the ecosystem obtained by applying the methodology of Inge et al. (2013) and the methodology for the EDI presented in this dissertation.....	77
Figure 4.6 - Comparison of results obtained for Almancil Civil Parish. Left: Coastal Risk Index (Antunes et al., 2019a), SLR Model: MOD.FC_2; Right: Multi-parametric Coastal Risk Index SLR Model: RCP 8.5. The figure on the left shows that the inclusion of the EVI allows for a more thorough classification of risk.....	78
Figure A.1 - Population Density (PD) Classification. Top: Overview of the Area of Study. Bottom Left: City of Faro and Surroundings. Bottom Right: City of Olhão and Surroundings. ....	105
Figure A.2 - Infrastructure (I) Classification. Top: Overview of the Area of Study. Bottom Left: City of Faro and Surroundings. Bottom Right: City of Olhão and Surroundings. ....	106
Figure A.3 - Transport Network (TN) Classification. Top: Overview of the Area of Study. Bottom Left: City of Faro and Surroundings. Bottom Right: City of Olhão and Surroundings. ....	107
Figure A.4 – Soil Use (SU) Classification. Top Left: City of Faro and Surroundings. Top Right: City of Olhão and Surroundings Bottom: Overview of the Area of Study. ....	108
Figure A.5 – Ecological Areas (EA) Classification. Top: Overview of the Area of Study. Bottom Left: City of Faro and Surroundings. Bottom Right: City of Olhão and Surroundings. ....	109
Figure C.1 - Multi-Parametric Coastal Risk Index (MCRI) with “Or” methodology. Top Left: Ecological Area Surrounding the Faro-Olhão Inlet and the Ilha do Farol Urban Area. Top Right: Ecological Area Surrounding the Armona Inlet and the Armona Island Urban Area. Bottom: Overview of the Area of Study.....	111
Figure C.2 - Multi-Parametric Coastal Risk Index (MCRI) with “Weighted” methodology (80% EVI, 20% SVI). Top Left: Ecological Area Surrounding the Faro-Olhão Inlet and the Ilha do Farol Urban Area. Top Right: Ecological Area Surrounding the Armona Inlet and the Armona Island Urban Area. Bottom: Overview of the Area of Study.....	112

## Table of Tables

Table 2.1 - Summary of methodologies used to determine the value of ecosystems, considering both Monetary and Non-Monetary Approaches and the different types of Valuation and Methodology. [Adapted from: Christie et al. (2012)].....	26
Table 3.1 - Full time resident population in the civil parishes that encompass the Ria Formosa in 2021 [Source: INE (2022)].....	33
Table 3.2 - Data used in this dissertation with sources, acquisition dates and observations.....	37
Table 3.3 - TWL Forecast for the Ria Formosa in 2100 with the IPCC RCP 8.5 scenario. Each probability of occurrence is related to an elevation interval, denoting how likely an area at that elevation is to flood in an extreme scenario. These intervals can then be normalised into the classes of hazard seen on the right.....	40
Table 3.4 - Change in erosion rates between 2010 and 2100. Stretches 5,6,7,17,18 and 23 are completely below the maximum swash in 2100. Stretch 14 is already below this value today. Stretch 21 represents the inlet area and the erosion algorithm was not used here, it is included for DTM completion purposes.....	45
Table 3.5 - Tide data from the Faro tide gauge from 2000-2010, 2015. For each of the values on high tide and low tide, the columns represent the maximum (Max), spring tide (ST), average (Avg), neap tide (NT) and minimum (Min). .....	46
Table 3.6 - Ecosystem classification by elevation. Each of the class boundaries correspond to the values in Table 3.5, with the midpoints being where an accretion rate transitions into the next one....	47
Table 3.7 – Excerpt of the tidal corrections table for secondary ports in the Ria Formosa (IH). For this correction the height of the tide at spring tide was used to create the anomalous tidal surface. ....	48
Table 3.8 - Reclassification of infrastructure, with examples of types of infrastructure (I) considered in each class.....	51
Table 3.9 - Reclassification of the Transport Network (TN) features and width factor used to convert line to polygon data.....	52
Table 3.10 - Reclassification of Soil Use (SU) based on level of alteration from their natural state....	52
Table 3.11 - Reclassification of Ecological Areas (EA). .....	53
Table 3.12 - Weights of each parameter for the SSI, according to the results of Antunes et al. (2019a). .....	54
Table 3.13 - Classification of the allocation variable based on a comparison between the number of buildings and the number of residential buildings present in a BGRI.....	55
Table 3.14 - Base value per allocation type, with the respective formula to determine this value.....	56
Table 3.15 - Allocation coefficients based on use type. .....	56
Table 3.16 - Allocation coefficient based on the BGRI allocation with the expression used to calculate it.....	56
Table 3.17 - Location coefficients by type of allocation, with the expression used to calculate them..	57
Table 3.18 - Antiquity coefficient by building age according to the CIMI. .....	57
Table 3.19 - Antiquity coefficient adapted to the census 2021 data .....	58
Table 3.20 - Ecosystem Boundaries. First column: Tide height (CD), Second column: Tide elevation (MSL), Third column: Tide elevation in 2100 (MSL).....	61
Table 3.21 - Susceptibility classification per ecosystem according to their ability to withstand extreme weather events. ....	62
Table 3.22 - Value attributed by the experts' survey to each ecosystem using a geometric x geometric averaging method. .....	64
Table 3.23 - Normalisation of damage values into classes.....	66

Table 4.1 - Exposure demographic statistics of the Ria Formosa's civil parishes to the extreme flooding scenarios of RCP 8.5 2100. Olhão is the most affected civil parish in this scenario. Conceição e Cabanas de Tavira has the second highest weighted damage even though there is a low number of residents due to a high density of hotels near the beach. Faro is the second most affected civil parish in terms of buildings and residents at risk.....	74
Table 4.2 - Evolution of ecosystem areas between 2010 and 2100. 1) Inland urban and agricultural area protected; 2) No protections. 3) Urban and agricultural area protected including on the Barrier Island System. ....	75
Table 4.3 - Comparison between the results obtained in this dissertation and the results of Inge et al. (2013) .....	76
Table B.1- Survey Results. Each Expert was Asked to Rank from 1 to 5 the Importance of the Contribution of each Ecosystem to each Ecosystem Service. A - Arithmetic Average; W - Weighted Average; G - Geometric Average.....	110
Table B.2 - Survey Results Averaged per Ecosystem. A - Arithmetic Average; W - Weighted Average; G- Geometric Average. e.g. AA = Arithmetic x Arithmetic .....	110

## Acronyms

<b>APA</b>	Portuguese Environmental Agency (from the portuguese: <i>Agência Portuguesa do Ambiente</i> )
<b>BGRI</b>	Base Reference Geographical Information (from the portuguese: <i>Base Geográfica de Referenciação de Informação</i> )
<b>CCS</b>	Climate Change Scenarios
<b>CD</b>	Chart Datum
<b>CN</b>	Climate Normal
<b>CSIRO</b>	Commonwealth Scientific and Industrial Research Organisation
<b>CVI</b>	Coastal Vulnerability Index
<b>DEM</b>	Digital Elevation Model
<b>DGT</b>	Portuguese Territory General-Directorate (from the portuguese: <i>Direção Geral do Território</i> )
<b>DEM</b>	Digital Elevation Model
<b>DSM</b>	Digital Surface Model
<b>DTM</b>	Digital Terrain Model
<b>EA</b>	Ecological Area
<b>EDI</b>	Environmental Damage Index
<b>ERI</b>	Environmental Risk Index
<b>ESI</b>	Environmental Susceptibility Index
<b>EVI</b>	Environmental Vulnerability Index
<b>GIS</b>	Geographic Information System
<b>GW</b>	Global Warming
<b>IH</b>	Hydrographic Institute (from the portuguese: <i>Instituto Hidrográfico</i> )
<b>INE</b>	National Statistics Institute (from the portuguese: <i>Instituto Nacional de Estatística</i> )
<b>IPCC</b>	Intergovernmental Panel on Climate Change
<b>IPMA</b>	Portuguese Institute for the Sea and Atmosphere (from the portuguese: <i>Instituto Português do Mar e da Atmosfera</i> )
<b>LiDAR</b>	Light Detection and Ranging
<b>MCRI</b>	Multi-parametric Coastal Risk Index
<b>MHT</b>	Mean High Tide
<b>MSL</b>	Mean Sea Level
<b>MSSH</b>	Mean Sea Surface Height
<b>MVI</b>	Multi-parametric Vulnerability Index
<b>NASA</b>	National Aeronautics and Space Administration
<b>NMHT</b>	Neap Mean High Tide
<b>NT</b>	Neap Tide
<b>OSM</b>	Open Street Map
<b>PD</b>	Population Density
<b>PVI</b>	Physical Vulnerability Index
<b>RCP</b>	Representative Concentration Pathway
<b>RNGAP</b>	High Precision Geometric Levelling Network (from the portuguese: <i>Rede de Nivelamento Geodésico de Alta Precisão</i> )
<b>SDI</b>	Socioeconomic Damage Index
<b>SLR</b>	Sea Level Rise
<b>SMHT</b>	Spring Mean High Tide
<b>SRI</b>	Socioeconomic Risk Index

<b>SS</b>	Storm Surge
<b>SSI</b>	Socioeconomic Susceptibility Index
<b>ST</b>	Spring Tide
<b>SVI</b>	Socioeconomic Vulnerability Index
<b>SU</b>	Soil Use
<b>TN</b>	Transport Network
<b>TWL</b>	Total Water Level
<b>WMO</b>	World Meteorological Organisation

# **1. Introduction**

## **1.1 Contextualising the Problem**

Climate change is an undeniable reality, as evidenced by the latest report from the Intergovernmental Panel on Climate Change (IPCC, 2021, 2022), which highlights the continuous rise in global temperatures and reinforces the urgent need for action. According to the report, the average temperature is projected to increase by up to 1.9°C by 2050 and potentially reach 5°C by 2100 under the most pessimistic scenarios. Such temperature increases threaten both natural and human systems worldwide. In Europe, specific risks are associated with the escalation in heat-related deaths, failure of agricultural crops due to heatwaves and drought, water scarcity, and coastal flooding.

One crucial consequence of global warming is the warming of oceans, particularly in the upper layers. This warming leads to thermal expansion, exacerbating the rise in sea levels, which poses significant threats to coastal areas, such as increased erosion rates, shoreline retreat, and vulnerability to flooding. In Portugal, this acceleration is already evident, as observed at the Cascais tide gauge, where the average sea level rose by approximately 1.6-1.9 mm/year (Antunes, 2011; Antunes & Taborda, 2009; Taborda & Ribeiro, 2015) between 1920-2000, 2.2 mm/year between 1992-2004 and 4.1 mm/year between 2005-2016 (Antunes, 2019).

The project "Climate Change in Portugal – Scenarios, Impacts, and Adaptation Measures" (SIAM) (Santos et al., 2002; Santos & Miranda, 2006) has identified vulnerabilities specific to Portugal. The rise in mean sea level has the potential to intensify storm surges and shorten the return period of violent storms, primarily impacting areas near river mouths and estuaries. Such changes will not only intensify flooding but also make drainage more challenging. Cardoso et al. (2023) highlighted how Portugal will be subject to a substantial increase in average temperatures, surpassing the global average, and how this will impact the quantity and severity of heat waves and hot stress conditions. This rise will result in a larger thermal amplitude, an increased thermal gradient between the ocean and the continent and a reduction in very cold days. Additionally, there will be a decrease in average precipitation and the length of rainy seasons, leading to more intense and frequent severe weather events due to the atmosphere's increased humidity-carrying capacity (IPCC, 2021). These factors will further aggravate the intensity of flooding events.

Sea level rise projections, even under the optimistic pathway of limiting global warming to 1.5°C, indicate a rise of at least 0.3 m between 2000 and 2100. However, if high rates of emissions trigger rapid ice sheet collapse, sea levels could potentially rise as much as 2 m by 2100 (IPCC, 2023). This rise will have severe consequences for Portugal's coastal areas, especially estuaries and lagoons such as Ria de Aveiro, Tagus Estuary, Sado Estuary and Ria Formosa. Erosion, increased aggradation in estuaries and lagoons, and loss of saltmarsh areas are among the main effects to be expected (Ribeiro, 2010).

Portugal's coastal areas are of paramount importance, as the country has experienced a growing concentration of economic and touristic activities in these regions, mirroring trends observed throughout Europe. With a densely populated coast, valuable economic activities, and significant infrastructure, Portugal faces unique challenges in managing the impacts of climate change. From an environmental perspective, these ecosystems also play a vital ecological role in supporting diverse fauna and flora (Savenije et al., 2008).

Given these circumstances, there is an increasing need for tools that can aid in the planning and management of coastal areas. The consequences of rapid climate change will be many, including rising

sea levels, increase of significant height of ocean waves (sea swell), meteorological forcing, temperature changes, and altered precipitation patterns. These factors significantly impact the sedimentary balance of shorelines, erosion rates, frequency and intensity of flooding, and the water quality of estuaries, lagoons, and aquifers, which can include contamination of soils and freshwater reservoirs by saltwater intrusion (IPCC, 2021, 2022).

To address these coastal challenges, this project aims to develop an integrated risk assessment framework for sea level rise in coastal areas with inland waters. It seeks to combine various tools developed in past dissertations (Costa, 2017; Ferreira, 2022; Rocha, 2016; Santo, 2022) that focused on the same subject matter, to create a comprehensive approach that incorporates physical, socioeconomic, and environmental vulnerability factors to facilitate the creation of multi-parametric risk maps, enabling improved management of sea level rise-related risks in these regions. By integrating different aspects of vulnerability, this framework will support administrative units in developing effective climate change adaptation strategies, contributing to the resilience and sustainable management of Portugal's coast, and ensuring the protection of both human and natural systems in the face of an uncertain future.

## **1.2 Objectives**

The aim of this study is to establish a methodology that allows for a thorough evaluation of the vulnerability and risk of a region to rising mean sea levels and to demonstrate its applicability using the Ria Formosa as a case study area. To achieve this, the following specific objectives have been proposed:

1. Creation of a Digital Terrain Model (DTM) of the coastal areas for future scenarios of mean sea level rise.
2. Create a Socioeconomic Vulnerability Map.
3. Create an Environmental Vulnerability Map for the intertidal ecosystems present in the Ria Formosa.
4. Develop a new methodological approach to calculate risk based on multiple vulnerability parameters
5. Create a Multi-parametric Risk Assessment Map of the Ria Formosa.

These objectives will be achieved through a combination of methodologies developed within the SNMPortugal working group ([www.smnportugal.pt](http://www.smnportugal.pt)) at the Science Faculty of the University of Lisbon, which this dissertation aims to combine into a single structured project. This dissertation contributes to the work frame with the development of a new methodology to evaluate environmental vulnerability and exposure and proposes a combined cartography that allows stakeholders to assess risk as a variable that encompasses social, economic, and environmental variables.

## **1.3 Motivation**

The motivation for this dissertation stems from the urgent need to enhance our understanding and management of coastal environments in the face of climate change. The work builds upon the methodologies developed by previous researchers, aiming to integrate dynamic models, environmental and socioeconomic factors to precisely identify and quantify risk zones. This comprehensive approach is intended to support the decision-making process for adaptation and mitigation measures, ensuring a robust evaluation of coastal vulnerability against future climate scenarios. By incorporating diverse components, this research seeks to significantly contribute to the assessment of coastal flood risks and inform sustainable territorial management strategies.

Moreover, the dissertation extends the scope of earlier studies by incorporating environmental vulnerability assessments alongside the existing methodologies. Recognising the socioeconomic significance and biodiversity of intertidal ecosystems, it addresses the urgent need for improved planning and adaptation strategies in response to sea level rise and climate change impacts.

## **1.4 Scientific Contribution**

This dissertation aims to make a significant scientific contribution by advancing the methodology for assessing coastal risk and vulnerability, integrating environmental and socioeconomic vulnerability maps into a multi-parametric risk index map. The inclusion of the environmental variables offers a holistic view of the impacts of climate change on coastal regions.

The applicability of this methodology is further demonstrated by using the case study of the Ria Formosa, a unique region in Portugal with a low-lying coast, areas of high urban density and a large natural protected area. The results obtained contribute to a better understanding of coastal dynamics and inform strategies to protect and preserve coastal environments.

## **1.5 Structure of the Dissertation**

This dissertation is structured in five chapters, beginning with this introductory chapter, followed by a state-of-the-art review, the methodological approach and results, the discussion of these results and the conclusions.

In the introduction the objectives and motivation that serve as a basis for this dissertation are introduced, while the state-of-the-art review presents the theoretical concepts necessary for the understanding of the processes involved in this study.

The third chapter describes the methodology used to produce the vulnerability and risk maps, including a thorough description of the study area, the intermediate results and considerations regarding the different data aggregation methods that can be used in these studies.

In the final two chapters the results obtained are discussed and the conclusions of this dissertation are presented, including some limitations of the methodology and future recommendations.

## **2. State-of-the-Art**

This section delves into essential concepts and theoretical foundations critical for comprehending the central themes of this dissertation: the assessment of risk to coastal areas exacerbated by the rising sea level, as well as concepts relating to vulnerability, hazard, susceptibility, damage, and exposure, and particular factors which need to be considered for this study. Each topic forming the basis for the comprehensive analysis will be briefly introduced. Due to the complexity of the field of study, this chapter will only address topics that are directly related to the main objective of this thesis, that being the establishment of a multi-parametric methodology to evaluate risk.

### **2.1 Coastal Risk**

The definition of risk in the context of natural disasters was established in an international convention by the Office of United Nations Disaster Relief Coordinator as “*the expected losses from a given hazard to a given element at risk, over a specified future time period, for example the expected loss of life, injury, property damage or economic disruption*” (Office of the United Nations Disaster Relief Coordinator, 1980). The IPCC characterises risk as “*the potential for consequences where something of human value (including humans themselves) is at stake and where the outcome is uncertain*”. In

more tangible terms, risk is often represented as the probability of occurrence of hazardous events or trends multiplied by the consequences if these events occur (IPCC, 2022).

The determination of risk involves three essential components: the likelihood of experiencing any hazard at a location or in a region (the hazard occurrence probability), the elements at risk (those affected by the hazard), and the potential damage to the elements at risk. For each of these components there are several factors that need to be evaluated, for example, the quantification of hazard probability requires assessing not only the probability of a storm occurrence but also the occurrence probability of various strengths. The elements at risk encompass a wide range of components that constitute society, people's lives and health, economic activities, jobs, houses, roads, and community services as well as the natural environment. Damage is similarly multi-dimensional, with each element being affected differently by hazards of varying severity - the higher the hazard, the greater the damage inflicted (Coburn et al., 1994).

Risk assessment is commonly used to estimate risk to a determined area in a determined time frame for a specific occurrence of hazard. Certain coastal areas, due to their location, low elevation, low or flat slopes, and type of soil, are considered more at risk for certain natural phenomena, such as tropical storms or hurricanes, which frequently result in coastal flooding and damage to people, nature, and infrastructure. The sea level rise, induced by global warming, will subject these areas to an increased risk of flooding. This risk will be further heightened by the subsequently elevated frequency of occurrence of extreme weather events, along with their increased severity.

Existing methods for assessing coastal vulnerability and risk differ in complexity, in the number of processes included and in the applications at various scales and outcomes. In recent decades, several methods for assessing coastal vulnerability have been developed on different scales, either presenting new approaches or adapting the existing ones. According to Satta (2014) the methodological sets can be grouped into four clusters: index/indicators-based methods, methods based on dynamic computer models, GIS-based decision support tools and visualization tools.

The most widely used methodology for coastal vulnerability assessment is the Coastal Vulnerability Index (CVI) (Gornitz et al., 1994). Since its inception, many authors have attempted to modify and incorporate different dimensions into this index. One noteworthy contribution was made by McLaughlin et al. (2010), who proposed an advanced CVI based on the integration of three sub-indices. The first sub-index evaluates the resilience and susceptibility of the coast to erosion based on environmental and morphological variables. The second sub-index characterises coastal forcing contributing to wave-induced erosion. Lastly, the socioeconomic sub-index assesses anthropogenic infrastructures potentially at risk, such as settlements, roads, and railways.

While it's still common to see studies where only physical factors are used when calculating risk (e.g. (Basheer et al., 2016; Ghoussein et al., 2018; Parthasarathy & Natesan, 2015; Royo et al., 2016), many authors are now integrating information on socioeconomic features with the assessment of the potential impact of climate change on coastal hazards (e.g. Behera et al., 2019; De Serio et al., 2018; Furlan et al., 2021; Satta et al., 2017). In Portugal, several authors have contributed to the study of coastal risk, in projects of both national and local scale (e.g. Barros et al., 2022; Ceia et al., 2010; Ferreira et al., 2021; Martins et al., 2012; Rocha et al., 2020; Silva et al., 2017).

However, there are still many variables which are not being considered by these studies. One area, in particular, where there is a significant gap in the literature is the assessment of the risk to natural environments, which are also threatened by hazards and have an intrinsic ecological value, therefore subjected to damage or losses.

According to Ramieri et al. (2011) there is a need for coastal vulnerability assessment to adopt an integrated strategy taking into account both the environmental changes caused by climate change and other causes, socioeconomic advancements, and the interactions between these elements. The risk assessment that constitutes the case study of the methodology presented in this dissertation follows the structure proposed by Rocha et al. (2023) for the particular scenario of a local scale, which can be seen in Figure 2.1, but aims to additionally include an approach to assess the SLR risks to natural ecosystems.

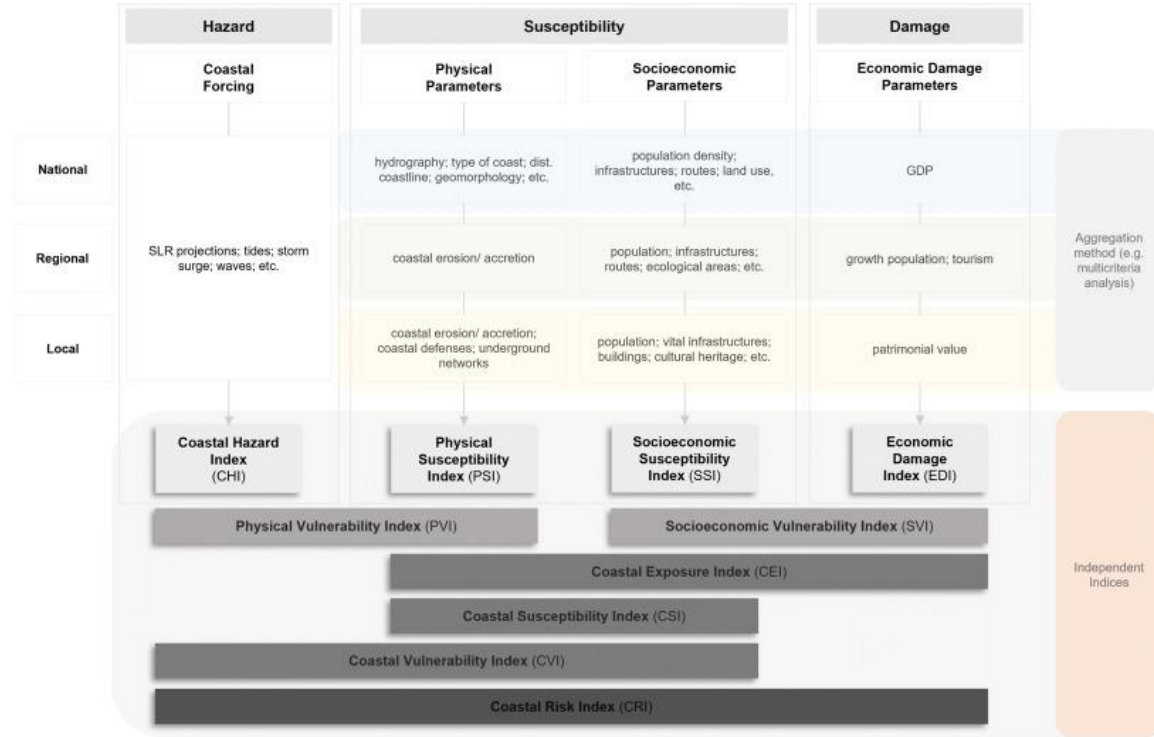


Figure 2.1 - Relationship between the different concepts associated with risk and the different indices that can be calculated. Each index in the first row is independent and can be used in conjunction with any others to obtain the combined indices of the three bottom rows [Source: Rocha et al. (2023)].

Following the interaction between concepts shown in Figure 2.1, risk can then be seen as the interaction between the physical vulnerability (PVI) and the socioeconomic vulnerability (SVI):

$$\text{Coastal Risk Index (CRI)} = \text{PVI} \times \text{SVI} \quad (2.1)$$

Where the PVI results from the product of coastal hazard index (CHI) and physical susceptibility index (PSI) and the SVI results from the product of socioeconomic susceptibility index (SSI) and economic damage index (here renamed socioeconomic damage index (SDI) for clarity):

$$\text{CRI} = (\text{CHI} \times \text{PSI}) \times (\text{SSI} \times \text{SDI}) \quad (2.2)$$

This can then be adapted to include the environmental vulnerability, creating a multi-parametric vulnerability index (MVI), where both the SVI and an environmental vulnerability index (EVI), composed of an environmental susceptibility index (ESI) and an environmental damage index (EDI), are considered:

$$\text{Multi - Parametric Coastal Risk Index (MCRI)} = \text{PVI} \times \text{MVI} \quad (2.3)$$

Where:

$$MVI = (SSI \times SDI) \times (ESI \times EDI)$$

(2.4)

The concepts of vulnerability, hazard, susceptibility, and damage will be explored in the subsequent chapters of this dissertation, as well as each of the parameters which will be used for this risk assessment.

## 2.2 Physical Vulnerability

The IPCC (2022) defines coastal vulnerability as the propensity of a system to be adversely affected by a hazard and encompasses a variety of concepts and elements, including susceptibility to harm and lack of capacity to cope and adapt. Vulnerability, together with exposure and hazard, is one of the key components of risk.

Vulnerability and susceptibility are related but distinct concepts used in the context of risk assessment. They both relate to the potential for harm or negative impacts, but they emphasize different aspects of risk: susceptibility refers to the inherent or intrinsic characteristics of a system (e.g., individuals, communities, or ecosystems) that make it relatively prone to being affected by a hazard, while vulnerability refers to the overall propensity of a system to suffer harm or damage when exposed to a hazard or stressor. It considers both the inherent characteristics (susceptibility) and external factors that can increase or decrease the risk of harm (Birkmann, 2007).

The most common way to evaluate coastal vulnerability involves the calculation of an index as a way to combine and simplify parameters or variables that are represented by many data sources, but that can be aggregated spatially. This results in an indicator that can be more easily understood and be used in decision making (McLaughlin et al., 2010; Rocha, 2016).

Physical vulnerability refers to the interaction between the hazard and the susceptibility of a determined location to that hazard, providing an understanding of how it is affected by various forcing factors.

### 2.2.1 Coastal Hazard Processes

A hazard is defined as a potential source of harm or danger, with the capacity to pose threats to people, property, and the environment. Various natural and human-made factors give rise to these hazards, which can take diverse forms. Coastal hazard processes concentrate specifically on perils linked to coastal areas, frequently instigated by natural forces that exert substantial impacts on these communities. Phenomena such as flooding, tsunamis, saltwater intrusion, coastal landslides, and hazardous material spills are all encompassed within the realm of coastal hazards. The effective management and mitigation of these hazards are deemed crucial for the safeguarding of coastal communities and their associated ecosystems (Coburn et al., 1994).

Coastal forcing encapsulates a spectrum of natural or environmental factors and processes that exert influence on and shape conditions within coastal regions, potentially amplifying hazards. In cases of severe flooding, as the case study examined in this dissertation, it is imperative to consider the collective of forcing components intricately linked to coastal hazards, in conjunction with sea level rise. This encompasses factors such as the astronomical tide, storm surges, and wave run-up (Rocha et al., 2023).

This chapter will explore the concepts related to physical coastal forcing as well as the parameters used for this portion of the study.

### 2.2.1.1 Mean Sea Level

The mean sea level (MSL) defines a reference surface and is used as a geodesic vertical reference, representing the average height of the sea surface in relation to a specified point or altimetric reference frame or system. It can be derived from a series of tide gauge observations over a defined period, ideally exceeding 19 years, or through the mean of mean sea surface height (MSSH) from satellite altimetry observations. For the tide gauge reference, the 19-year period encompasses the astronomical nutation period (18.6 years) — a periodic variation in the orientation of the Earth rotation axis and, therefore, the node lines of the Moon's translation plane with the Earth equator. In Portugal, the conventional MSL was established based on observations from the Cascais tide gauge, reflecting the average of annual averages recorded between 1882 and 1938. This dataset defines the National Altimetric Datum, known as Cascais 1938.

Given that the MSL is intricately tied to different time scales, due to sea level variations, analyses often involve considering various MSL values, focusing, for example, on the monthly and annual variations. This approach allows for a nuanced examination of the sea level's fluctuations, beyond tides and wave oscillation. To ensure the analysis accuracy, any phenomena causing variations within a period smaller than the chosen scale are typically disregarded. This results in a filtering process being applied to tide gauge observations, refining the dataset to align with the selected temporal scale for a more targeted and meaningful assessment of MSL variations (Silva et al., 2008).

The absolute variation of the MSL is a non-linear process, resulting from different mechanisms with different temporal scales (Rahmstorf, 2007). According to Dias & Taborda (1988) and Titus (1986), the three major factors that influence the MSL are the total mass of water present in the oceanic basins, the temperature of the water at different depths (influencing the density) and the shape (bathymetry) of the oceanic basins. These factors are mainly modified by eustatic processes, namely:

- Glacio-Eustatic Processes: changes in sea level resulting from the growth or retreat of ice sheets, such as continental glaciers and polar ice caps.
- Glacio-Isostatic Processes: isostatic adjustment of Earth's crust over the mantle due to the weight change of ice sheets (long-term surface changes).
- Hydro-Isostatic Processes: variations in sea level caused by the redistribution of water masses on Earth's surface, such as changes in the amount of water stored in glaciers, ice caps, or groundwater.
- Tectonic-Eustatic Processes: changes in the sea level due to the dynamics of tectonic plates that can change the shape of ocean basins.
- Techno-Eustatic Processes: sea level changes resulting from human activities or anthropogenic factors, like land subsidence due to groundwater extraction or the construction of large reservoirs.
- Sediment-Eustatic Processes: these processes are associated with changes in sea level due to the deposition or erosion of sediment on the ocean floor.
- Geoid-Eustatic Processes: changes in the Earth's gravitational field reference surface (geoid) can impact sea levels.

Due to global warming (GW), which imposes an ice loss from continental glaciers and polar caps, as well as an increase in the ocean heat content, the global MSL has exhibited an upward trend since 1880 (Church & White, 2011), and projections suggest that this rise will persist throughout the current and next century (IPCC, 2021; Taborda & Ribeiro, 2015). Several internationally recognised organizations, such as the Commonwealth Scientific and Industrial Research Organisation (CSIRO) and the National Aeronautics and Space Administration (NASA), estimate the average global sea level

rise to be in the range of 3.4-3.5 mm/yr since 1995. In Portugal, the 20th-century observations from the Cascais and Lagos tide gauges have been analysed by Dias & Taborda (1988), revealing an average increase of  $1.3 \pm 0.1$  mm/yr and  $1.5 \pm 0.2$  mm/yr, respectively. Additional studies (Antunes, 2011; Antunes & Taborda, 2009; Taborda & Ribeiro, 2015) suggest a MSL increase in Cascais during the 1920-2000 period of approximately 1.6-1.9 mm/yr. More recent data indicates a MSL rise in Cascais at a rate of 2.2 mm/yr between 1992-2004 and 4.1 mm/yr between 2005-2016 (Antunes, 2019). The rise in MSL will exacerbate coastal flooding, particularly impacting low-lying areas.

Depending on the Climate Change Scenarios (CCS), represented by the well-known Representative Carbon Pathways (RCP), global MSL may rise from a few meters to more than ten meters in the next centuries to millennia (IPCC, 2023).

#### 2.2.1.2 Tides

Ocean tides manifest as periodic oscillations in sea level regulated by the gravitational forces exerted by the Sun and Moon, in conjunction with the Earth's rotation. While both celestial bodies contribute to tidal patterns, the Moon holds the predominant influence. Despite its smaller mass compared to the Sun, the moon's proximity compensates for this difference, making it the primary factor shaping tidal behaviour (Pugh, 2004).

From a mathematical standpoint, ocean tides can be expressed as a series of harmonic functions (sinusoidal waves), each possessing a known period and relying on astronomical and local oceanic basin factors. These functions form the foundation for characterising tidal behaviour in a particular location and can be precisely determined through a mathematical method referred to as harmonic analysis (Antunes & Godinho, 2011; Instituto Hidrográfico, 2023).

Due to the elliptical orbits of the Earth and the Moon, coupled with the Earth's orbital obliquity (orbital plane deviating from the Equatorial plane), a disturbance effect occurs on the Earth's axis and, consequently, its orbital plane. This phenomenon induces changes in the alignment among the Earth, Moon, and Sun. Additionally, the Moon's orbital plane maintains an almost constant angle with the ecliptic plane, while the line of intersection between these two planes undergoes a gradual rotation over an 18.6-year period - nutation period.

The main periods of the tidal wave depend on the Moon's phases, as defined by its alignment or quadrature with the Sun concerning to the Earth. During Full Moon and New Moon, when the Moon aligns with Earth and the Sun, in opposition or conjunction, the tidal range reaches its maximum values due to the combined gravitational forces of both these celestial bodies. This phenomenon results in what is known as spring tides (ST). In contrast, during the First Quarter or Last Quarter phases, when the positions of the Moon and the Sun are at right angles in relation to the Earth (Moon's position in quadrature), tides with the lowest amplitudes occur. These are known as neap tides (NT) (Ribeiro, 2010; Rolim, 2014).

The annual movement of the Earth in relation to the Sun also causes a variation in tidal amplitude. When the Earth is closer to the Sun, the tidal amplitude increases, particularly during the equinoxes. On the other hand, in the summer solstice, when the Sun is farther from the Earth, spring tides typically have the lowest amplitudes of the year (Antunes, 2012).

Three distinct types or tide regimens can occur: diurnal tides, semidiurnal tides, or mixed tides. Semidiurnal tides, observed across the entirety of Portugal, occur when two high tides and two low tides occur within a single day, with different or similar amplitudes, depending on the diurnal inequality. In contrast, diurnal tides are characterised by only one high tide and one low tide per day. Mixed tides exhibit variability, alternating between periods with one and two tides per day. Tides can

also be classified by their wave height (Antunes, 2012): microtidal (< 2 meters), mesotidal (2 – 4 meters), and macrotidal (> 4 meters). The Ria Formosa, as in all Portugal mainland, is classified as a mesotidal system (Newton & Mudge, 2003).

The variability of sea level encompasses not only the regular periodic oscillation of the astronomical tide but also irregular variations spanning short, medium, or long periods. Notably, meteorological forcing emerges as a significant factor, contributing to sea level changes that can surpass astronomical tide predictions by considerable margins. Along the Portuguese coast, for instance, increases of up to 80 cm are observed, illustrating the potential for extreme consequences (Antunes et al., 2019b). The impact of meteorological forcing is particularly pronounced during storms, driven by atmospheric conditions associated with the passage of low-pressure systems and strong winds, resulting in sea level surges. Additionally, short-period variations involve high-frequency fluctuations induced by local wind forcing or strong sea state (Dias & Taborda, 1992). Atmospheric pressure also plays a key role in sea level variations, with low pressures associated with elevated water levels and high pressures linked to a decrease in sea level.

Traditional tidal observation involves the use of tide gauges equipped with diverse measurement technologies, including mechanical, hydrostatic pressure, acoustic, or radar systems. These instruments capture the instantaneous sea surface level with respect to a reference mark. The recorded sea level observations are then converted into either tidal elevation (reflecting the variation in sea level relative to MSL) or tidal height (indicating the variation relative to the chart datum). Tidal height is derived by combining the tidal elevation with the local Chart Datum (CD) value (Antunes, 2012).

In this context, tidal elevation exhibits fluctuations around the MSL, without accounting for effects related to SLR and meteorological surges. Tidal elevation assumes positive values during high tides and negative values during low tides. Conversely, tidal height is consistently represented as a positive value owing to the definition of CD, which is located below the lowest of the low tides recorded in a nodal period. Exceptions to this positive value occur only in extreme situations involving meteorological forcing or other phenomena that lead to a substantial decrease in the tide below the CD (Antunes, 2012).

Tide tables are produced utilizing harmonic prediction models tailored for each tide gauge. These models enable the determination of average and extreme levels for both high tide and low tide during spring tide and neap tide. The aim is to characterise the annual amplitudes of the corresponding tidal oscillations. It's crucial to emphasize that these values exclusively pertain to astronomical tide, excluding the meteorological forcing component of the tide.

To characterise the tidal dynamics of the Ria Formosa, tidal harmonics were employed to the Faro tide gauge, located at Faro Island, near the Faro-Olhão inlet. Tidal harmonics serve as phase and amplitude parameters for the concordance method applied to tidal wave transferring between two ports that share the same tidal regimen, usually between a primary port and a secondary port in the vicinity (Instituto Hidrográfico, 2023). These concordance parameters are instrumental for determining tide tables at secondary ports or any other location where a full year of tide records may not be available.

### 2.2.1.3 Storm Surge

A storm surge is an atmospheric forcing that triggers an elevation in sea level during a storm. This phenomenon arises from strong winds propelling water towards the shore, and the low pressure at the centre of the storm enables the sea surface to ascend, surpassing the expected astronomical tide (Andrade et al., 2006).

The variability of storm surge is contingent upon geographical location and temporal factors, and its estimation is achievable through the harmonic analysis of hourly tide records. Storm surge values can fluctuate between positive and negative values. A positive surge, particularly when aligning with a period of spring tides, has the potential to induce severe flooding, emphasizing the critical role storm surges play in shaping the impact of extreme weather events.

This phenomenon is intricately linked to low-pressure and cyclonic systems, with its significance heightened in cases where the low-pressure system is more pronounced. The impact is further intensified when the accompanying wind field, due to its direction and intensity, induces a setup of sea level toward the coast (Andrade et al., 2006).

Storm surge is conventionally defined by return periods, derived from the analysis of maximum storm surge events over an extended period. In Portugal, the maximum observed storm surge between 1960 and 2018 ranged from 50 to 70 cm for the west coast. Harmonic analysis revealed the highest values to be 82 cm at the Viana do Castelo tide gauge on October 15, 1987, and 83 cm at the Lagos tide gauge on March 4, 2013. The latter instance's magnitude is attributed to the additional wave setup effect due to the tide gauge location and the southwest wave direction of the storm event. According to Antunes et al. (2019b), the Lagos tide gauge, situated closest to the Ria Formosa in the southern coast of Portugal, has a maximum predicted storm surge of 82 cm, 91 cm, and 100 cm for return periods of 50, 100, and 200 years, respectively.

#### 2.2.1.4 Sea Swell

The propagation of swell waves near the coast depends on the open sea state, bathymetry, and seafloor geometry within the propagation zone (Freire, 1999).

In a broad context, a wave is characterised as an oscillatory disturbance propagating through a medium, be it liquid, solid, or gas, and typically signifies a transfer of energy. In the context of maritime agitation, ocean waves specifically refer to surface mechanical waves that carry energy through the water. This energy is transferred to the ocean through various mechanisms, including the influence of the wind, the gravitational forces of the Moon and the Sun, seismic events, or any other processes leading to abrupt modifications in the seafloor (Blumberg & Bruno, 2018). Sea swell are waves generated by the wind friction that propagate for hundreds of kilometres through the gravity force and represent the highest energy waves that reach the coast.

As a wave enters the surf zone (see Figure 2.2), its height increases due to the rapid reduction in depth until the wave slope reaches a critical value, defined by the ratio between its height and the water depth, and then breaks. In shallow waters, the wave speed becomes dependent on depth, diminishing as the depth decreases. To maintain a constant energy flux, the wave's height (proportional to its energy) gradually increases. In very shallow depths, a notable disparity in speed arises between the wave crest (where the depth is greater) and the wave trough (propagating at a shallower depth). This difference continually expands. Consequently, the wave crest advances over the trough, where it lacks support, leading to its breaking (Blumberg & Bruno, 2018). The nature of wave breaking is predominantly influenced by the beach slope and wave steepness.

The sea state is typically characterised based on values related to significant wave height ( $H_s$ ), which represents the average of the third percentile of wave heights. It is further characterised by the mean wave period, indicating the average duration of the waves used in the calculation of significant height. Additionally, the peak period is considered, corresponding to the period with the highest spectral density and representing the most energetic waves. Directional information associated with the peak period is also a key aspect in characterising maritime waves (Coelho, 2005).

The monthly average significant wave height exhibits variations, ranging between 1.1 m and 2.8 m in wave buoy records from Figueira da Foz and Sines, and between 0.6 m and 1.5 m for Faro. Along the Portuguese west coast, wave directions are predominantly from the northwest, with some increase from the west during the winter, while the southern Algarve coast experiences waves predominantly from the west. Monthly maximum significant height values display significant variability, reaching values of 11 m in December and January, and 4 m in July, with the potential for even higher values during storm events. The most frequent significant wave period values range from 9 s to 11 s, with the observed minimum value being 6 s and the maximum reaching 18 s (Mendes & Oliveira, 2021).

Other crucial concepts related to the ocean wave's impact include the effects of run-up and set-up. Run-up (denoted as  $R$  in Figure 2.2) refers to the swash maximum level reached by the water on the coast after swell wave breaks. Essentially, run-up represents the vertical distance between the highest points reached by the wave swash and the tide level at that moment.

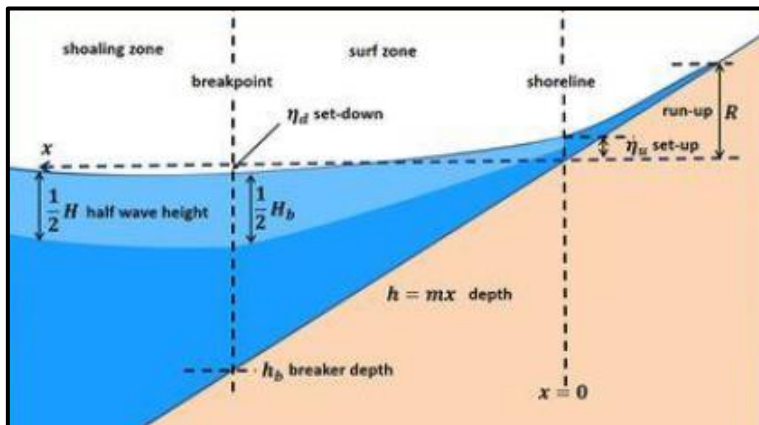


Figure 2.2 - Schematization of the concepts of run-up, set-up, surf zone and breaker depth [Source: Sistema Nacional de Informação de Recursos Hídricos (2022)]

Wave set-up (denoted as  $\eta_u$ ) is essentially the increase in tide surface elevation at the shoreline resulting from the stacking effect caused by wave breaking in the surf zone (Bowen et al., 1968). This elevation includes both a static and a dynamic component. The static component represents the average value of set-up over the considered period, while the dynamic component captures the oscillation of the set-up (Figure 2.3) (Dean et al., 2005). Set-up, which encompasses both the dynamic and static components, is a constituent of the total run-up, along with the incident run-up ( $R - \eta_u$ ).

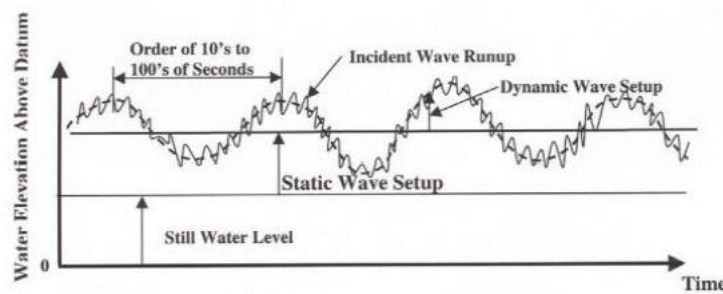


Figure 2.3 – Definitions of static and dynamic wave setup components [Source: (Dean et al., 2005)]

Due to the morphology of estuaries, swell waves cannot penetrate the interior through the inlet channel, as their energy dissipates within this configuration (Freire, 1999). The type of waves observed within these systems are primarily caused by local winds. While the Ria Formosa is not strictly an estuary, but rather a coastal lagoon system, it shares a similar morphology but with multiple inlet channels, leading to wave energy dissipation. In this context, the barrier islands act as barriers

where wave energy is dissipated, contributing to the creation of relatively calmer waters within the lagoon.

## 2.2.2 Physical Susceptibility

Physical susceptibility refers to the inherent characteristics of a coastal environment, including its natural features and geological attributes. These attributes can make it more or less prone to the impacts of rising sea levels.

The study area in Ria Formosa is dominated by the lagoon system, composed of barrier islands and tidal inlets, which form a protective layer to the intertidal wetlands. This translates to an area of sandy dunes immediately followed by a flat, low elevation area. Both in some of the barrier islands as well as the area immediately adjacent to the wetlands there are significant human settlements.

In order to evaluate the physical susceptibility of this system the main processes which will be discussed are sedimentation, coastal erosion, and coastline evolution.

### 2.2.2.1 Erosion, Sedimentation and Coastal Evolution

Coastal erosion and the consequent retreat of the shoreline are primarily influenced by two major factors: sediment deficit, or imbalance, and coastal forcing parameters (tides, currents, storm surges, and storm wave action). These factors differ significantly in terms of the temporal scale at which coastal erosion occurs. The sediment deficit, being a systemic process, operates on a larger time scale, spanning decades to centuries, with its effects not immediately noticeable in day-to-day life. Conversely, coastal forcing parameters are associated with extreme events that induce rapid and episodic erosion on the coast.

The combination of these two factors characterises the erosion experienced along most of the Portuguese coast over the last 60 to 100 years.

In addition to these factors, there is the secular variation of MSL on a longer timescale. The SLR results in systematic coastline retreat, while its fall leads to coastline expansion, as observed during glacial (decrease in MSL) and interglacial (rise in MSL) periods (Santo, 2022).

Another additional factor, distinct from natural processes, is artificial beach nourishment. This intervention has been implemented since the end of the 20th century to mitigate the effects of coastal erosion. It aims to compensate for sediment lost due to the sediment deficit.

The concept of sediment deficit requires an understanding of the sediment balance or budget. The sediment balance is defined as the difference between the volume of sediments entering in the system of a coastal section and the volume of sediments leaving the same system. Under normal circumstances, a positive sediment budget (where sources exceed losses) results in sediment deposition, leading to the advancement of the shoreline (accretion). Conversely, in a situation where the sediment budget is negative, the coastal stretch experiences sediment deficit, and the shoreline undergoes retreat (erosion).

Quantifying the sediment balance in a coastal stretch is a complex task that often involves estimating the order of magnitude, adjusting variables, and utilizing historical erosion/accretion or coastline advance/retreat data (Rosati, 2005).

Human activities and climate change can induce alterations in sediment budgets. For instance, dam construction and the subsequent reduction in river flows result in the diminished transport of sand by the rivers to the river mouth. This intensifies the coastal sediment budget deficit, reducing the availability of sand on coastal beaches and exacerbating erosion. Similarly, reduced average

precipitation can lead to a decrease in the amount of sediment transported to the sea by rivers, fostering a tendency for shoreline retreat (Andrade et al., 2006).

According to Lira et al. (2016), the coastline evolution of the Portuguese mainland from 1958 to 2010 reveals an overall erosion tendency for the low-lying sandy coast, with a mean rate of  $-0.24 \pm 0.01$  m/yr. Notably, the most significant contributors to this erosion are located on the west coast of Portugal, particularly in the stretches of Espinho - Torreira, Costa Nova - Praia de Mira, Cova da Gala – Leirosa, and Cova do Vapor – Costa da Caparica.

The southeast coast of Algarve exhibits a more complex evolution pattern, with sections experiencing erosion alternating with sections undergoing accretion, as seen in Figure 2.4. This pattern appears to be related to the morphological evolution of the tidal inlets in the Ria Formosa. Despite the variations in behaviour across these stretches, the mean rate of change for this section falls within the uncertainty range ( $+0.01 \pm 0.01$  m/year), indicating an overall balanced coastal sediment budget. The stretch of the coastline that corresponds to the boundaries of the Ria Formosa is currently experiencing an average erosion rate of  $-0.10$  m/yr.

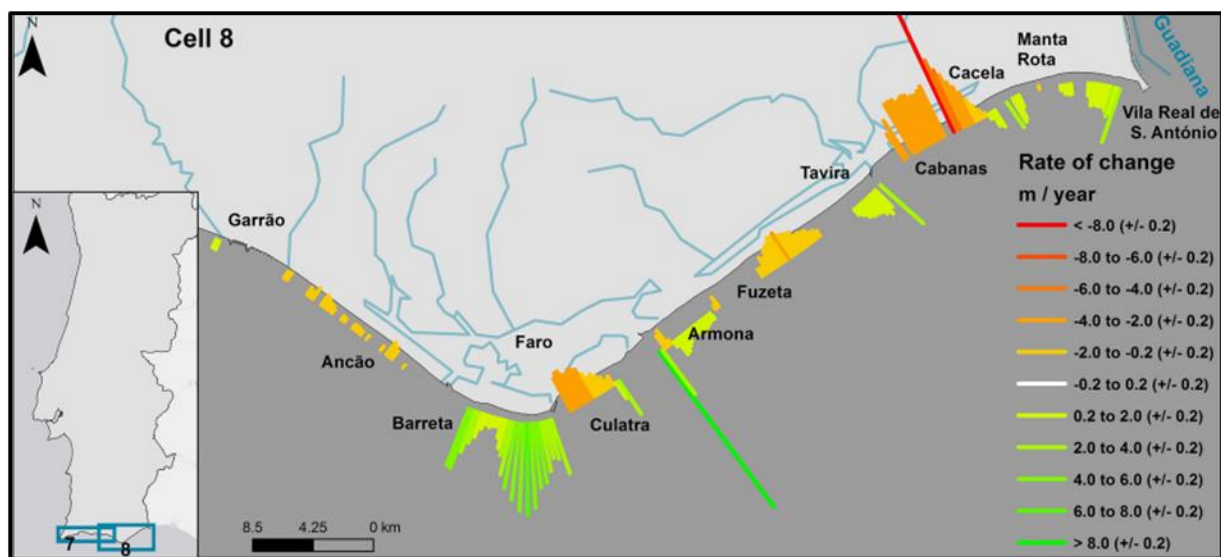


Figure 2.4 - Long-term coastline rates of change for the southeastern region of Portugal. Notable rates of coastline advance are seen in the Barreta Island and on the western end of the Armona Island. Coastline retreat is especially significant in the stretch between Cabanas Island and Cacela and on the western end of Culatra Island. [Source:Lira et al. (2016)]

Natural barrier island systems typically respond to sea level rise in one of two ways: either they wash over landward and remain intact, or they break up and drown in place. The specific outcome for a particular island is challenging to forecast with certainty, but island disintegration seems to be more prevalent in areas experiencing high rates of relative SLR, or high levels of hydrodynamic currents. Developed islands form a particular case for concern, as most are wider than the critical width required for island migration, leading to erosion from the ocean side and inundation from the bay side.

Moreover, human development tends to hinder landward migration. Structures disable the transport of sand toward the land, and after storms deposit sand onto streets, local public works departments typically redistribute it back onto the beach rather than allowing it to migrate naturally to the bay side. Consequently, even islands narrow enough to migrate landward under natural conditions may become narrower if there is no explicit decision to protect against ocean encroachment or fill part of the bay (Titus, 1990).

#### 2.2.2 Coastal Protection Measures

To counteract the impacts of coastal erosion stemming from both sediment deficit and coastal forcing parameters, coastal protection infrastructure is routinely implemented. These interventions aim to shield the coast from erosion or sediment loss. In Portugal, the most employed coastal protection measures are artificial beach nourishment and artificial protection structures (Pinto et al., 2018). Artificial beach nourishment involves depositing substantial amounts of sand on the shoreline (over the beach or under water levels), fostering expansion towards the sea, and enhancing volumetric and altimetric strength. On the other hand, coastal protection structures encompass the construction of significant structures such as groynes, breakwaters, adherent longitudinal structures (seawalls), and jetties. A notable concern associated with larger protections is their potential to disrupt sedimentation patterns, often leading to sedimentation deficits downstream (Bouhmadiouche & Hemdane, 2016).

Unlike artificial structures, beach nourishment is designed to offer a dynamic, more natural and flexible response that aligns with the inherent seasonality of the natural system and the rate of sediment deficit (Hamm et al., 2002; USAID, 2009). However, it is dependent on the sediment budget available nearby. It's important to note that any operation involving the deposition of sandy sediments in the coastal area, extending from depths of -10 m CD to the high beach at +10 m CD, is typically considered and categorised as artificial beach nourishment. In recent decades, artificial beach nourishment has been the preferred approach both in Portugal and globally.

In addition to its flexibility, artificial beach nourishment provides enhanced protection against ocean overtopping phenomena, potential flooding, and reduces the erosive effects caused by storms on the coastline and associated damage to structures. This protective capacity primarily stems from the greater effectiveness of artificial nourishment in dissipating wave energy compared to heavy artificial structures. Furthermore, sand nourishment has an immediate protective effect, allowing for the rapid restoration of the morphology of the beach-dune system. This contrasts with heavy coastal defence structures, whose collateral and reverse effects, such as the intensification of erosion downstream, become evident after some time (Martins & Veloso-Gomes, 2011).

In the context of climate change, beach nourishment is recognized as one of the most crucial measures to mitigate or reverse coastal erosion and overtopping phenomena, which are anticipated to worsen due to SLR and the heightened intensity of extreme storms (USAID, 2009). According to Nave & Rebêlo (2021) and Pinto et al. (2018), between 1950 and 2017, 134 artificial beach nourishment operations were recorded in mainland Portugal. Approximately 67% of these interventions were carried out on the western coast, with the remaining 33% on the southern coast of the Algarve. During this period, over 2,500,000 cubic meters of sand were artificially deposited along the southeastern coast of Portugal, with the regions of Tavira and Cabanas being the primary beneficiaries.

### **2.3 Socioeconomic Vulnerability**

Socioeconomic vulnerability refers to the degree to which individuals, communities, and economies are vulnerable to the impacts of SLR considering their intrinsic characteristics and living conditions. This concept recognizes that the impacts or consequences of SLR are not solely determined by physical factors but are also significantly influenced by societal and economic factors (Magnan et al., 2022).

Risk results from the intersection between hazard, susceptibility, and damage. Both physical and socioeconomic vulnerability are a part of risk. For instance, a piece of land may present a high physical vulnerability to SLR with low socioeconomic vulnerability if it holds little economic or social

significance. In contrast, another area may have lower physical vulnerability but, due to its high socioeconomic importance, presents a greater overall socioeconomic vulnerability.

Coastal hazards such as flooding, erosion and salinization pose a wide array of potential harm to people, settlements and activities including agriculture, tourism, fisheries, and aquaculture (IPCC, 2022). They can also harm the environment and ecosystems, such as the impact, even temporary, on some ecosystem services.

According to the IPCC (2014), approximately 2% of the world's land area is situated in low-lying coastal regions and houses a population exceeding 600 million people. In 2005, the total value of assets exposed to coastal flooding accounted for approximately 5% of the global Gross Domestic Product (GDP). Looking ahead to 2070, due to climate change, estimates suggest an increase to 9% global GDP. These costs are associated only with the direct costs related to damage inflicted on infrastructure and property (Nicholls et al., 2007).

Even under the assumption that the population of the low elevation coastal zone remains constant and without accounting for potential changes in natural and human-made coastal protection or shifts in storm patterns linked to extreme sea levels, the population residing below anticipated annual flood levels is projected to more than double in the event of a 1-meter global SLR (Kulp & Strauss, 2019). Considering the potential for additional coastal population growth, this figure is likely to be even higher.

Socioeconomic variables play a crucial role in contributing to coastal vulnerability and risk assessment, primarily because socioeconomic changes occur more frequently and rapidly than changes in physical processes (Szafsztein & Sterr, 2007). According to Boruff et al. (2005), determining the overall vulnerability of coastal areas requires the integration of social, economic, built-environment, and physical characteristics. Any coastal vulnerability assessment that neglects its social aspects is deemed insufficient because the occurrence and magnitude of coastal impacts from SLR depend on various future environmental and socioeconomic developments (Klein & Nicholls, 1999). Therefore, it is essential to incorporate socioeconomic data in these studies to assess the vulnerability associated with people living in coastal areas facing pressure from coastal hazards. These disasters only escalate into catastrophes when human lives are affected, making the inclusion of socioeconomic factors crucial for a comprehensive understanding of regional vulnerability (Murali et al., 2013).

In light of these risks, societal adaptation to climate change, and to SLR in particular, is recognized as essential, even at lower levels of warming (IPCC, 2022; Magnan et al., 2021, 2022). This highlights the need for the inclusion of socioeconomic vulnerability in risk assessments. Socioeconomic vulnerability results from the interaction between the socioeconomic susceptibility and the potential damage that a hazard can cause in that location.

### 2.3.1 Socioeconomic Susceptibility

Contrarily to physical susceptibility, socioeconomic susceptibility refers not to the intrinsic characteristics of a location but is entirely contingent on human occupation and activity.

The Ria Formosa is surrounded by urbanised areas, present both on the barrier islands and inland. It is home to many economical activities, some of which, like salt harvesting, aquaculture, and fishing, are extremely dependent on the characteristics of the lagoon. Tourism is the main source of income in the region and is also an activity that is highly dependent on the presence of beaches such as those found in the barrier islands.

In order to evaluate the socioeconomic susceptibility of this system this dissertation will follow a methodology similar to Antunes et al. (2019a), focusing on five essential variables to characterise the area: the population, infrastructure, transport network, land use and ecological areas. The following subchapters delve into each of these topics.

### 2.3.1.1 Population

Population data is crucial for comprehending the impact and scale of a natural disaster. Human susceptibility is viewed as a social condition or a measure of society's resilience to a disaster (Murali et al., 2013). Population density correlates with the level of socioeconomic development, and regions with varying population densities exhibit diverse impacts and responses to coastal erosion (Li et al., 2015). Generally, areas characterised by high population density are deemed highly vulnerable (Hegde & Reju, 2007).

Population pressure plays a pivotal role in coastal risk, as individuals in densely populated regions often take measures to safeguard their properties from erosion (Devoy, 1992; Dilley & Rasid, 1990) and flooding, as they are reluctant to abandon homes, land, and infrastructure developed over the years. Geographical areas with sparse populations may not face the same environmental pressure or possess comparable resources for protection (Mahapatra et al., 2014). Nevertheless, the population can also be seen as a direct "erosion-inducing" variable, as the presence of large numbers of people near the coast can have detrimental impacts on the coastal zone (McLaughlin et al., 2010).

Gornitz et al. (1994) excluded population from vulnerability calculations but acknowledged that future studies should incorporate coastal populations to enhance the risk assessment of vulnerable areas. More recent studies focusing on socioeconomic susceptibility include population or population density as a crucial variable (e.g. Behera et al., 2019; Bera & Maiti, 2021; De Serio et al., 2018; Furlan et al., 2021) for risk estimation.

### 2.3.1.2 Infrastructure

Infrastructure is strategically positioned and influenced by the concentration of properties crucial to society, whether they are public institutions like hospitals, public safety facilities, and schools or private entities. The relocation or repair of such infrastructure incurs significant costs due to their active importance within the community.

In addition to these critical facilities, private properties owned by citizens or cultural heritage sites are sometimes integrated into studies under the broader category of infrastructure (Ferreira et al., 2021; Zhu et al., 2019). Alternatively, they may be considered as a distinct category of their own (Bagdanavičiūtė et al., 2019; Kantamaneni et al., 2018).

Infrastructure plays a pivotal role in estimating the risk to a coastal area. The location and density of essential societal assets impact the overall socioeconomic susceptibility of a region. The potential damage or disruption to these facilities during coastal hazards can have far-reaching consequences, both in terms of economic costs and societal well-being. Therefore, a comprehensive assessment of coastal risk must consider the critical role of infrastructure in shaping the overall vulnerability and resilience of the area.

### 2.3.1.3 Transportation Network

The transport network is a crucial socioeconomic factor for assessing coastal vulnerability and risk, particularly in terms of local accessibility concerning the distance from cities and vital transport infrastructures such as railways, roads, bridges, highways, parking lots and stations. In coastal settlements, this often also includes port infrastructure and the navigation network. This information is

essential for understanding the spatial distribution and clustering of human settlements and structures, playing a key role in quantifying damages to human life, services, and economies. Immediate effects resulting from events like inundation or surges are critical considerations in this evaluation (De Serio et al., 2018).

Transport networks function as vital communication lines and primary means of mobility for the population, facilitating the distribution networks of goods, equipment, and services. However, their high construction, maintenance, and repair costs make them susceptible to financial strain when partially destroyed or damaged in coastal areas, necessitating substantial financial efforts (McLaughlin et al., 2010). Moreover, road networks prove to be indispensable during natural calamities, serving critical roles in emergency response efforts and enhancing early warning systems. Disruptions in these networks can lead to resource scarcity, significantly magnifying the impact of calamities (Murali et al., 2013; Rocha et al., 2023).

#### 2.3.1.4 Land Use

Land use is a critical factor influencing coastal susceptibility, reflecting various morphological behaviours, ranging from natural vegetation cover to paved areas, exposed soil, or agricultural areas. The degree of change in the natural state of land covering is considered indicative of susceptibility, with greater changes implying higher susceptibility (Li et al., 2015). Understanding land use and land cover classes in a specific region is paramount for assessing vulnerability, with anthropogenic activities and climate changes contributing to the evolution of land use/land cover patterns (Murali et al., 2006).

Moreover, the types of land use/land cover play a significant role in determining coastal vulnerability. Protection considerations are influenced by the economic, cultural, or environmental importance of an area. According to McLaughlin et al. (2002), vulnerable areas are those deemed “important” in economic, cultural, or environmental terms, justifying protection efforts. Assessable value variables, including economic value, provide insights into the locations of economically valuable areas. The value of land use and land cover can be defined in various ways, such as monetary terms, replacement cost, aesthetic terms, or conservation value.

#### 2.3.1.5 Ecological Areas

The Ecological Classification focuses on environmentally protected areas with clearly defined geographic spaces, established, and managed through legal processes or effective means to ensure long-term preservation (Laffoley et al., 2019).

This assessment parameter does not consider the environmental impact of risk to ecological areas, but rather their value in terms of economic benefits (i.e. increased property values, touristic attractivity). As such, in this dissertation the classification will encompass not only protected areas but also urban green spaces.

A more in-depth assessment of the environmental vulnerability will be explored in chapter 2.4.

#### 2.3.2 Socioeconomic Damage

In the aftermath of any natural disaster, evaluating the economic damage incurred is not only imperative but also poses an academic challenge. This assessment usually occurs post-event or amid an ongoing emergency. However, conducting damage assessments rooted in hazard predictions provides an avenue for implementing potential policy measures aimed at future mitigation (Hayashi, 2012).

In the context of coastal risk, measuring socioeconomic damage is an intricate process involving various variables from both social and economic perspectives. While these variables are often quantifiable, they might pose challenges in terms of accessibility due to data availability restrictions, as well as spatial resolution (region, district, municipality, parish, or neighbourhood).

A considerable amount of literature has concentrated on incorporating economic variables into indices to indicate heightened risk in areas with substantial economic value. However, most of these efforts fall short of providing a direct quantification of monetary damage. Kantamaneni et al. (2018) and Zhu et al. (2019) both utilize GDP and fiscal revenue as factors but introduce indices that do not directly calculate damage; instead, they incorporate it as a vulnerability factor or a separate vulnerability index. Similarly, Satta et al. (2017) employs economic figures to express sub-indices of vulnerability and exposure.

In a more detailed exploration, Thatcher et al. (2013) goes beyond GDP figures by providing actual monetary loss ranges associated with different building types and their locations. However, despite the availability of this information, it is not integrated with hazard and vulnerability data to derive a comprehensive estimate of potential damage; once again, it is only included as a factor in indices. Taking a step further, Barros et al. (2022) identified the infrastructure at risk with specific methodologies for each class. Unfortunately, a methodology to calculate damage is absent in this study as well.

Antunes et al. (2019a) introduced a methodology for estimating damage to apply in Loulé's municipality coastal risk assessment. Such methodology consisted in creating a Coastal Socioeconomic Value Index (CSV). This index comprises five parameters explored in the socioeconomic vulnerability, with the contribution of each parameter weighted using the Analytic Hierarchy Process (AHP) (Saaty, 1988) based on a survey conducted among Specialists and Non-Specialists.

The damage parameter was derived using the municipal realty tax code (*CIMI – Código do Imposto Municipal sobre os Imóveis*) outlined in the Portuguese national law by Law-Decree n.<sup>o</sup> 287/2003 (*Decreto-Lei n.<sup>o</sup> 287/2003*). The formula was adapted to the project needs, being able to use either census data or building footprint data as the bases for the damage calculation.

This dissertation will aim to replicate and apply the methodology proposed by Antunes et al. (2019a) to provide a damage estimation for the affected area.

## 2.4 Environmental Vulnerability

The loss of land and ecosystems is of particular concern worldwide, yet quantifying this loss remains challenging due to uncertainties surrounding local ecosystem and shoreline responses to rising seas, as well as uncertainties regarding how effectively humans will safeguard shorelines (Hinkel et al., 2014).

In the face of SLR, crucial ecosystem services may be compromised, particularly if coastal defences and human infrastructure disable the natural adjustment capacity of coastal ecosystems, for example, by hindering inland migration (IPCC, 2022; Schuerch et al., 2018; Titus, 1990). The loss of coastal protection services (Beck et al., 2018; Duvat, 2019) is of paramount importance, given that mangroves, corals, saltmarshes, and seagrass meadows currently play a critical role in shielding hundreds of millions of people worldwide from storm surges and waves (Chaplin-Kramer et al., 2019; Van Coppenolle & Temmerman, 2020).

For instance, considering the RCP 8.5 scenario (IPCC, 2021) by 2100, a 1-meter reduction in coral reef height would more than double the global area susceptible to flooding during a 100-year event

(Beck et al., 2018; Magnan et al., 2021). This underscores the profound implications of ecosystem service loss on coastal resilience and the urgent need for comprehensive strategies to address these vulnerabilities.

A notable gap exists in the literature when it comes to recognizing ecological coastal risk as a distinct entity, as highlighted in the reviews conducted by Nguyen et al. (2016) and Rocha et al. (2023). These assessments of indices for coastal vulnerability underscore a prevalent absence of ecological variables in the existing literature. Notable studies, including those by Peduzzi et al. (2002) and Kubal et al. (2009) simply attempt to incorporate an environmental parameter as part of their socioeconomic analysis, as seen in chapter 2.3.1.5.

Yusuf & Francisco (2009) attempted to consider biodiversity-protected areas at risk of coastal flooding by employing a binary value approach. However, this method utilized biodiversity protected areas simply to distinguish between areas with equal socioeconomic vulnerability. In this context, the protected area was identified as more vulnerable than the non-protected area. ATEAM (2004) investigated the response of different land coverages, including ecological areas, to climate change but without quantifying these findings in a vulnerability assessment.

Meyer et al. (2009) pursued a more intricate approach in measuring environmental risk, particularly for river flooding impacting ecological systems. Nevertheless, their vulnerability values were determined through binary responses to three selected variables, which given the similar characteristics of the whole study area did not allow for much differentiation beyond the flooding levels. Torresan et al. (2008) explored coastal vulnerability in an environment protected by barrier islands, considering wetland migratory potential. However, the Ria Formosa presents a unique scenario, where the ecosystem is already stressed by nearby urban areas. In this context, the likelihood of urban areas being abandoned for ecosystem migration is highly improbable.

In this dissertation, a new index will be introduced to assess environmental vulnerability, aiming to independently evaluate the vulnerability and resultant damages inflicted on natural areas due to rising sea levels, focusing specifically on ecosystem services. As such, in the upcoming chapters, the ecosystems of Ria Formosa will be explored, along with an examination of the theory of ecosystem services. The new methodology will be thoroughly presented in chapter 3.6.

#### 2.4.1 Environmental Susceptibility and Intertidal Ecosystems

In the context of this environmental vulnerability assessment, environmental susceptibility constitutes the propensity of the system to withstand and adapt to the hazard. As ecosystems are more adaptable than urbanised areas to extreme flooding scenarios, the major hazard here will be the mean SLR without the extra coastal forcing parameters.

Environmental susceptibility in this context is then intrinsically linked to the type of intertidal habitat and its characteristics.

This dissertation will examine these ecosystems: intertidal flats, saltmarshes and sand dunes. Saltmarshes can be further divided into low marsh and high marsh. These ecosystems serve as transitional zones between the sea and land, situated in intertidal areas. Dunes typically manifest as mounds or hills, formed through the deposition of sand by wind or water, from land or sea reservoirs. In contrast, flat surfaces with intricate canal systems characterise mudflats and saltmarshes, serving as drainage and sediment deposition networks, subtly sloping toward the maritime boundary (Silva, 2013). Distinguishing these ecosystems involves analysing sediment granulometry, elevation, and the prevalent vegetation (Inácio, 2017). A visual representation of these ecosystems, highlighting their distinctive features, is provided in Figure 2.5.

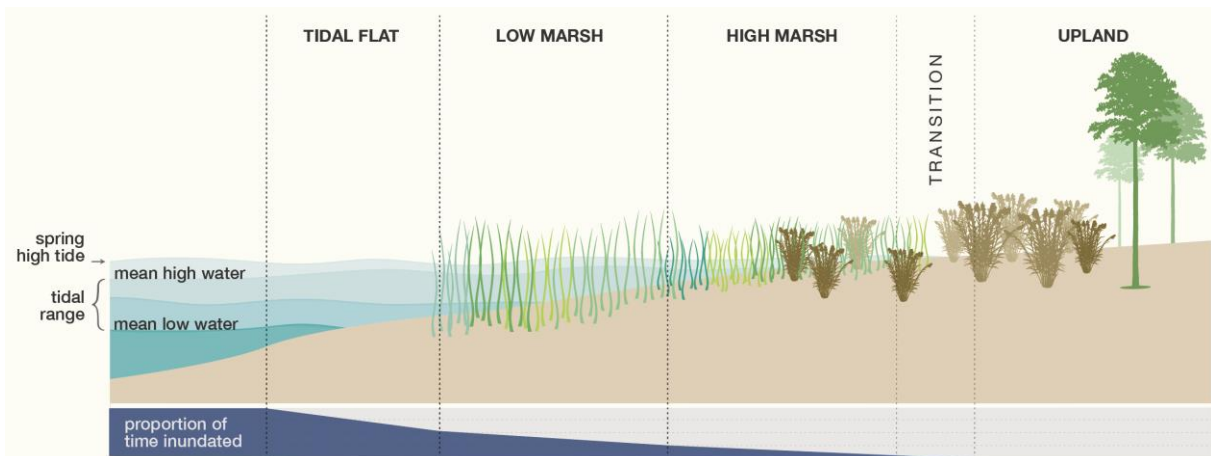


*Figure 2.5 - Segmentation of the intertidal zone. As elevation rises and time inundated diminishes, subtidal environments give way to tidal flats, low marsh, high marsh and finally an upland region. Transition zones have mixed characteristics, with dunes being an example of such areas [adapted from: <https://www.chesapeakequarterly.net/>].*

The rationale behind selecting these environments is grounded in their significant ecological roles:

- Their function as essential sites for feeding, refuge and nidification of various bird species.
- The value they offer as a study area for analysing coastline evolution, recognizing significant climate changes, and identifying sea level variations, due to their specific sedimentation processes (Silva, 2013).
- Their wave and tidal energy dissipation capacity, which serves as a natural protective barrier against SLR and extreme weather along the coast (Inácio et al., 2022).
- Their critical role in mitigating climate change impacts. The reduction or destruction of these areas may contribute to increased CO<sub>2</sub> emissions to the atmosphere, or reduction of carbon storage. The destruction of wetlands accounts for 3–19% of the increase in CO<sub>2</sub> emissions related to deforestation (Pendleton et al., 2012). This emission increase is attributed to the release of organic carbon stored in these environments, commonly referred to as blue carbon (Laffoley & Grimsditch, 2009). Additionally, the carbon stored in European saltmarshes alone represents 4% of all carbon accumulated in coastal areas (Luisetti et al., 2013).

The subsequent subchapters will delve deeper into each of the intertidal ecosystems to understand their differences. This will be essential for the environmental susceptibility index which will be proposed in chapter 3.6.1.

#### 2.4.1.1 Intertidal Mudflats

Intertidal mudflats, characterised by very sparse or absent vegetation, represent sedimentary accumulation environments within the intertidal zone. Typically found along the shorelines of bays, estuaries, lagoons, barriers, and deltas, they thrive in areas with low current strength. These mudflats can extend to oceanic shorelines associated with low energy and minimal wave action, forming low tide terraces (Inácio, 2017).

These shallow, nearly flat surfaces exhibit a low altimetric gradient and are predominantly influenced by tidal movements, although wave action can be influential in specific circumstances. Tidal variations lead to the rise and fall of water levels, driving the inflow and outflow of water in estuaries or lagoon systems during flood and ebb tides. The resulting currents, ranging from a few centimetres to one meter per second, play a crucial role in shaping these environments (Davis & Dalrymple, 2012).

The extent of intertidal mudflats is contingent on factors such as tidal range, local morphology, and sediment availability. Larger tidal ranges, lower gradients, and increased sediment supply contribute to a greater expanse, with macrotidal conditions resulting in the maximum extension. Sediment sources, whether from rivers, the marine environment, cliff erosion, or internal sediment resuspension, further influence the tidal flat's dimensions.

These tidal flats experience vertical accretion up to the level of Neap Mean High Tide (NMHT) locally, situated above the MSL. Beyond this point, the flats tend to be colonized by vegetation, transforming into saltmarsh areas (Allen, 2000). The flat surface is often intersected by meandering channels, forming a network reminiscent of river systems. Notably, water flow within these channels occurs bidirectionally—toward land during flood tide and toward the sea during ebb tide.

#### 2.4.1.2 Saltmarshes

Saltmarshes are characterised as intertidal areas featuring fine sediment transported by water and stabilized by vegetation (Boorman, 1995). Comprising vegetation that can tolerate the salinity of the surrounding water, saltmarshes are integral components of estuarine, coastal, and occasionally lagoon systems, particularly prevalent in middle latitudes. They span from polar zones to subtropical regions (between 30° N and 30° S), where they give way to mangroves. Mangroves, distinguished by their tree-dominated composition, represent tropical intertidal zones. Despite variations in vegetation, saltmarshes and mangroves share similar ecological complexities (Chmura, 2009).

Saltmarshes' formation and maintenance depends on processes and inputs of larger systems where they are inserted. They function as sediment banks within estuaries or bays, typically accumulating very fine sediments with significant absorption capacity. This unique property allows saltmarshes to retain and neutralize suspended or diluted pollutants in the water through their plant life (Gonçalves, 2016). The collective elements of saltmarshes work synergistically to filter, retain, and degrade various substances. Consequently, saltmarshes are essential for reducing water pollution levels in the estuaries or bays to which they are connected. Numerous studies have demonstrated their ability to effectively retain pollutant compounds, including herbicides, pesticides, and heavy metals (e.g. Almeida et al., 2011; Boorman, 1999; Giuliani & Bellucci, 2019). The presence of these pollutants, often attributed to human activities, poses environmental risks when they persist in estuarine and river waters.

Furthermore, saltmarshes (along with mangroves) are widely acknowledged for their substantial contribution to coastal defence by dissipating wave energy and temporarily storing floodwater (Inácio et al., 2022). The existence of saltmarshes significantly reduces the expenses associated with maintaining coastal fronts, requiring less robust protection structures. Though it is important to note that their protection effectiveness diminishes under extreme maritime agitation conditions. Nevertheless, the intrinsic value of saltmarshes as a natural, functional, and sustainable form of protection is widely recognized (Gonçalves, 2016).

The saltmarsh stands out as one of the most productive zones in the biosphere, particularly in biomass production. Nutrients naturally reach this environment through the constant ebb and flow of tides, sediment transport from the continental zone, settlement of living organisms (such as birds, fishes, molluscs, and other animals), and decomposition processes. Comprising a marshy substrate of silt and clay, saltmarshes host plants adapted to the salinity levels typical of brackish and salty water (Allen, 2000).

As described by Inácio (2017), the surface of a saltmarsh tends to be flat and almost horizontal, intersected by channels inherited from the intertidal mudflats. Within saltmarshes, two distinct zones can be identified: the high marsh and the low marsh. The relationship between vegetation and local

tide boundaries is crucial, with specific flora species being conditioned by the duration of tidal immersion, which is related to its salt tolerance. Elevations below the NMHT level experience prolonged immersion, hindering vegetation maintenance and constituting the upper limit of the intertidal mudflat. Levels compatible with the characteristic vegetation of the low marsh range from NMHT (lower) to Mean High Tide (MHT) (upper). In contrast, the high marsh's characteristic vegetation extends from MHT (lower limit) to Spring Mean High Tide (SMHT) (upper limit).

The vegetation within saltmarshes is highly specialized, requiring specific conditions to thrive in this unique environment. Tidal dynamics significantly influence saltmarshes, with water levels submerging portions of the marsh and its plant inhabitants. These plants must possess the ability to withstand periodic submersion for varying durations, depending on the tidal cycle. As a result, saltmarsh vegetation is exposed to rapid fluctuations in salinity levels, a challenge that most species are unable to endure. The plant species adapted to such conditions are referred to as "halophytes," exhibiting distinct adaptations to their surroundings (Gonçalves, 2016).

The low marsh represents the portion of the saltmarsh that experiences prolonged submersion, typically ranging from 7 to 11 hours per day and becoming exposed only during low tide. Positioned between the average level of NMHT and the MHT, or slightly above it, this zone is characterised by pioneer plant formations. Among these, saltmarsh grass (*Spartina maritima*) stands out as the most representative species, demonstrating resilience to extended submersion periods (Costa, 2001). Additionally, formations in the low marsh often include aquatic plants like eelgrass (*Zostera noltii*), seagrass (*Zostera marina*), and plants from the genera *Potamogeton* and *Ruppia*, along with some algae species (Gonçalves, 2016).

The high marsh is characterised by shrubby or shrub-tree vegetation, usually less than 1 meter in height, occupying the emergent soils of SMHT platforms. During tidal phases, this zone experiences a submersion period lasting a maximum of 10 hours per day (Moreira, 1987). Notably, the high marsh undergoes significant salinity variations, influenced by rainwater reducing salinity and sequences of submersion and water evaporation, which increase salinity levels. In Mediterranean climatic conditions, a crystalline layer of salt can form on the soil surface.

Within the high marsh, where salty and freshwater mix, earlier species gradually give way to the sea rush (*Juncus maritimus*) and three-cornered bulrush (*Bolboschoenus maritimus*, *Scirpus maritimus*). As the proportion of freshwater increases, characteristic hygrophytes of marshes begin to appear, including the common club-rush and the common reed (*Phragmites australis*). The tamarisk shrub (*Tamarix africana*), occurs at the transition to terrestrial environments (Gonçalves, 2016).

Human activities and climate-induced changes in external factors pose threats to the delicate systems of saltmarshes, endangering the crucial services they offer. Globally, extensive regions of saltmarshes have undergone conversion into agricultural land, industrial areas, or port facilities, contributing to significant losses despite recent reductions in such transformations for alternative purposes (Davy, 2009).

#### 2.4.1.3 Dunes

Coastal dunes are dynamic, intricate ecosystems with unique functionality and significant ecological value. These ecosystems take shape along low-lying coastal margins, where the interplay of sand carried by oceanic waves and wind, along with the presence of vegetation, gives rise to dynamic geomorphic structures. In regions outside arid areas, coastal dunes tend to be partially vegetated, fostering a complex system characterised by feedback loops among vegetation types, sediment

dynamics, and dune morphology (Hesp, 2004). Dunes can occur at all latitudes on earth but comprise a relatively limited global area (Hardisty, 1994).

The frontal portions of coastal dunes exhibit dynamical connections with the nearby beach, contributing sediment during erosion events typically associated with storms. Inland sections beyond the reach of periodic wave erosion may undergo stabilization through vegetation or continue evolving influenced by wind action (Jones et al., 2008).

Coastal dunes exhibit a rich ecological diversity with variable species composition, featuring characteristic vegetation that includes unique species adapted to environmental conditions (Kutiel, 2001). Unfortunately, due to significant anthropogenic pressures on coastal areas, particularly coastal dunes, many of these ecosystems and their hosted species face global threats, demanding conservation efforts in numerous countries (Doody, 2012). Among the most severe threats to coastal dunes are degradation and negative impacts from the expansion of invasive species (e.g. Conser & Connor (2009); Vallés & Cambrollé (2013)).

Beyond being specific habitats, coastal dunes are integral components of the larger dynamic coastal sedimentary system. Consequently, they are influenced by a multitude of variables and processes, including littoral sediment budgets, wave and wind climate, tidal regimen, and sediment characteristics (Delgado-Fernandez et al., 2019). This complexity results in diverse physical dune forms, creating a variety of habitats at various stages of maturity within individual dune fields and between different locations.

Coastal dunes have a long history of human interaction, initially utilized for their shelter and foraging resources, and later for their agricultural and grazing potential. Unfortunately, their proximity to coastal settlements has led to the destruction of many dunes, either through construction or mining activities (Feagin et al., 2005). Van der Meulen & Salman (1996) noted that 75% of Mediterranean coastal dunes had been damaged or destroyed in the previous 30 years. In the broader European context, 25% of coastal dunes have been lost since 1900, and 55% of the remaining coastal dune area has seen a decline (Heslenfeld et al., 2004). Consequently, there has been a significant emphasis on the conservation of existing coastal dunes, driven in part by the essential ecosystem services they provide (Cooper & Jackson, 2021; Everard et al., 2010).

#### 2.4.2 Ecosystem Services

The Convention on Biological Diversity (United Nations, 1992) defines biodiversity as “*the variability among living organisms from all sources, including terrestrial, marine, and other aquatic ecosystems, and the ecological complexes of which they are part. This includes diversity within species, between species, and of ecosystems.*”

This encompassing definition demonstrates that biodiversity extends to diversity within species populations, the number of different species and the diversity of ecosystems. Understanding the intricate connections between nature, economic activity, and human well-being requires evaluating the various dimensions of biodiversity (TEEB, 2010).

Human economy, health, and survival rely extensively, though often indirectly, on natural resources (Reid et al., 2005). A wide array of advantages can be derived from the resources and processes provided by natural ecosystems, collectively referred to as ecosystem services (Inge et al., 2013).

The Millennium Ecosystem Assessment (2005) first proposed a globally recognized definition for ecosystem services, “*the functions and products of ecosystems that benefit humans, or yield welfare to society*”. The Economics of Ecosystems and Biodiversity project (TEEB, 2010) built upon that

assessment and introduced an updated classification that clearly separates ecosystem services from benefits. According to TEEB, ecosystem services are "*the direct and indirect contributions of ecosystems to human well-being*," emphasizing that services can have multiple indirect benefits for people.

The Millennium Ecosystem Assessment proposed a classification encompassing four categories of ecosystem services, each rooted in biodiversity (Millenium Ecosystem Assessment, 2005):

- Provisioning Services: Products obtained from ecosystems, including food, fresh water, wood, fibre, genetic resources, and medicines.
- Regulating Services: Benefits derived from the regulation of ecosystem processes, such as climate regulation, natural hazard regulation, water purification, waste management, pollination, and pest control.
- Cultural Services: Non-material benefits, such as recreation, spiritual and aesthetic values, and education, that people obtain from ecosystems.
- Supporting Services: Essential functions within the ecosystem, including soil formation, photosynthesis, and nutrient cycling, supporting the overall diversity within the ecosystem.

Decisions regarding natural resources are commonly influenced by the values humans attribute to ecosystems and the associated benefits (Daily et al., 2009). This becomes especially crucial in biodiversity conservation, where a clear definition of service units facilitates their identification, mapping, and measurement across diverse ecosystems. Standardized assessments of ecosystem services serve as the foundation for enhancing environmental policies (Lele et al., 2013).

Ensuring the continuation of ecosystem services and, consequently, long-term human well-being, requires the preservation of nature. This entails gaining a thorough understanding of how ecosystems function, deliver services, and the intricate interplay between biodiversity and the supply of ecosystem services, including the resilience of ecosystems in the context of changing conditions, particularly climate change. Under the current climate change trend, numerous ecosystems are nearing critical thresholds, potentially jeopardizing their capacity to provide essential services, elevating the necessity to adopt a precautionary approach to safeguarding healthy ecosystems and sustaining the continuous provision of ecosystem services in the long run (TEEB, 2010).

The anticipated global climatic changes, including temperature increase, sea level rise, and changes in precipitation patterns and extreme weather events, are expected to have varied and region-specific impacts on coastal lagoons (IPCC, 2022). Due to their shallow depth, coastal lagoons are particularly vulnerable to temperature increases, influencing vital biological processes (Lloret et al., 2008). Elevated water temperature can lead to decreased levels of dissolved oxygen, crucial for many organisms, posing risks to the services offered by coastal lagoons. SLR is another significant factor with potential impacts, affecting light availability at the bottom, potentially disrupting benthic primary producers and altering the food web structure (Brito et al., 2012). Changes in precipitation pattern can impact watershed runoff and erosion, resulting in increased sediments and pollutants entering coastal areas (Anthony et al., 2009). In regions with decreased precipitation, reduced freshwater input can cause extreme changes in salinity regimes, water circulation, and flushing rates in coastal lagoons (Lee & Park, 2013). These changes in precipitation patterns will also influence freshwater and nutrient inputs carried by rivers, subsequently affecting lagoon biogeochemistry (Solidoro et al., 2010) and provisional services (Newton et al., 2018).

Understanding the potential impact of hazards on ecosystem services provides a valuable means to quantify nature's vulnerability. The preservation of healthy ecosystems, guided by a thorough

understanding of their functioning and resilience, remains crucial for ensuring the continuous provision of essential ecosystem services.

### **2.4.3 Environmental Damage**

Valuing biodiversity and the related ecosystem services has become an increasingly crucial aspect of effective conservation and development policies (TEEB, 2010).

Initially, biodiversity valuation studies primarily concentrated on assessing the value of individual species or habitats (Nunes & van den Bergh, 2001). Contemporary research has embraced a more comprehensive perspective, employing an ecosystem services approach for biodiversity valuation (Christie et al., 2012).

Ecosystem services encompass the social, economic, and ecological benefits of biodiversity, however, the majority of research on valuing biodiversity has concentrated on its economic benefits (Farber et al., 2002). Measuring ecosystem value in monetary terms facilitates decision-making, enabling a direct comparison between the benefits of maintaining biodiversity and the associated costs.

Pearce (1993) introduced the concept of total economic value (TEV), as a method to encompass all the components of utility which can be derived from ecosystem services. This value can be expressed as a monetary amount or any other market-based unit of account. TEV encompasses the following notions of value (Häyhä & Franzese, 2014):

- Market Value – Value of a commodity in the open market
- Direct Use Value – Value of products and services provided by nature for direct consumption or human activities.
- Indirect use value – Value attached to indirect utilization of ecosystem services (e.g. flood protection, carbon sequestration).
- Intrinsic Value – Value of environment and life forms present in it.
- Existence value – Value attached to the knowledge that species, natural environments and other ecosystem services exist even if they are not actively being used by humans.
- Bequest Value – The willingness to pay to preserve the environment for present use.
- Option value – The willingness to pay to preserve the environment for future use.

While TEV serves as a widely used framework for valuing economic benefits derived from biodiversity, it has limitations and may not encompass all its benefits. Biodiversity contributes to numerous ecological processes, including the maintenance of essential life support through soil formation and nutrient cycling. However, the complexity and indirect nature of these benefits often make them challenging to express through monetary valuation techniques, demanding the use of non-monetary methods to fully appreciate their importance (Farber et al., 2002).

Various techniques have been employed to measure the economic, social, and ecological benefits stemming from biodiversity and associated ecosystem services. Table 2.1 provides a short summary of monetary and non-monetary approaches to valuing biodiversity.

Monetary approaches offer a means to quantify the economic value of various elements within TEV. However, their application can be particularly challenging, especially when dealing with complex ecosystem services. In such cases, researchers have turned to non-monetary approaches to gauge people's preferences for biodiversity, employing methods detailed in Table 2.1. While these methods may not yield monetary valuations of biodiversity, they provide valuable insights into the significance of biodiversity to individuals in ways that monetary approaches may not capture (Christie et al., 2012).

*Table 2.1 - Summary of methodologies used to determine the value of ecosystems, considering both Monetary and Non-Monetary Approaches and the different types of Valuation and Methodology. [Adapted from: Christie et al. (2012)]*

	<b>Valuation Approach</b>	<b>Methodology</b>	<b>Description</b>	<b>Examples of Application</b>
Monetary Approaches	Market Price Approach	Market Prices	Uses prices from markets related to environmental goods as a proxy for value.	Turpie, 2003
	Market Cost Approaches		Uses costs from a market good related to the environmental good as a proxy for value.	
		Replacement Cost	Cost of replacing an environmental service	Möller & Ranke, 2006
		Damage Avoided Cost	Cost of mitigating environmental damage	Barbier, 2007
		Production Function Approach	Cost of an environmental service to the production of a marketed good	Barbier, 2007
	Revealed Preference Method		Uses observations from markets related to the environmental good to measure value	
		Travel Cost	Cost of travel to a natural resource is used to evaluate the recreational benefits of that resource.	Shrestha et al., 2002
		Hedonic Pricing Method	Measures value through observations in a related market: usually house price	Nicholls, 2019
	Stated Preference Methods		Estimates value by asking survey respondents to report their willingness to pay (WTP) to obtain a specified good, or willingness to accept (WTA) to give up a good	
		Contingent Valuation	Measures WTP for a single policy option	Turpie, 2003
		Choice Modelling	More complex contingent valuation, allows values of the attributes of the policy to be assessed.	Christie et al., 2006
Non-Monetary Approaches	Participatory Approaches to Valuation		Joins Stated Preference Methods with deliberative processes from political science.	
		Deliberative Valuation	Value determined by participants collecting information, reflecting, and participating in group activities.	Bunse et al., 2015
		Habitat Equivalency Analysis	Calculates the service losses and the scale of restauration projects to compensate the public.	Dunford et al., 2004
	Value Transfer	Value transfer	Infers economic value from information collected at another location.	Gaodi et al., 2010
	Consultative Methods		Uses inquiries into people's perceptions of an environmental issue	
		Questionnaires	Focus on gathering quantitative data	Struhsaker et al., 2005
		In-depth interviews	Focus on gathering qualitative data	Gareau, 2007
	Non-Monetary Participatory Approaches		Uses group-based activities and participatory approaches to attain detailed information about people's relationship with the natural environment.	
		Participatory Rural Appraisal, Participatory Action Research	Used in developing countries, promotes knowledge and enables local people to make their own appraisal, analysis, and plans.	King & Faasili, 1999
		Citizen Juries	Involves a court-like process in which participants review evidence and make judgements on the future of the environmental good	Kenyon et al., 2001
		Health-Based Approach	Measures the contribution of the environmental good to health-related factors on the quality and length of a human life.	Doctor et al., 2004

Inge et al. (2013) introduced a methodology for valuing ecosystem services in estuaries, covering various services and outlining the required information for calculating their value. Additionally, it

provided a comparative analysis of different land use classes within an ecosystem, ranking their diverse contributions to various ecosystem services. This allows for an analysis that encompasses both a monetary and non-monetary approach.

Van der Biest et al. (2017) applied a comparable methodology to assess the economic loss associated with fixed dunes compared to dynamic dunes. The study conducted an in-depth analysis of the ecosystem services provided by each type of dune, evaluating the costs through factors such as taxes on groundwater extraction, drinking water prices, estimated societal benefits from nitrogen retention, expenses related to dyke maintenance and adaptation to rising sea levels, carbon storage capacity, and recreation.

The objective of this dissertation was to establish a framework for applying a similar methodology, in any geographic context that contains estuarine zones or other internal waters, addressing the existing gap in literature. The focus of the study is on non-monetary valuation rather than monetary valuation, given the limited availability of such information for the Portuguese coast. The approach involves adapting the methodology introduced by Inge et al. (2013), utilizing a consultative method with specialist input. As the sea levels rise, certain habitats will face environmental pressure but possess the capacity to adapt, such as a high saltmarsh transitioning to a low saltmarsh or a low saltmarsh becoming an intertidal mudflat. As such, the methodology needs to account not only for the ecosystem value of each specific ecosystem but also how much each area will change. This adaptation is necessary because although the ecosystem services provided by each habitat differ, the hazard impact may not result in a complete loss.

## 2.5 Exposure

Exposure is a key concept of risk assessment, encompassing the location, attributes, and value of assets crucial to communities, including people, buildings, factories, farmland, and more, that may be harmed by hazards. The significance of exposure lies in its direct correlation with risk—if an area lacks exposure to a hazard, the risk is minimal (IPCC, 2022; Satta et al., 2017).

Following the characterisation of risk in chapter 2.1, exposure can be interpreted as being a combination of all the physical, socioeconomic, and environmental assets that can be impacted by a hazard:

$$CRI = CHI \times Coastal\ Exposure\ Index\ (CEI) \quad (2.5)$$

Where:

$$CEI = PSI \times SSI \times SDI \times ESI \times EDI \quad (2.6)$$

Various factors contribute to the dynamic nature of exposure. Processes like population growth, migration, urbanization, and economic development concentrate people and assets in hazard-prone areas. Disasters can force people to relocate from increasingly unsafe regions, altering exposure over time. Hazard-prone areas, like coastlines and floodplains, attract economic development, increasing the value of exposed assets (UNISDR, 2004, 2009).

Measuring exposure involves considering the number of people and types of assets and respective intrinsic value in the hazard area. Combining exposure data with vulnerability and capacity assessments provides a basis for quantitative risk estimation associated with specific hazards. Exposure modelling plays a critical role in risk assessment, using data from diverse sources and methods.

Addressing the upward trend in economic exposure in high-hazard areas is crucial for mitigating risk. Effective strategies include land use planning, location decisions, structural and non-structural measures, and early warning systems to minimize the impact of exposure on disaster risk.

The quantification of the damage that a certain natural hazard can cause results from the combination of the physical, socioeconomic, and environmental susceptibilities and the assets valuation of a certain area. Obtaining the damage parameter with maximum accuracy can be highly challenging due to its association with dynamic and occasionally volatile costs or market values (Cardona et al., 2012).

While exposure is intrinsically related to many other topics explored in this dissertation, coastal exposure indices will not constitute part of the products. This is due to the methodology applied for the physical vulnerability not allowing for a dissociation of physical susceptibility and hazard. Calculating exposure without this variable would encroach on the definition of vulnerability, therefore in this scenario producing a separate exposure index is not feasible.

## 2.6 Other Concepts

This chapter encompasses concepts in geospatial sciences that, while being relevant to the understanding of this dissertation, are not directly related to the components of risk and, as such, need to be addressed separately.

### 2.6.1 Vertical Reference Systems in Portugal

#### 2.6.1.1 Altimetric Datum Cascais

In continental Portugal, the orthometric altitude reference system is based on the Altimetric Datum of Cascais 1938. This datum was established by averaging sea level observations recorded by the Cascais tide gauge between 1882 and 1938, resulting in the vertical reference frames by the average sea level, usually referred as “Cascais 1938” (Antunes, 2012). The benchmark located in the tide gauge is the starting point to the geometric levelling in the whole national levelling network. The establishment of an altimetric system allows for precise and standardized height measurements by relating any point on the Earth's surface to a well-defined reference surface (the average sea level of Cascais 1938) and the actual topographic surface (*ibid*).

The national vertical reference system is defined by a set of orthometric altitudes stretching the entire continental national territory and connected through networks of geometric levelling and the national geodesic network. Any DTM in continental Portugal uses the Vertical Datum of Cascais 1938 as altimetric reference for the altitude of its points (Antunes, 2012).

The sea level elevation records are referred to a reference mark located near the tide gauge, that serves as a starting point for the geometric levelling in the whole national network of high precision geodesic levelling that establishes the national system of orthometric heights (Antunes, 2012). This reference mark, that materializes the national altimetric datum, is found at an altitude of 4.31 m in relation to the MSL of Cascais 1938, i.e., the MSL of Cascais 1938 is located 4.31 m below this reference benchmark.

#### 2.6.1.2 Chart Datum

The Chard Datum (CD) referred to in Portuguese as Hydrographic Zero (ZH – *Zero Hidrográfico*), corresponds to the reference surface in relation to which the hydrographic probes and the isobathymetric lines of nautical maps are referred to, as well as the tide forecasts that are published in the Tide Tables of the National Institute of Hydrography (IH – *Instituto Hidrográfico*).

The CD defines the vertical datum for nautical cartography, referring the values of tide heights and ocean floor depth to this referential. To harmonize these values with the altimetric information present in cartography the tide values must be reduced of the CD of the respective reference port. Knowing that this value depends on the tidal amplitude of each hydrographic port, the CD varies from region to region.

In Portugal, the definition of CD is given by the lowest of low tides registered in a nodal period (18.6 years), added of a value of 30 cm as a safeguard. Along the Portuguese continental coast, the CD in use is 2.00 m below the MSL of Cascais 1938, with the exception of the hydrographic ports of Cascais, Lisbon and the rest of the Tagus Estuary, where the CD is 2.08 m, and the archipelagos of Madeira and Azores, with 1.40 m and 1.00 m, respectively to their MSL, due to the lower amplitude of ocean tides when compared to coastal or estuarine areas (Antunes, 2012).

### 2.6.2. Digital Terrain Models

The Digital Elevation Models (DEMs), in the context of cartography, describe the relief of the surface of the Earth. They consist of continuous functions with discrete representation, where each point of planimetric coordinates (X, Y) has one corresponding value of height. This representation is often complex, and the degree of similarity with the real terrain depends on the quality and density of the 3D coordinates of the terrain point samples used to create it. Several types of DEMs with different purposes can be considered (Li et al., 2005) with the Digital Terrain Models (DTMs) and Digital Surface Models (DSMs) being the most recognizable division – DTMs represent the relief at ground level while DSMs represent the surface including built up structures and natural features such as trees and tall vegetation. This difference can be seen in Figure 2.6.



Figure 2.6 - Differences between DSM (surface model that includes structures and vegetation) and DTM (terrain model, represents relief at ground level) [Source: <https://3dmetrica.it/>]

There are several methods to collect the information needed for the construction of DEMs, such as stereophotogrammetry, automatic image correspondence, LiDAR (Light Detection and Ranging), and radar interferometry.

In the context of SLR risk assessments, DTMs form the basis without which it is impossible to spatialize coastal flooding. Particularly in the case of local assessments, high quality terrain models with high spatial and vertical resolution are essential as they allow for more detailed results.

In this dissertation, the data was acquired with Bathymetric LiDAR, a method that utilizes a laser pulse aimed at the terrain, in order to obtain the distance between the surface and the origin of the pulse (Li et al., 2005). This distance is obtained measuring the time interval between the emission of the pulse and the detection of the received reflected signal. In the particular case of Bathymetric LiDAR, the laser pulses use two different wavelengths: the regular pulse has a wavelength of 1064 nm (infrared), and the other pulse is artificially generated by halving that wavelength, resulting in a green pulse of 532 nm. The green pulse can penetrate the water body of ocean or river and be reflected by sea floor (up to a certain depth, usually 50-70 m depending on the model), while the infrared pulse is reflected by the surface of the water, allowing for the depth to be determined by calculating the difference between these two signals. Over the solid surface of the earth both signals reflect simultaneously.

Data acquired by stereophotogrammetry was then used to complete the land side data, a classical method which involves estimating the three-dimensional coordinates of points on an object, measured in two or more photographic images taken from different positions through an aircraft.

The DTM is then built by combining both data sources and transforming the point data into a continuous surface composed by adjacent planes, a Triangulated Irregular Network (TIN), following a specific criteria (Delauney, 1934). From here, the TIN can then be interpolated to generate a 3D continuous surface in a rectangular grid format, with a resolution compatible with the source data and the objective of the study.

### **3. Methodology and Data**

#### **3.1 Area of Study**

##### 3.1.1 Physical and Geographical Description

The Ria Formosa is a barrier lagoon system located in the southernmost region of Portugal, Algarve, delimited by the coordinates 36°58'N, 8°02'W to 37° 39'N, 7°32'W. It exhibits an extremely complex geometry with innumerable channels and straits and several inlets. This system has some unusual characteristics, such as the lack of a significant river, the tide range conditions, and its triangular shape, which set it apart from conventional coastal ecosystems (Sousa et al., 2019).

The rich ecological value of the Ria Formosa is protected by a statute of natural reserves. In Portugal, it was first established as a natural reserve in 1978 by Decree n.º 45/78 (*Decreto n.º 45/78*) and then as a natural park in 1987 by Law-Decree n.º 373/87 (*Decreto-Lei n.º 373/87*), whereas internationally it is part of conservation and protection protocols such as the Natura 2000 network (Birds Directive 79/409/EEC and Habitats Directive 92/43/EEC) and the Ramsar Convention (UNESCO, 1971).

The national park comprises 18 000 ha, where the sheltered intertidal environment covers an area of approximately 8 400 ha. Of these, only around 14% are permanently flooded (Andrade et al., 2004). The unique conditions of Ria Formosa have also made it attractive for economic activities, such as saltponds, fish farms and bivalve aquaculture ponds, which extend for over 2 000 ha.

Five barrier islands (Barreta, Culatra, Armona, Tavira and Cabanas) and two mainland attached sand spits (Ancão and Cacela) constitute a beach/dune system that functions as a natural barrier to protect many habitats such as saltmarshes, dunes, intertidal mudflats, and saltponds. This large intertidal zone extends for a length about 55 km (E-W) and reaches a width of 6 km (N-S) at its broadest point (Newton & Mudge, 2003). A general view of the system can be seen in Figure 3.1.

The origin of the system is debated. The most accepted model (Dias, 1988; Pilkey et al., 1989) of its genesis points to sea level fluctuations resulting from glaciations and de-glaciations. During the Last Glacial Maximum, approximately 18 000 years ago, several sandy bodies formed parallel to the coastline. As the sea level rose from 120 m below the current level to the levels observed today, these sand bodies migrated landward to form islands, reaching their current position circa 7 000 years ago. Since then, the morphology and evolution of these islands was mainly influenced by waves, tides, extreme events, and SLR.

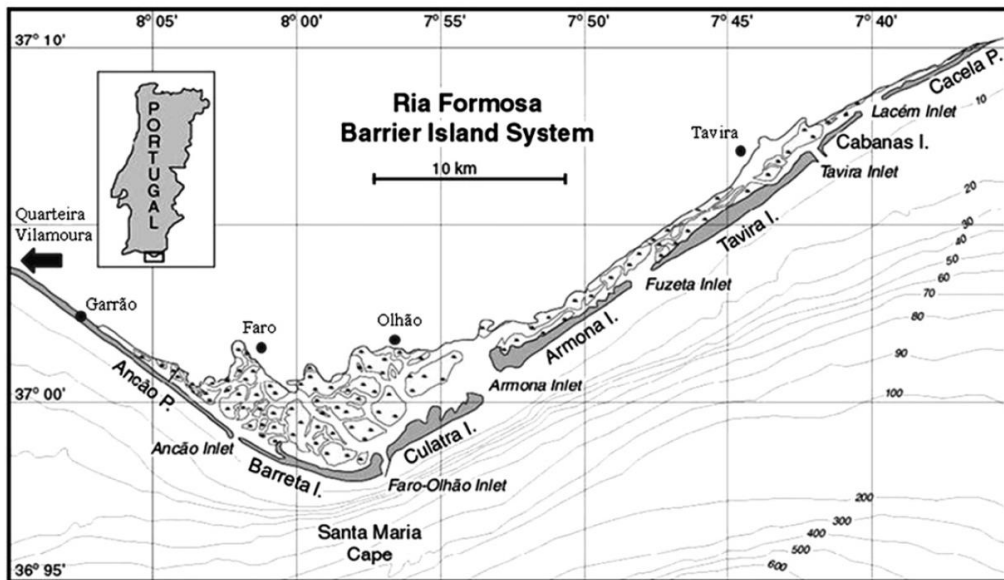


Figure 3.1 - The Ria Formosa barrier island system, located in the south of Portugal. The barrier system is composed of, from west to east, the Ancão Peninsula, the Barreta Island, the Culatra Island, the Armona Island, the Tavira Island, the Cabanas Island and the Cacela Peninsula. They are divided by six inlets, from west to east, Ancão Inlet, Faro-Olhão Inlet, Armona Inlet, Fuzeta Inlet, Tavira Inlet and Lacém Inlet. [Source: Ceia et al.(2010)]

The Ria Formosa is a mesotidal lagoon, with a semi-diurnal tidal regime, in contrast with other Mediterranean lagoons, that are microtidal (Kerambrun, 1986; UNESCO, 1979). The average range of the tides is between 2.80 m and 1.30 m during spring and neap tides, although 3.50 m can be reached on equinoctial tides (Pacheco et al., 2010).

The scarcity of fluvial contribution is a feature that distinguishes the Ria Formosa from other coastal lagoons worldwide (Aníbal et al., 2019). There are five small rivers and fourteen streams that flow into the Ria Formosa but most of these dry out in the summer (Newton & Mudge, 2003). The most important watercourses in the basin are River Gilão and streams Almargem, S. Lourenço, Zambujosa, Seco and Cacela. Their mean annual discharge of water into the Ria Formosa is  $1.74 \times 10^5 \text{ m}^3/\text{yr}$  (PROT Algarve, 2004).

There are six inlets, Ancão, Faro-Olhão, Armona, Fuzeta, Tavira and Lacém which allow the link between the ocean and the lagoon marshes. These inlets are then fundamental for water quality, navigability, and the transport of nutrients, chemicals, and sediments (Ceia et al., 2010). Tidal currents are the main factor in water circulation inside the lagoon, with a small influence from wind (Salles et al., 2005). There is an exchange of 40-70% water mass during each tide (Sprung, 1994). The low fluvial input and the high rate of water renewal through the inlets results in a vertically well-mixed system, where the average salinity values are very similar to open ocean waters (Newton & Mudge, 2003).

Maritime storm waves and tidal currents are responsible for intense morphodynamics in the Ria Formosa barrier island system (Pilkey et al., 1989). While some islands experience high growth rates that have been observed in studies over the last fifty years, globally, the system is in an active phase of landward migration, likely as a response to SLR, which is resulting in an overall shrinking of the lagoonal area (Andrade et al., 2004; Ferreira et al., 2016; Kombiadou et al., 2018). Ocean overwashes and sand dunes play a pivotal role in the system's evolution, as sedimentary dynamics emerge as the primary mechanism underpinning the development and perpetuation of its barrier islands (Dias, 1988; Ferreira et al., 2016; Pilkey et al., 1989).

The sea swell in the region is characterised by a significant wave height ( $H_s$ ) of 1.0 m. Wave heights higher than 3 m represent less than 2% of the waves registered. The mean wave period ( $T_m$ ) is 4.7 s with a peak period ( $T_p$ ) of 8.2 s. The wave direction is predominantly from SW-W (71%), followed by SE (23%). The most frequently observed waves have under 1 m in height, peak period below 11 s and originate from the west (31%). Waves over 3 m of height are generally observed during winter and originate mostly from southwest (Costa et al., 2001).

Inlets tend to show an eastward migration until a limiting position is reached, resulting in an infilling of the inlet and the start of a new cycle, with the opening of a new inlet close to the initial one. The exception is the Armona inlet, which is the only naturally stable inlet, although its width has been decreasing (Andrade, 1990; Cunha, 2019; Dias, 1988; Salles, 2001). The Faro-Olhão and Tavira inlets were artificially created during the 1920s and later stabilised with jetties during the second half of the 20th century (Ceia, 2007).

Human activity has further influenced the natural processes of the Ria Formosa. Barrier islands are among the most vulnerable natural systems to sea level variations, extreme events, and anthropic activities (Aníbal et al., 2019). The system responds quickly and intensely to coastal engineering projects, such as inlet stabilizations or construction of groynes, which disrupt the flow of sediments (Dias, 1988). Storm surge events associated with spring tidal periods have also intensified the coastal erosion, which will continue to be further aggravated by the SLR.

### 3.1.2 Socioeconomic Characterisation

In terms of administrative regions, the Ria Formosa extends over twelve civil parishes, shown on Figure 3.2.

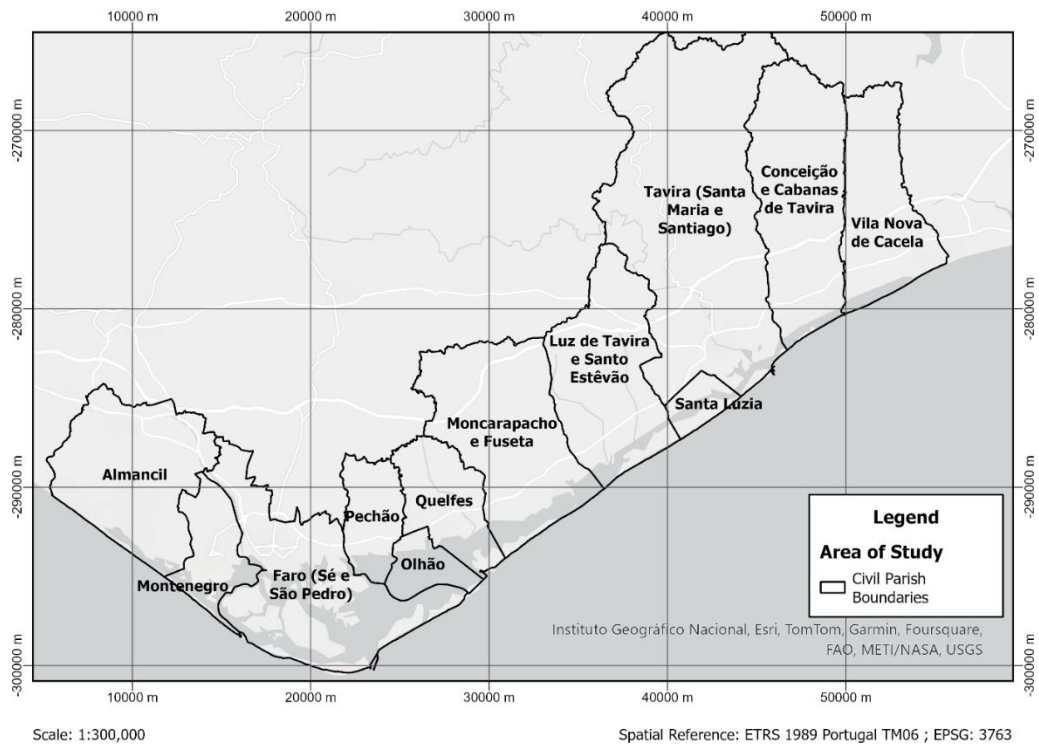


Figure 3.2 – Area occupied by the twelve civil parishes that encompass the area of the Ria Formosa

The region of Algarve experienced the largest population growth in the country during the last decade, with a population increase of 3.62% since 2011. The three main urban centres of the Ria Formosa, Faro, Olhão and Tavira have experienced a steady population increase since 1981, with the resident

population in 2021 being over 30% higher than in the early 1980s (Falcão et al., 2003; Instituto Nacional de Estatística, 2022).

The results of the most recent census of the population of the twelve civil parishes over which the Ria Formosa extends can be seen in Table 3.1.

*Table 3.1 - Full time resident population in the civil parishes that encompass the Ria Formosa in 2021 [Source: INE (2022)]*

Municipality	Civil Parish	Population (2021)	Municipality	Civil Parish	Population (2021)
<b>Loulé</b>	Almancil	11 291	<b>Faro</b>	Montenegro	8 613
<b>Olhão</b>	Pechão	3 888		Faro	46 299
	Olhão	14 206		Luz de Tavira	4 730
	Quelfes	17 253		Santa Luzia	1 589
	Moncarapacho e Fuseta	9 267		Tavira	15 432
<b>Vila Real de Santo António</b>	Vila Nova de Cacela	3 873		Cabanas de Tavira	3 428
				<b>Total</b>	139 869

In summer, a significant population increase occurs due to tourism. During this season, population can often reach double the size of the population in winter.

Human occupation of the Ria Formosa, particularly the barrier islands, began at the end of the 19<sup>th</sup> century in the form of communities of fishermen (Bernardo et al., 2002). The system management problems started to increase since the 1960s, as tourism became intense on several islands, particularly on Praia de Faro and in the Ancão Peninsula, with the construction of infrastructures (such as buildings and parking lots) in the dune ridge. In the last few decades, the settlements have increased, with structures becoming more permanent and located in areas at great risk (Dias et al., 2004). Some of these structures have been damaged during storm events and there has been a push from the Portuguese government and environmental agencies to relocate the population that resides in the barrier islands. Not only is this urban development very vulnerable to erosion and storm exposure, but it also places increasing pressure on the ecosystem and adds an additional layer of concern when it comes to the adaptability of the system and the impact of SLR. Human activity has also further increased coastal erosion in the Ria Formosa, particularly due to engineering projects on the updrift area or in the Natural Park, such as the construction of groyne fields (e.g. Quarteira), marina jetties (Vilamoura) and the stabilization of the artificial inlets of Faro-Olhão and Tavira. The disruption of the equilibrium conditions associated with the excess coastal erosion and the SLR rise leads to greater overwash susceptibility (Ferreira et al., 2008).

The Ria Formosa's resource-rich environment has made it a valuable regional asset, fulfilling a myriad of socioeconomic roles, each intricately interwoven with the delicate ecosystem. Main economic activities include fishing, aquaculture, salt extraction, and tourism.

The natural characteristics of the system gave rise to a significant aquaculture sector, contributing with almost 40% of the national production and 81% of the total number of aquaculture units. Bivalve production is typically reared in the lagoon's intertidal flats (Guimarães et al., 2012) and represents 84% of the Ria Formosa's aquaculture productions, whereas the remaining 16% comes from fish farming.

Excluding the fish farms, most other methods of catching fish are prohibited inside the lagoon area due to its importance as a nursery for many bivalve and fish species (Serpa et al., 2005). Fishing is mainly performed in the oceanic waters and is then unloaded in the nearby ports (Falcão et al., 2003). The most important fishing ports of the eastern part of Algarve are located on the Ria Formosa (Instituto Nacional de Estatística, 2019).

Currently, most of the national production of salt comes from the active saltpans in Algarve. There are three major groups of saltpans in the region, located in Castro Marim, Tavira and Olhão. Both the saltpans in Tavira and Olhão are in the Ria Formosa. Beyond their economic value, these saltpans contribute to the ecological harmony of the region, serving as sanctuaries for diverse avian species, especially migratory birds.

Tourism is one of the foremost contributors to the region's economy. Over the decades, the lagoon has evolved into a premier destination for both leisure seekers and nature enthusiasts. The surge in tourism activities has led to the development of accommodations, dining establishments, and recreational facilities, transforming the Ria Formosa into a bustling tourist haven. As a consequence of such increased activity, the tertiary sector is the most important productive sector in Algarve, with approximately 70% of the region's employed population working in tertiary sector activities. This number reaches up to 87% in the municipalities of Faro and Vila Real de Santo António (Serpa et al., 2005).

### 3.1.3 Biological Characterisation

The habitats present in the Ria Formosa can be classified in four main units: intertidal saltmarshes, intertidal flats, subtidal channels, and the beach/dune system. This diversity supports a rich biodiversity of flora and fauna.

Different species of flora thrive in different conditions. The intertidal flats of the Ria Formosa host one of the most important populations of seagrass (*Zostera noltii*) in Portugal (Guimarães et al., 2012), which is important for fish fauna (Ribeiro et al., 2008), bivalve populations (Cabaço et al., 2005), and microbenthic species (Gamito, 2008). Large areas of the bottom of the subtidal channels are covered by other species of seagrass, like the *Zostera marina*.

The sand dunes, particularly the lagoon-facing side, are home to species like sea rocket (*Cakile maritima*), prickly saltwort (*Salsola kali*), marram grass (*Ammophila arenaria*), sea-spurge (*Euphorbia paralias*) and sea cottonweed (*Otanthus maritimus*), among many others. These plants hold back the movement of sand by the wind and favour the formation of dunes (Cassar & Stevens, 2002).

Saltmarshes are considered one of the highest productive areas of the biosphere constituting nursery places for many marine species and have a high purification and carbon capture ability. There are well defined zonation patterns for saltmarsh vegetation. In the low saltmarshes, species like *Spartina*, *Arthrocnemum perenne*, *Salicornia nitens*, *Suaeda maritima* and *Limonium algarvense* are dominant. Going toward the upper limit of high saltmarshes, the vegetation changes to species such as *Artemisia campestris*, *Suaeda* and *Cistanche phelypaea* (Falcão et al., 2003).

The lagoon serves as an important spawning and nursing area for many aquatic species due to a combination of high nutrient levels, insolation, tidal water exchange and sheltered environment (Newton & Mudge, 2003). Over fifty species of fish and a great variety of bivalves have been identified in the lagoon. The most sought after due to their commercial value are the *sparidae*, *triglidae*, *scombridae* and *clupeidae* families of fish (Serpa et al., 2005) and the crosscut carpet shell

(*Venerupis decussate*) and the common cockle (*Cerastoderma edule*) bivalve families (Newton & Mudge, 2003).

The Ria Formosa is also a natural habitat for various species of birds, with more than 20 000 wintering birds counted on a regular basis in the lagoon system. The lagoon's proximity to Africa also makes it an important stop in the routes of many migratory birds. It is an important beach-nesting area for species such as *Sterna albifrons* and *Charadrius alexandrinus*, and for migratory species such as *Calidris alpina*, *Pluvialis squatarola*, *Limosa limosa*, *Recurvirostra avosetta* and *Tringa tetanus* (Sousa et al., 2020).

### 3.2 Methodology

The diagram in Figure 3.3 illustrates the workflow process of the major steps in this dissertation. The methodology is split into five main stages, one for each of the components of risk: the SLR scenario, physical vulnerability, socioeconomic vulnerability and environmental vulnerability and a final stage which will cover the different methodologies to compose indices, the different products that can be obtained with each component and the multi-parametric risk index cartography of the Ria Formosa. More in-depth diagrams can be found from chapter 3.4 onwards, further detailing the steps taken to generate each of the indices.

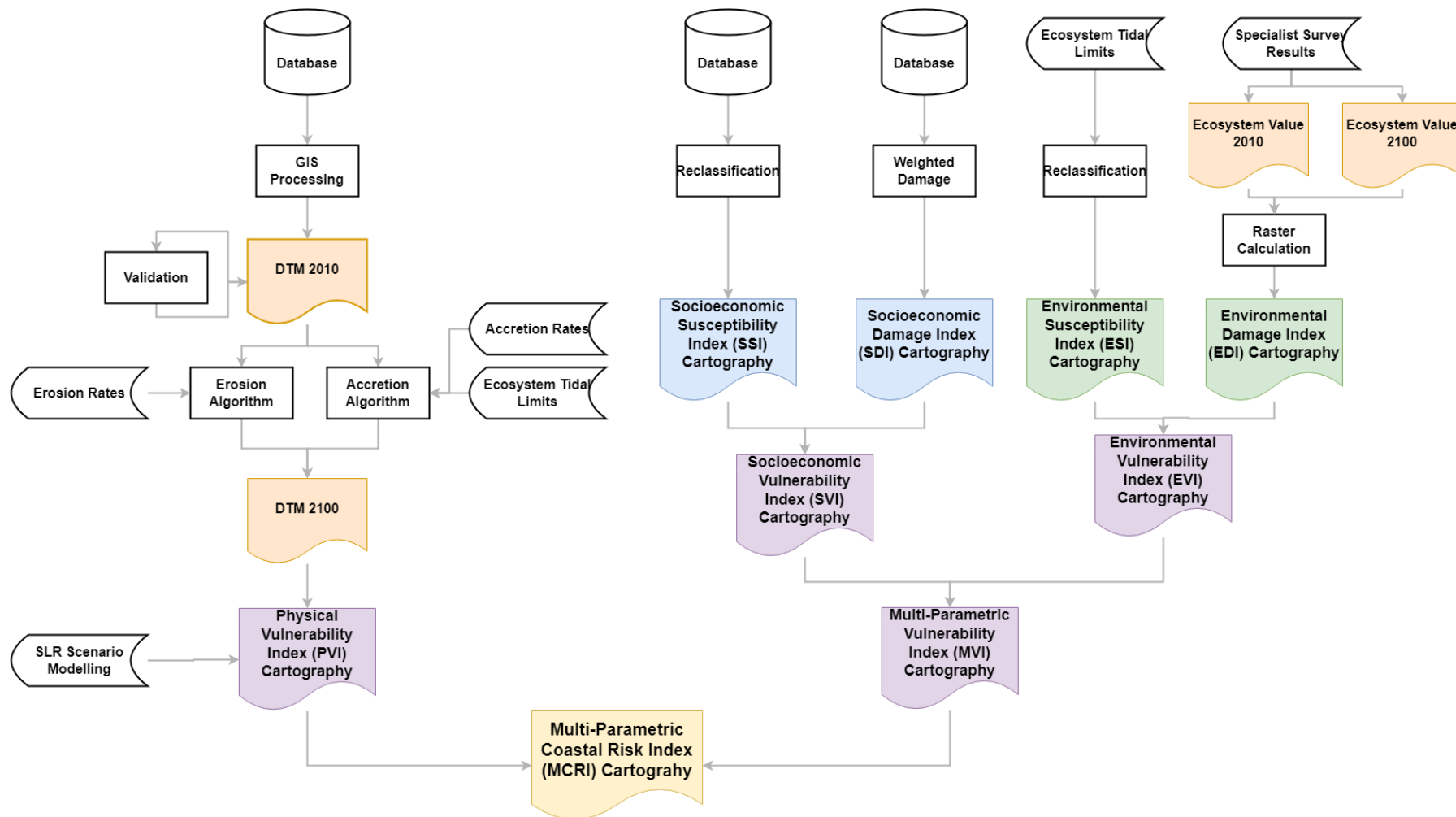


Figure 3.3 - Workflow of the methodology applied in this dissertation to reach the Multi-Parametric Coastal Risk Index Cartography. The complete process is divided into three main stages from where the first three products of this dissertation are obtained: First, the determination of the Physical Vulnerability Index (PVI) on the left, which includes the determination of the hazard and the inclusion of erosion and accretion algorithms to simulate a terrain model for 2100. On the right, the Multi-parametric Vulnerability Index (MVI) results from the Socioeconomic Vulnerability Index (SVI), which is based on the reclassification of layers of information and the determination of the potential damage to the region, and the Environmental Vulnerability Index (EVI), a new index developed for this thesis using ecosystem reclassification by using historical tide data and the results of a survey of experts in the field.

### 3.3 Data

In order to obtain the results proposed by this dissertation, several types of data from multiple sources are required. The use of LiDAR and stereorestituted points sourced from DGT is essential for the creation of the DTM, whereas the bathymetry was completed using data from IH for the Canal de Faro and data from EMODnet for the Atlantic Ocean. Forecasting of SLR for the scenario considered is critical to obtain a good hazard model. Rates of erosion and accretion are crucial data to correctly forecast the evolution of the area of study. Multiple sources of socioeconomic data such as the Soil Use Cartography (Carta de Uso e Ocupação do Solo – DGT) or the locations of infrastructure, points of interest or communication networks are essential to understand the socioeconomic vulnerabilities and tidal information is necessary to identify the ecosystems in the Ria Formosa.

A more thorough description of all the data and sources used can be found in Table 3.2.

*Table 3.2 - Data used in this dissertation with sources, acquisition dates and observations.*

Data	Source	Acquisition Date	Observations
Stereorestituted Points	DGT	2014-2015	Spatial Resolution 2 m
LiDAR	DGT	2011	Spatial Resolution 2 m
Bathymetry – Canal de Faro	IH	2009	Spatial Resolution 25 m
Bathymetry - Ocean	EMODnet	2020	Spatial Resolution 100 m
High Precision Geometric Levelling Network (RNGAP)	DGT	2000	
Secondary Port Tide Corrections	IH	2024	
Tide Gauge Data - Faro	FCUL	2015	
Soil Use	DGT	2021	Carta de Uso e Ocupação do Solo
Socioeconomic Data	OSM	2024	Infrastructure, Transport Networks, Green Areas
Ecological Areas	RNAP	2018	
Ecological Areas	Natura 2000	2021	
Census 2021	INE	2022	Population Density, Habitation Data
Location Coefficients	AT	2015	
Aerial Photography	DGT	2018	

### 3.4 Physical Vulnerability

#### 3.4.1 Hazard

To evaluate vulnerability or susceptibility to a certain risk several scenarios are usually considered, encompassing a wide range of possibilities from the most to the least likely. The IPCC frequently considers RCP scenarios 2.6, 4.5, 6.0 and 8.5, with 8.5 being the most extreme scenario considered. Other studies, in particular from NOAA (NOAA, 2017) consider that the IPCC RCP projections are too conservative and don't take into account a faster melting of polar ice caps that could lead to a much faster increase in SLR, as seen in Figure 3.4. Antunes (2019) presents the FCUL models generated with data from the Cascais tide gauge, which also considers SLR projections that go beyond those of the IPCC. In this context, the RCP 8.5 is not viewed as an extreme hazard scenario but rather an intermediate one. For this reason, this was the model chosen for this project.

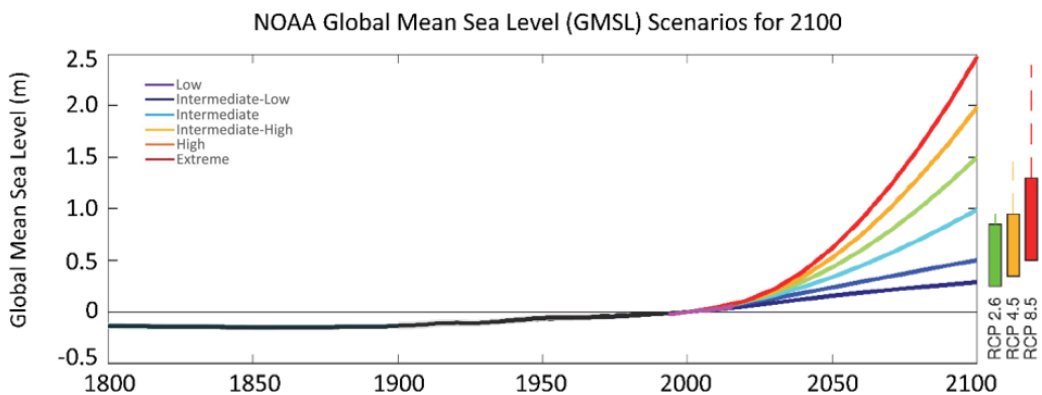


*Figure 3.4 – NOAA global mean sea level scenarios for 2100. The graphic highlights the uncertainty of the RCP 8.5 model, considering it an Intermediate-Low to Intermediate-High scenario. [Adapted from: NOAA (2017)]*

As discussed during chapter 2.2.1, the sea level variation is not a linear process but rather results from the combined action of several processes. Of the various processes of sea level variation relevant for this project, the astronomical tides, the mean sea level rise, the storm surge, and the setup, resulting from the sea swell and surface winds, are used to model the hazard scenarios. As this methodology to determine hazard scenarios was already included in several other projects (Antunes, 2019; Antunes et al., 2018, 2023; Santo, 2022), this chapter will focus mostly on the key steps as well as specific changes made for the Ria Formosa SLR.

The workflow followed for this section of the project can be seen in Figure 3.5.

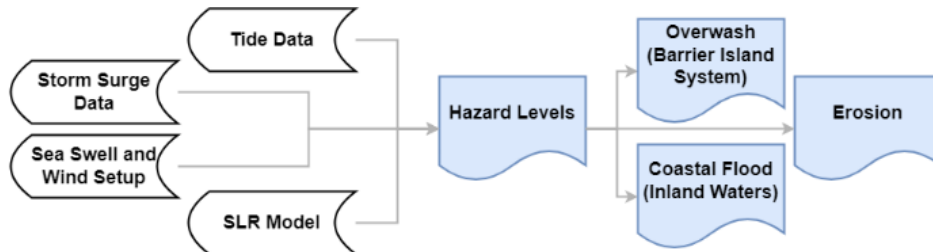


*Figure 3.5 – Workflow for Chapter 3.4.1. The objective of this chapter was the determination of a table of hazard levels, which can then be used to determine the elevation of coastal floods and the overwash that can hit the barrier island system. This data is also critical for the erosion mode used in chapter 3.4.2. The items on the left are the coastal forcing parameters that are used to determine the hazard.*

### 3.4.1.1 Tide

Long series of astronomical tide observations in Portugal exist only for the tide gauges in Cascais and Lagos. For most other locations, port tide gauges maintained by IH have registered observations short periods, ranging up to 20 years. The tide forecast for the port tide gauge in Faro-Olhão (located on the Faro-Olhão Inlet) was calculated by Antunes (2007) and made available by FCUL and Dom Luiz Institute, using data obtained from IH between the years of 2007 and 2010 and periodically reviewed.

As the tide maximums have a periodic variation, with intervals of 4 to 5 years, the reference tide for this study corresponds to a maximum amplitude tide, coinciding with years where the Moon is closer to Earth. The year chosen for this was 2015, where the maximum tide reached 4.00 m in Faro, relative to CD.

The harmonic model of tides allows the tide forecasting and the consequent calculation of extreme tides for future periods and the analysis of tide variations over time. The tide forecast models (Antunes, 2007) already include the modelling of the SLR adjusted to the data in the Cascais tide gauge (Antunes, 2011), therefore the tide values obtained for the Mainland Portuguese Coast already

include the variation in the sea level. However, and since the SLR model is here applied separately, this component is previously removed from the tide model of Antunes (2007).

The tide regimen in the inland waters of the Ria Formosa barrier island system differs from the one observed at the Faro-Olhão inlet tide gauge in both amplitude and phase. To correctly model the maximum height of the tides inside the Ria Formosa a series of corrections were measured in various points of the lagoon and a tidal surface anomaly model was applied. This process is further detailed in chapter 3.4.2.

Based on the SLR forecasts and the tide model for a reference year it's possible to estimate the evolution of the maximum high tides for a long period in the future. Using this data the percentage of submersion or emersion of a specific height in the terrain can be calculated, resulting in a cumulative frequency of submersion during the year, or in an extreme flood level probability.

#### 3.4.1.2 Storm Surge

The storm surge is a disturbance or anomaly of the sea level normally forced by meteorological phenomena, such as highly energetic storm with variation in air pressure and surface winds. As previously discussed in chapter 2.2.1.3, the SS on the Portuguese Atlantic coast can reach 50-70 cm, according to the tide gauge data analysis (Antunes, 2019a), with the possibility of reaching 80-100 cm for long return periods (>100 years).

Due to the lack of data for the Faro-Olhão tide gauge, data from the nearby tide gauge in Lagos was used to update the maximum tide and the return periods of extreme levels of SS: 82 cm, 91 cm, and 100 cm for return periods of 50, 100 and 200 years, respectively. These extreme values, when compared to the data from the Portuguese Atlantic Coast, reflect occasional occurrence of higher-than-average SS for the region, with values of 83 cm and 60 cm reached in 2013 and 2018, respectively.

The relative position of Lagos, west of the Ria Formosa, can result in an overestimation of SS values for this area, as this SS is associated with subtropical storms, usually from the southwest (Antunes, 2014).

#### 3.4.1.3 Sea Swell and Wind Setup

Sea level extremes are also influenced by the setup effect, resulting from both the coastal sea swell and the presence of strong winds. The sea swell setup must be considered when estimating extreme values of the sea surface level near the coast, while the wind setup must be considered in the internal waters of the Ria Formosa.

Antunes (2014) describes the methodology applied for this modelling. The data for sea swell was obtained from the Faro wave buoy (IH). As no references for wind setup values were found for this region, the average velocity of the wind (38 Km/h) was used.

#### 3.4.1.4 SLR Models

The SLR models obtained globally (Figure 3.6) need to be locally adjusted in order to consider factors like long period variations of the tides, gravity field variations, Earth rotation variations, vertical surface velocities, the variability of oscillation of the ocean-atmosphere system and other non-climatic factors.

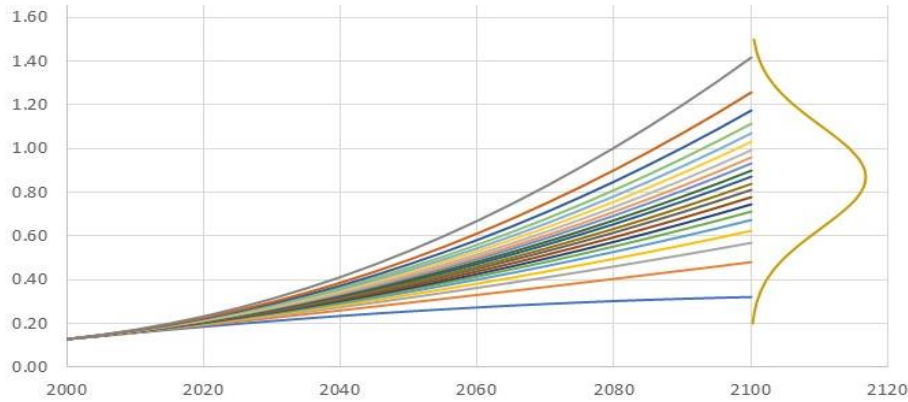


*Figure 3.6 – Model statistics representing the probability distribution of global mean sea level (in meters, on the left) per year for the IPCC RCP 8.5 scenario.*

Knowing the dynamic variation factors of SLR and based on the studies of the temporal series of the Cascais and Lagos tide gauges, temporal series of the permanent GPS stations in Cascais and Lagos (Serpelloni et al., 2013) and neotectonics (Cabral, 1995; Figueiredo et al., 2013), for this project only the uplift effect deduced from the comparative analysis of the 100-year and 10-year series of the Cascais tide gauge with the global sea level series of Jevrejeva et al. (2014) and Church & White (2011) and the satellite altimetry series from NASA, CNES and CSIRO was considered (Antunes, 2019).

From this analysis of Antunes (2019) resulted an average value of +0.20 mm/yr, corresponding to the relative difference between the sea level of Cascais and the global sea level. Cabral (1995) and Figueiredo et al. (2013) consider a 0.10-0.20 mm/yr uplift in the southern region of Portugal when compared to the northern regions.

Based on the SLR rates determined from the data of the Cascais tide gauge it's possible to deduce an acceleration value and determine a model that can forecast for the near future the increase in sea levels. The same approach can be used for the Algarve region, in this case the altimetric data was extracted from the Sea Level Change portal (NASA), to obtain a model for the southern region similar to the ones existing for Cascais, with the coastal uplift correction (0.20 mm/yr).

Using the extreme tide amplitudes of 2015 as a reference, the estimates of TWL (Total Water Level) in Table 3.3 were obtained for the Ria Formosa.

*Table 3.3 - TWL Forecast for the Ria Formosa in 2100 with the IPCC RCP 8.5 scenario. Each probability of occurrence is related to an elevation interval, denoting how likely an area at that elevation is to flood in an extreme scenario. These intervals can then be normalised into the classes of hazard seen on the right.*

	Internal Waters		Barrier Island System	Hazard Class
	2100 + SS			
Probability of Occurrence	min (m)	max (m)	Overwash (m)	
1% to 20%	3.80	4.65	6.78	1
21% to 40%	3.40	3.80	6.07	2
41% to 60%	3.15	3.40	5.50	3
61% to 80%	2.75	3.15	4.92	4
81% to 99.9%		2.75	4.18	5
Uncertainty of the Scenario	0.45 m			
Central Estimate	3.30 m			

### 3.4.2 Physical Susceptibility

The determination of the physical susceptibility was classically done, in earlier works, with a series of layers of data identifying factors that could contribute to exacerbate a flood scenario, such as the land use, distance to the coastline, hydrographic network and type of coast (Antunes et al., 2018; Rocha et al., 2020). According to Rocha et al. (2023), while these kinds of information may be relevant for studies at a national level, the most important factors when considering the physical susceptibility at a local or regional scale are the coastal sedimentation processes and the possible existence of coastal defences. In some cases, this has been done through the normalisation of variables like the erosion/retreat rate, the coastal slope and the sea level rise (e.g. Ghoussein et al. (2018); Islam et al. (2016)). A more complex approach that allows for a “snapshot” into the future is the use of programming algorithms to simulate the erosion/accretion of an area, combined with the extra forcing caused by the SLR (Antunes et al., 2023; Antunes et al., 2024a; Santo, 2022).

As the area of study is a small region of the country, the objective was to attempt to model these geological processes, both the erosion on the ocean side and the accretion on the lagoon. This is a process comprising of various steps. A workflow diagram of the process followed in this chapter can be seen in Figure 3.7.

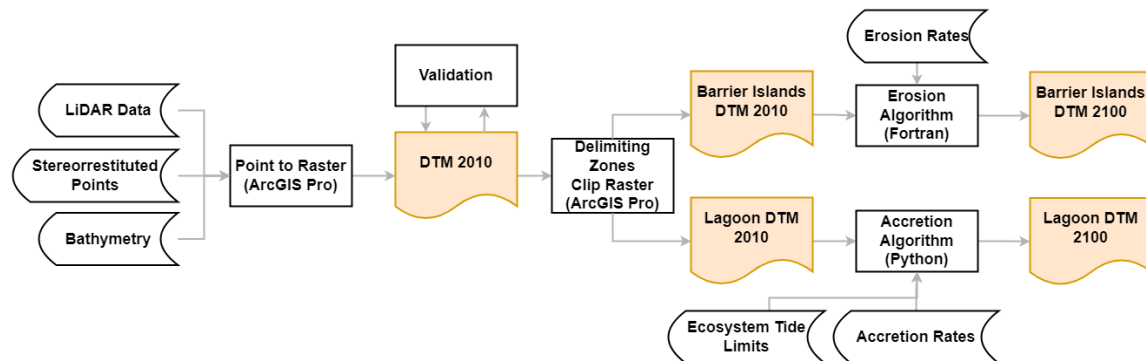


Figure 3.7 - Workflow for Chapter 3.4.2. The focus of this chapter was the determination of two DTMs for 2100, the Barrier Islands and the Lagoon, using the erosion and accretion algorithms, respectively. Before reaching this step, it was necessary to create a reference DTM, here called DTM 2010, using the data sources on the left of the diagram.

#### 3.4.2.1 Reference Digital Terrain Model

The first step in determining physical susceptibility is the creation of the base digital terrain model, considered here as the reference DTM for the year 2010 (with the most recent data of 2011 and 2015), as both the stereorestituted points and LiDAR data were acquired in this decade.

The LiDAR data used for the DTM corresponds to surveys of the littoral of the Portuguese Mainland, with an extension of approximately 600 m of the maritime side and 400 m of the land side of the coastline. The LiDAR survey was conducted in 2011 and the resulting data has a resolution of 2 m. The stereorestitution for this acquisition, for an area of approximately 513 400 ha, was done between 2014 and 2015 and also has a resolution of 2 m. Both were made available by DGT as part of a partnership with the Portuguese Environmental Agency (APA - Agência Portuguesa do Ambiente). Both data sources were divided into files of 3D point-grids and a shapefile with the geographic location corresponding to each set of files was also provided with the data.

The first iteration of the DTM was produced in an automated manner, using a Python code that reads each sheet of points for each of the files being used and joins them together in a single file to facilitate its input in ArcGIS Pro. This was done for each of the data sources, which were then combined in ArcGIS Pro, giving priority to the LiDAR data as it is the more accurate data. Once this step was

completed, a gap was detected in the Canal de Faro, which is the main navigable channel in the Ria Formosa, where a section had been filled in with null data, needing the addition of extra data sources.

The bathymetry data was obtained from EMODnet (European Marine Observation and Data Network) and IH, at a much lower resolution than the terrain data. In order to blend the bathymetry data smoothly with the first DTM, both data sources were joined in a TIN model, with the overlapping areas manually edited to ensure a smooth transition. The resulting DTM can be seen on Figure 3.8.

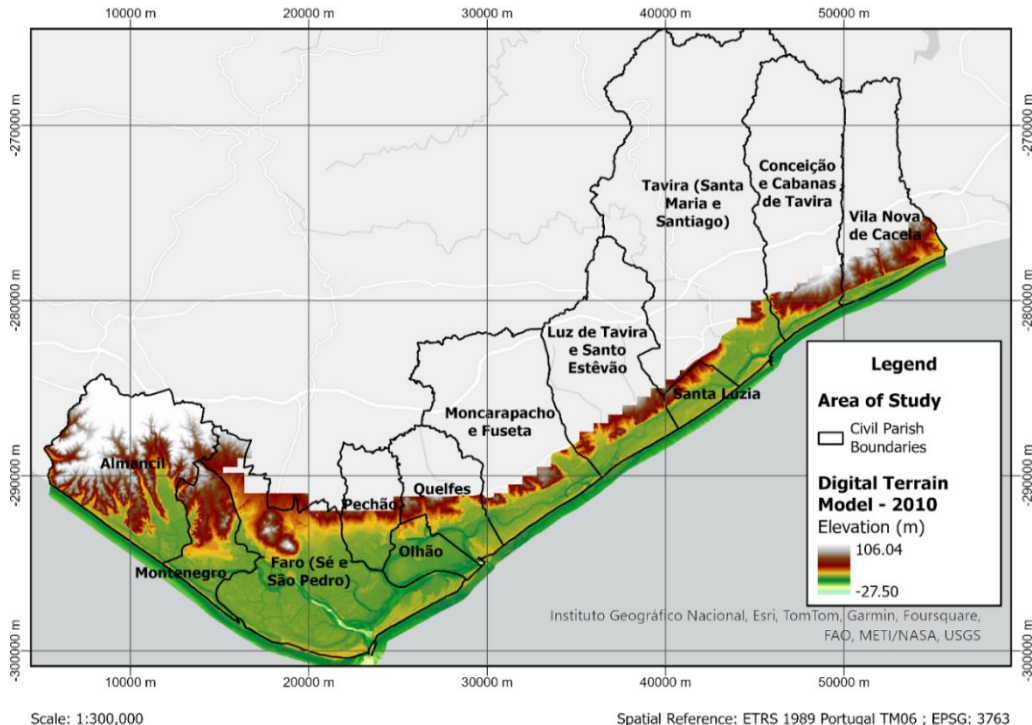


Figure 3.8 - Reference Digital Terrain Model for the Ria Formosa in 2010, overlaid with the civil parish boundaries shown in chapter 3.1.1. With the exception of the western side of the Almancil civil parish, the whole area has a coastline which is mostly flat and at low elevation.

Altitude quality control is indispensable for physical vulnerability assessments as the DTM is the element that allows for these studies to be made. The elevations of the points used to produce the DTM were obtained using photogrammetric methods, and despite these methods being efficient and accurate, they are not error-free (Höhle & Höhle, 2009). Specifically, errors in accuracy related to the vertical reference, while having little influence on topographic cartography due to being within the precision of their respective methods, are of extreme importance within the scope of this project's evaluation.

The validation of this DTM was carried out through a direct comparison made to a set of levelling benchmarks belonging to the *Rede de Nivelamento Geométrico Alta Precisão* (RNGAP – National High Precision Levelling Network) of the DGT. For this purpose, 27 marks were identified, spread out over the length of the study area. Some of the control points had to be excluded due to being placed on structures and therefore not being a good reference for the DTM ground data. Unfortunately, due to time and geographic constraints, it was not possible to obtain field observation data.

By comparing the elevation values (orthometric height) of the levelling marks with the corresponding values of the produced DTM, a set of residuals was obtained as estimates of the respective error of the altimetric model, as follows (Figure 3.9):

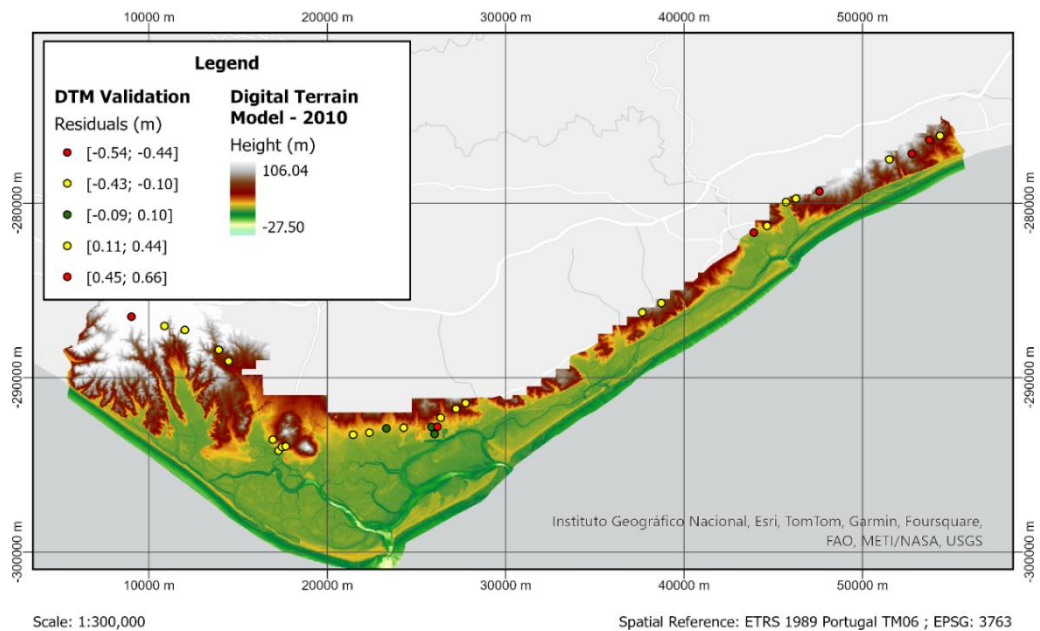


Figure 3.9 - Location and residuals of levelling benchmarks used for DTM validation. Most of the benchmarks for RNGAP are located along main roads or in urbanised areas, so there is a lack of validation data in the lagoon area.

A statistical analysis of these calculated residuals marks allowed for the determination of a standard deviation of 0.27 m, corresponding to the estimate of the precision of the DTM, and a residual mean of 0.05 m, corresponding to the absolute deviation (bias) of the model relative to the altimetric reference datum (Vertical Datum Cascais 1938).

The model could then be further corrected, using the mean of the residuals, however, it was concluded that due to the spread of the study area, the lack of field survey data, and the random distribution of the residuals, the current DTM is of acceptable accuracy for this study.

#### 3.4.2.2 Geological Processes

To simulate the transition from 2010 until 2100 and the impact of geological processes on the area of study, the area of the Ria Formosa was divided into two sections. In Figure 3.10, such sectioning is shown - in yellow the section most affected by coastal erosion processes, comprised of the barrier island system and the sand spits (both beach/dune systems). In green, the intertidal area of the lagoon, where sedimentation processes are the dominating change factor.

The algorithm used to simulate coastal erosion is an adaptation of the methodology applied by Santo (2022), which was developed by Antunes (2017) and is based on the modified Bruun Rule (Rosati et al., 2013). Bruun (1962) proposed a formula for estimating the retreat of sandy shorelines as a response to changes in the sea level. The Brunn Rule has been widely adopted by the scientific community as a method to interpret coastal alterations, however, it falls short by its failure to consider landward sediment deposition and its inability to be adapted to different sediment deficit coastal conditions. The modified Bruun Rule, while still a limited method, accounts for situations where the sediment transport occurs both seaward and landward. The modifications introduced by Antunes (2017) and Santo (2022) allowed for the modified Brunn Rule to be applied to DSMs (a combination of DTM and Bathymetry) and introduced an elasticity function to manage the distribution of sediments between the landward and seaward directions.

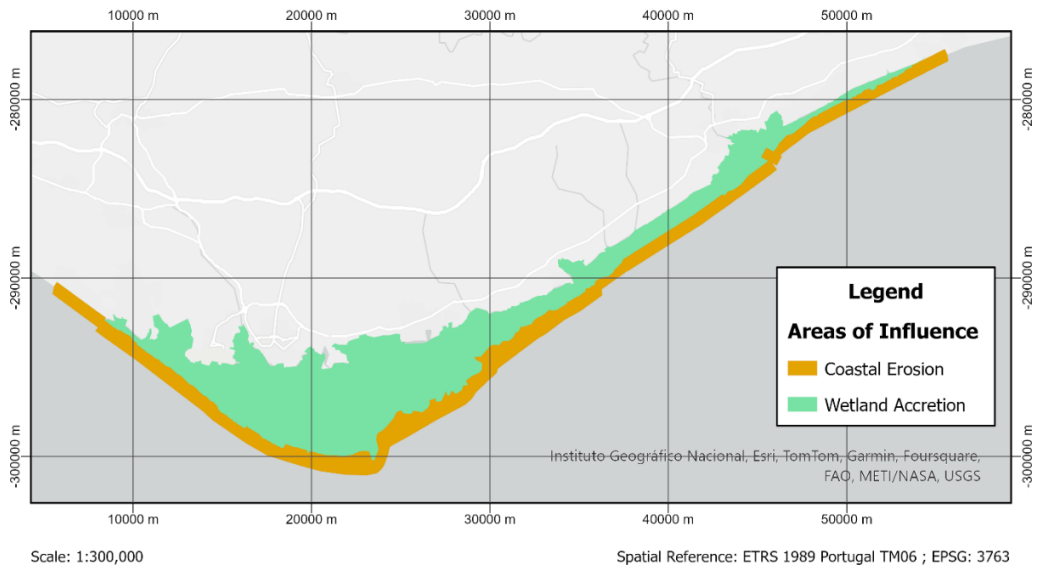


*Figure 3.10 – Sectioning of the areas where each algorithm will be applied. The division of the areas was made along the northern side of the barrier islands, with a slight overlapping area to ensure a smooth transition in the resulting DTM.*

The method was also applied to the study of the national project of the Roadmap for Adaptation 2100 developed by Dom Luiz Institute and FCUL for APA. In a way to improve and solve earlier limitations found on the application, and for the purpose of this dissertation, a further modification was introduced into the algorithm by Antunes et al. (2024a), to allow the additional accounting of both erosion and accretion related to the sediment deficit. It is based in simple shifts, landward or seaward, that corresponds to the known erosion rates.

According to Lira et al. (2016) the Southern coast of Portugal is currently a system approximately in sedimentary equilibrium, meaning the sediments lost in one location are then deposited in a different location. However, this is likely to be tilted towards a sedimentary loss due to the rise in the mean sea level (e.g. Anderson et al., 2015; Bird, 1996; Jiménez et al., 2017; Leatherman et al., 2000). To understand the erosion behaviour in the barrier island system, the erosion rates obtained by Lira et al. (2016) were adopted as a baseline for 2010 and then the predicted SLR and coastal erosion algorithm were used to determine both the shoreline retreat and the simulated DTM for 2100.

After sectioning the area of the DTM where the coastal erosion algorithm will be applied, the first step was to manually identify the orientation of the coastline, which was marked by a set of line features drawn along the coast of the Ria Formosa (Figure 3.11). Further divisions were necessary when the erosion/accretion behaviour had large variations within the same stretch, allowing for a more accurate model. With the aid of a Python code that uses ArcGIS commands, these line features were then used as a reference to draw perpendicular profiles. The spacing between these profiles can be defined by the user. At the start, this was defined as 2 m, the same resolution as the original DTM. Using these profiles, the program then determines the 3D coordinates (X, Y, Z) of points along the profile, with a point registered every 2 m. These coordinates are then exported to text files to allow for further processing.

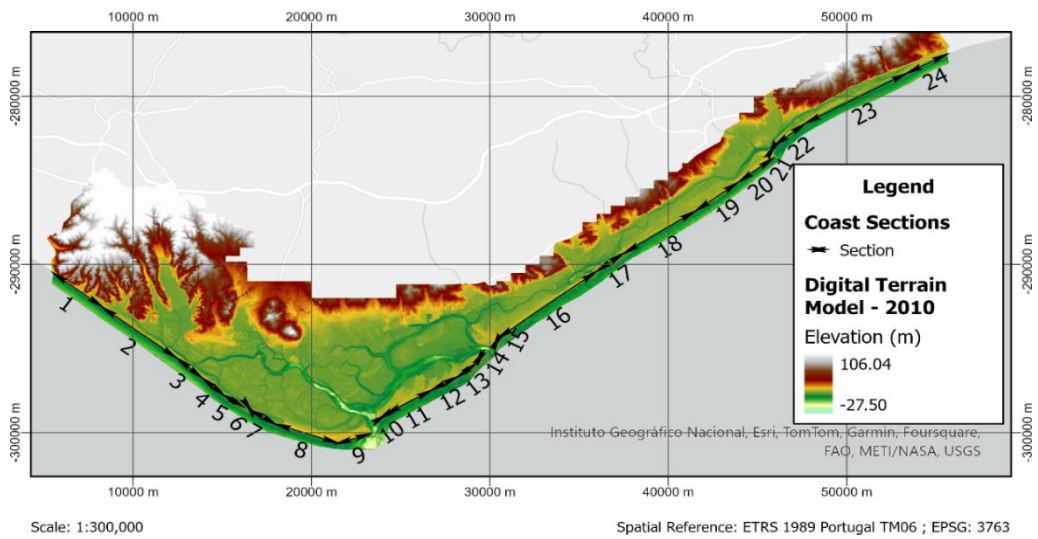


Figure 3.11 - Sectioning of the Barrier Island System Coastline. Stretches were separated according to erosion tendencies and orientation of the coastline, with a slight overlap to prevent any gaps in the model.

The coastal retreat is then simulated using these perpendicular profiles, the model of mean SLR and a series of factors which can be input in the program such as the erosion rate, the search distance for the next maximum in the profile and the elasticity scale of the profile. The erosion rate for each segment was given by the average of the profiles calculated by Lira et al. (2016) for each subsection. Using this algorithm, firstly the erosion along each profile was simulated to match the current erosion rates and the parameters were then adjusted to allow for a more realistic scenario considering the mean sea level rise and climate change predictions.

One issue that still exists within the algorithm is the way in which it calculates coastal retreat and erosion rates. The way these are estimated is based on the first profile point over the maximum swash, used here to identify the coastline, and composed of the SLR, the maximum high tide, the maximum storm surge in a 10-year period and the wave total run-up. With the additional erosion and the increase in overwash derived from the SLR, many of the profiles never reach a height above the maximum swash. In such cases, the reference point for the retreat takes the highest value of the profile, which results in an estimated erosion and retreat lower than what is expected. In total, 16 663 profiles were considered and 10 302 of these will be completely below the maximum swash in 2100. Table 3.4 shows the variation in erosion rates for each section. Positive values represent accretion areas and negative values erosion areas.

Table 3.4 - Change in erosion rates between 2010 and 2100. Stretches 5,6,7,17,18 and 23 are completely below the maximum swash in 2100. Stretch 14 is already below this value today. Stretch 21 represents the inlet area and the erosion algorithm was not used here, it is included for DTM completion purposes.

Stretch	1	2	3	4	5	6	7	8	9	10	11	12
Base Erosion Rate (m/yr)	-0.65	-0.25	-0.50	0.05	0.05	0.14	2.18	2.34	4.36	-1.05	-2.04	-0.36
2100 Erosion Rate (m/yr)	-0.80	-0.48	-0.64	-0.47	-0.18	0.05	0.15	0.24	0.65	-0.86	-1.40	-0.67
Stretch	13	14	15	16	17	18	19	20	21	22	23	24
Base Erosion Rate (m/yr)	1.57	3.59	2.41	0.36	-1.31	-1.30	-0.10	1.54	N/A	-1.65	-3.46	-0.84
2100 Erosion Rate (m/yr)	0.49	0.71	0.63	-0.36	-0.63	-0.80	-0.40	0.74	N/A	-0.18	-0.19	-0.81

After applying this erosion algorithm, the resulting profiles are then input back in ArcGIS Pro, where they are merged and transformed into a raster dataset, with special attention paid to areas of overlap to ensure smooth transitions. To maintain the smoothness of the model, as well as to account for the uncertainty of the predictions, the final model has a spatial resolution of 10 m.

In the intertidal area, the process used to simulate accretion over time is an adaptation of Ferreira (2022). According to Bricker-Urso et al. (1989) the maximum sedimentation rate possible in natural coastal environments is 16 mm/yr. In the case of Ria Formosa, Andrade (1990) estimated an average sedimentation rate of 2 mm/yr, however, the distribution of sedimentation is very uneven, with the region east of the Faro-Olhão inlet reaching 2.5 times the average rate (NEMUS, 2005). Due to the lack of more detailed information that would allow for a distinction of the accretion rate of different regions inside the lagoon, the reference value of 5 mm/yr was used as this corresponds with the widest area of the lagoon.

Several studies (e.g. Christiansen et al. (2000); Ma et al. (2018); Moskalski & Sommerfield (2012)) have shown that the sedimentation dynamics also change with the distance to the water channels. The intertidal mudflats immediately adjacent to the channels, especially in the case of the Ria Formosa, where the ocean tides are a dominating factor in the dynamic of the system, are often subjected to the ebb and flow of the currents, diminishing their capability to retain sediment. As the distance to the channel increases, so does the sedimentation rate up to a point where the tides are still able to reach frequently. Approaching the high saltmarsh, the submersion period diminishes and so this area has less opportunity to retain sediment. The modelling to account for these differences in accretion behaviour then would begin with a lower sedimentation rate in the subtidal areas, increasing steadily in the intertidal mudflats as the distance to the subtidal area increases and peaking around in the low saltmarsh, before steadily decreasing again in the high saltmarsh.

The first step to implement such an approach was to define height limits for each of the intertidal ecosystems considered in the study. As explained in chapter 2.4.1, these limits can be defined based on the heights the tides can reach during different periods of their cycle. Using data from the Faro tide gauge between 2000-2010 and 2015, Table 3.5 was compiled, showing the average tide values reached during this period.

*Table 3.5 - Tide data from the Faro tide gauge from 2000-2010, 2015. For each of the values on high tide and low tide, the columns represent the maximum (Max), spring tide (ST), average (Avg), neap tide (NT) and minimum (Min).*

	High Tide (m)					MSL (m)	Low Tide (m)				
	Max	ST	Avg	NT	Min		Max	ST	Avg	NT	Min
Min	3.79	3.44	3.11	2.73	2.31	2.09	1.71	1.41	1.03	0.69	<b>0.25</b>
<b>Mean</b>	<b>3.92</b>	3.47	<b>3.14</b>	<b>2.76</b>	2.39	2.11	1.84	1.46	1.07	0.73	0.40
Max	4.00	3.56	3.22	2.85	2.58	2.14	1.92	1.49	1.10	0.77	0.42

The values highlighted in Table 3.5 (in bold) will define the ranges necessary to the classification of the intertidal ecosystems, however, these are referred to the CD and as such they need to be reduced of 2 m to be referred to the MSL. Since this is a simulated accretion for 2100, the SLR also needs to be considered, with an expected +0.884 m according to the IPCC RCP 8.5 (Tide Value – 2 m + 0.884 m). Table 3.6 shows the final threshold classification obtained for each ecosystem:

*Table 3.6 - Ecosystem classification by elevation. Each of the class boundaries correspond to the values in Table 3.5, with the midpoints being where an accretion rate transitions into the next one.*

Ecosystem	Min h (m)	Midpoint (m)	Max h (m)
Subtidal			-0.87
Intertidal Mudflat	-0.86	0.38	1.64
Low Saltmarsh	1.65	1.83	2.01
High Saltmarsh	2.02	2.39	2.80

With the aid of a Python algorithm and using the 5 mm/yr sedimentation rate as the base value, the segmentation in Figure 3.12 was applied, with the changes in each rate occurring at the midpoint of each class, except for the subtidal class. The algorithm will then receive the 2010 DTM as the input, identify the pixels in the range of (-3.00 m, 2.80 m) and apply the corresponding base sedimentation rate, multiplied by the calculated rate percentage and by number of years between the two models, in this case 90 years.

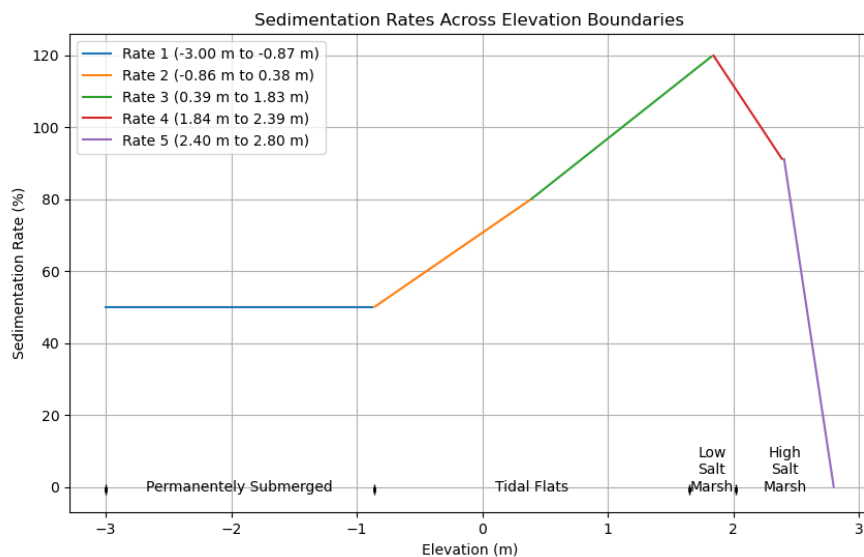


*Figure 3.12 - Sedimentation rates across ecosystem elevation boundaries, in % relative to the base value of 0.5 mm/yr. The sedimentation increases from the subtidal area until the low saltmarsh, rapidly dropping to as it transitions into the high saltmarsh and reaching zero at the higher limit of the intertidal zone.*

### 3.4.2.3 Digital Terrain Model for 2100

With the modified DTMs obtained for both the erosion and accretion zones, the process was concluded by creating a mosaic of the two areas where these algorithms were applied and the third area, not subject to any of these geological processes, which resulted in the simulated DTM for 2100 that can be seen in Figure 3.13.

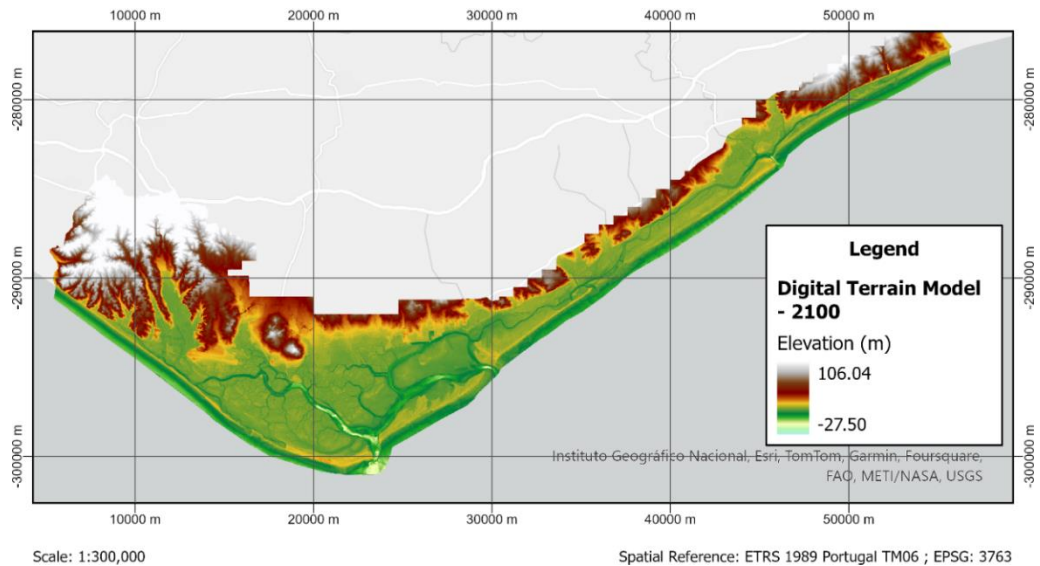


Figure 3.13 - Digital Terrain Model for 2100 – this DTM is the composition of the Barrier Island DTM resulting from the erosion algorithm, the Wetland DTM resulting from the accretion algorithm and the remaining area where no change algorithms were implemented.

### 3.4.3 Physical Vulnerability Index (PVI)

With the projected DTM for 2100 and the hazard elevation intervals obtained in chapter 3.4.1, the physical vulnerability index can now be calculated. Figure 3.14 details the workflow followed in this chapter.

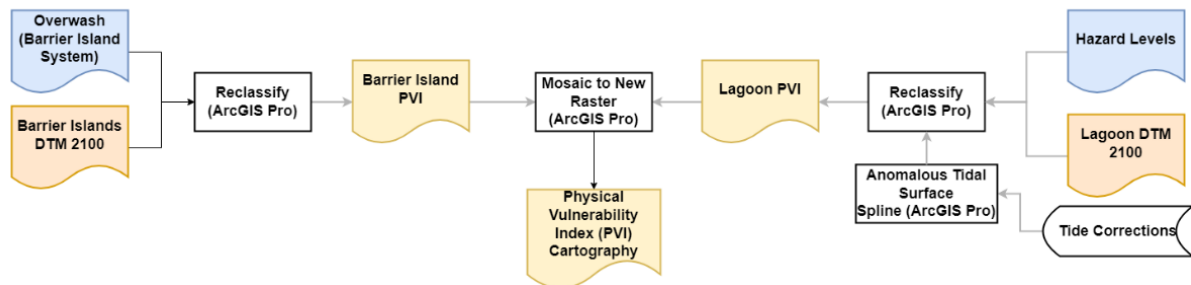


Figure 3.14 - Workflow for Chapter 3.4.3. The objective of this chapter is to obtain the Physical Vulnerability Index (PVI). This is accomplished by applying the hazard level values in Table 3.3 to their respective area of influence. For the Lagoon, an anomalous tidal surface was also introduced to account for the inland waters' tidal variations.

#### 3.4.3.1 Tide Corrections

The hazard values on for the overwash (Table 3.3) are enough to reclassify the barrier islands area, but the tides inside the intertidal area are more similar to those of an estuary, with a different pattern of HT/LT and time differences to the tide registered at the Faro gauge. To model the tides more accurately inside the Ria Formosa an anomalous tide surface was created, using the IH Table for height corrections of secondary ports, seen in Table 3.7.

Table 3.7 – Excerpt of the tidal corrections table for secondary ports in the Ria Formosa (IH). For this correction the height of the tide at spring tide was used to create the anomalous tidal surface.

Faro-Olhão Ports	Height Corrections HTst (m)
Barra do Ancão	-0.07
Faro (Cais Comercial)	0.02
Olhão (Cais da Lota)	-0.04
Barra da Armona	-0.02
Barra de Tavira	-0.03
Barra de Cacela	-0.03

The coordinates of each port as well as the tide height corrections were imported into ArcGIS Pro and a spline interpolation function is used to obtain the anomalous tidal surface with a 2 m spatial resolution. This anomalous tidal surface and the location of the secondary ports can be seen in Figure 3.15.

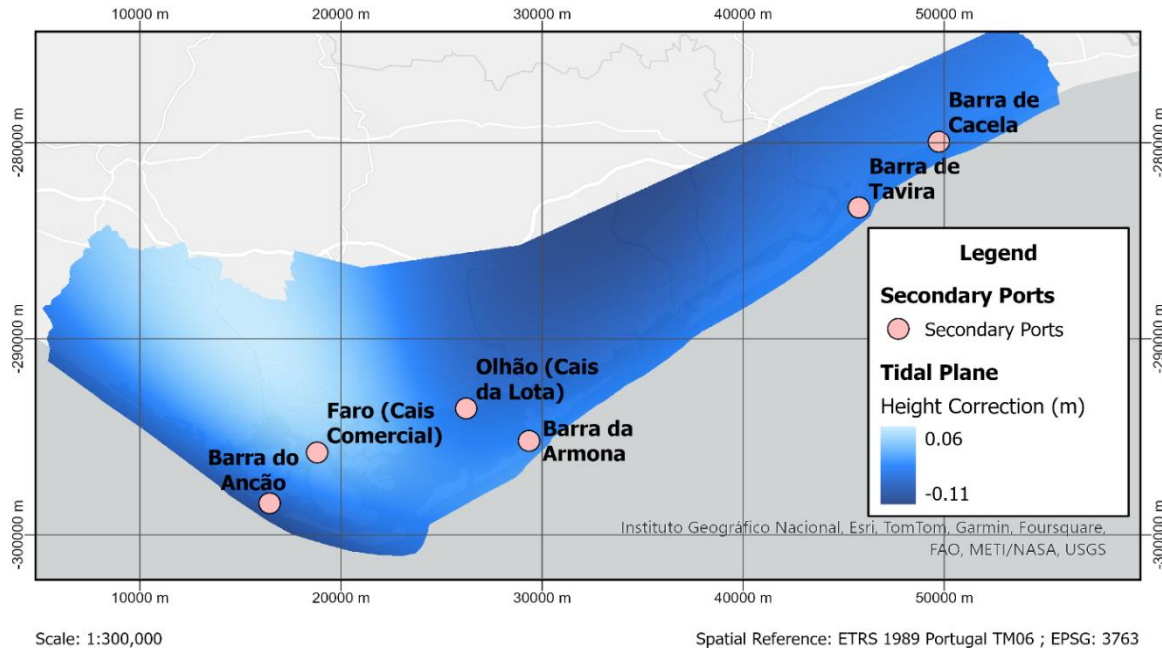


Figure 3.15 – Anomalous tidal plane for the Ria Formosa and the location of the secondary ports from Table 3.7. This region has a very slight variation in tidal heights, ranging from +0.06 to -0.11, with the area surrounding Faro (Cais Comercial) having the largest difference to the tide observed at the Faro-Olhão tide gauge.

### 3.4.3.2 Physical Vulnerability Index Cartography

The process to calculate the Physical Vulnerability Index (PVI) is split into two parts, using the segmentation and reclassification tools. The methodology used for this step is based on Costa (2017). Considering the limits established for each class in Table 3.3, surfaces are calculated using the tide surface and the higher boundary of each class. This is then used to segment and reclassify the DTM, using, for each class, the higher and lower boundary surfaces and intersecting these to determine the area that corresponds to each class.

Once the boundaries for each class have been determined these operations can then be combined using the raster mosaic tool resulting in a single raster file. However, before obtaining the final version of the PVI there is a final step that needs to be taken to guarantee the coherence of the data, that is the logical interpretation of the results obtained and clean-up of areas that are incorrectly classified.

As this model, also used for flooding hazard assessment, is based on a reclassification of the DTM it will always identify risk flood areas if they are below the maximum tide height. However, there are real situations where lower altitude areas are naturally or artificially protected by barriers of higher elevation, which should prevent flooding to those zones. To correct such issues and to facilitate the interpretation of the data, an extra step was included before joining the PVI classes, which consisted of a semi-manual clean-up of this data, by transforming the raster of each class into a polygon feature and eliminating any parts that were not contiguous with the rest of the class. Further works using this methodology, particularly for larger areas, would benefit from the implementation of image processing algorithms to automate this process. One such algorithm has been in development and is currently awaiting publication (Antunes et al., 2024b).

Once this step was completed, the classes were then able to be merged into a single raster, which represents and spatialises the Physical Vulnerability Index. One final step in the process that serves to improve the results readability is the exclusion of the areas which are already permanently submersed from the result. This data was acquired using the water classification from the COS, obtained from DGT. The Physical Vulnerability Index can be seen on Figure 3.16.

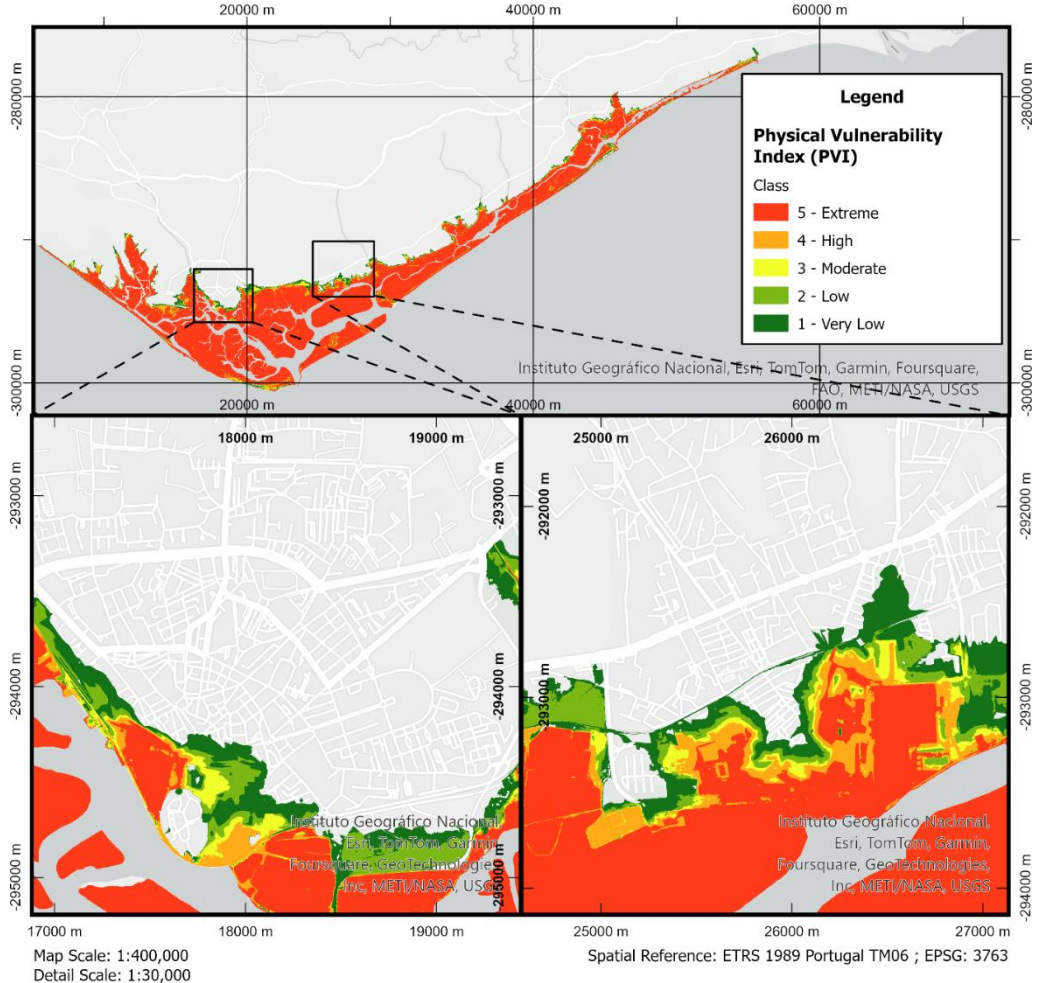


*Figure 3.16 - Physical Vulnerability Index Cartography. Each class represents the hazard levels from table 3.3. Most of the region exhibits an extreme PVI level, diminishing as it reaches the upper boundary of the lagoon. Top: Overview of the study area. Bottom Left: City of Faro and surroundings. Bottom Right: City of Olhão and surroundings.*

### 3.5 Socioeconomic Vulnerability

#### 3.5.1 Socioeconomic Susceptibility Index (SSI)

The Socioeconomic Susceptibility Index (SSI) methodology was based on Antunes et al. (2019a) and follows a similar classification criteria and weighting distribution of each parameter for the final index calculation. Consequently, the socioeconomic parameters considered for the study are the population density (PD), infrastructures (I), transport network (TN), soil use (SU), and ecological area (EA). Each of these parameters will be normalised in five classes, on a scale of 1 to 5, to express their contribution to the calculation of the SSI. Each of the following sub-chapters will explain the classification of each class in further detail. Figure 3.17 below details the workflow for the SSI.

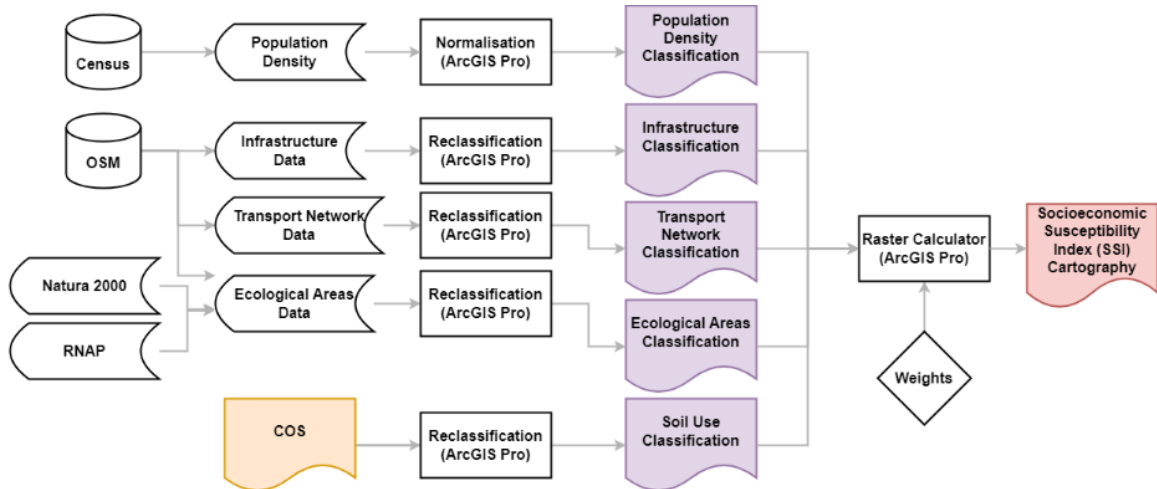


*Figure 3.17 - Workflow for chapter 3.5.1. The objective of this chapter was the calculation of the Socioeconomic Susceptibility Index (SSI). The five variables chosen for this index were Population Density, Infrastructures, Transport Network, Ecological Areas and Soil Use. This data was obtained from various sources, most notably OSM, and normalised or reclassified in ArcGIS Pro.*

The results of this classification for each of the components of the SSI for the city of Faro can be seen on figure 3.18. Maps displaying the full extent of the classified area can be found in annex A.

### 3.5.1.1 Population Density

Using the census data from 2021 (INE, 2022), the population density (PD) was calculated for each statistical sub-unit (denominated BGRI - *Base Geográfica de Referenciação de Informação*).

$$PD = \frac{\text{Inhabitants } (n)}{\text{BGRI Area } (\text{km}^2)} \quad (3.1)$$

The population density of each BGRI in the study area falls between a minimum value of 0 inhabitants/km<sup>2</sup> and a maximum value of 63 989 inhabitants/km<sup>2</sup>. The data was then classified, firstly by excluding the uninhabited areas and then utilizing a quantile distribution with five classes.

A large area of the Ria Formosa natural park is uninhabited or sparsely populated, with the main population centres located in the cities of Faro, Olhão and Tavira.

### 3.5.1.2 Infrastructures

The infrastructures (I) parameter was obtained by reclassifying information obtained from Open Street Maps (OSM) (OpenStreetMap contributors, 2017) and defining classes that account for the social and economic importance of each type of infrastructure. Three classes were considered, classes 5, 3 and 1, corresponding to critical infrastructure, local commerce, and other locations with touristic or cultural importance. Table 3.8 shows a more detailed description of the infrastructure considered in each reclassification class.

*Table 3.8 - Reclassification of infrastructure, with examples of types of infrastructure (I) considered in each class.*

Class	Description	Examples of Infrastructure
5	Critical Infrastructure	Clinics, banks, hospitals, police stations, schools, universities, fire stations, wastewater plants, communication towers, pharmacies.
3	Local Commerce	Bars, cafes, cinemas, clothes stores, restaurants, furniture shops, nightclubs, shoe shops, theme parks.
1	Cultural / Tourist Destinations	Archaeological sites, castles, forts, golf courses.

As this data was obtained from OSM (OpenStreetMap contributors, 2017) the infrastructure classification is limited by the information available on that platform. Both the cities of Faro and Olhão have a low amount of Local Commerce classification which probably does not correspond to reality. This gap in information could be solved in further local projects by obtaining information directly from city councils and town halls, whenever possible.

### 3.5.1.3 Transport Network

The transport network (TN) class is calculated based on the type and importance of the existing roads and railways. Transport networks are vital for the mobility of the population and for the distribution of goods and services. Good condition transport networks are also essential for emergency response.

The TN data was obtained from OSM (OpenStreetMap contributors, 2017) in a shapefile with line data, which necessitated a reclassification. To be able to combine this information with the other parameters, the information needed to be transformed into polygon data. This was done by attributing a width factor to each of the different classes of transport networks considered. The width factor was obtained from Antunes et al. (2019a), where the information was inferred from measurements of orthophotos in the Loulé municipality.

Table 3.9 shows the full classification of the TN, as well as the width factor used for each TN type.

*Table 3.9 - Reclassification of the Transport Network (TN) features and width factor used to convert line to polygon data.*

Class	Description	Width Factor (m)
5	Main Roads and Railway	6.0
4	Secondary Roads	5.0
3	Residential Roads	5.0
2	Tracks	5.0
1	Pedestrian Paths	2.4

### 3.5.1.4 Soil Use

The soil use (SU) parameter accounts for the different types of soil use and occupation. According to Rocha (2016), soils are more vulnerable to flooding and erosion when there is a higher level of alteration from their natural state. The soil use information was obtained from the Portuguese *Carta de Ocupação e Uso do Solo – COS2018* and accounting for the higher levels of soil alterations, the classification used is shown on Table 3.10.

*Table 3.10 - Reclassification of Soil Use (SU) based on level of alteration from their natural state.*

Class	Category
5	Urban and Industrial Infrastructure
4	Agriculture
3	Forests, Woods, Pastures
2	Naked Soil or Low Vegetation
1	Water Masses, Marsh

### 3.5.1.5 Ecological Area

The ecological area (EA) parameter has the largest disparity between the classification chosen for this dissertation and the classification adopted by Antunes et al. (2019a). As part of this project involves the development of a specific index for the environmental risk, the ecological areas appear in the socioeconomic index not due to their environmental importance and contribution to biodiversity but as assets to socioeconomic development and population well-being.

The classification adopted for the study area is then shown on Table 3.11:

Table 3.11 - Reclassification of Ecological Areas (EA).

Class	Category
5	Natural Reserves
3	Urban green areas

Natural reserves are considered to be any sites designated by either the Portuguese national protected areas network (*RNAP – Rede Nacional de Áreas Protegidas*, established by Law-Decree n.º 142/2008, *Decreto-Lei n.º 142/2008*), the European Natura 2000 network (Directorate-General for Environment (European Commission) et al., 2008) or the international Ramsar Convention (UNESCO, 1971). In the study area there are two natural reserves, namely the Ria Formosa, declared as protected area by all three of the conventions, and the Cerro da Cabeça, a national protected area. The area also includes several municipal parks and other urban green spaces, of a much smaller size.

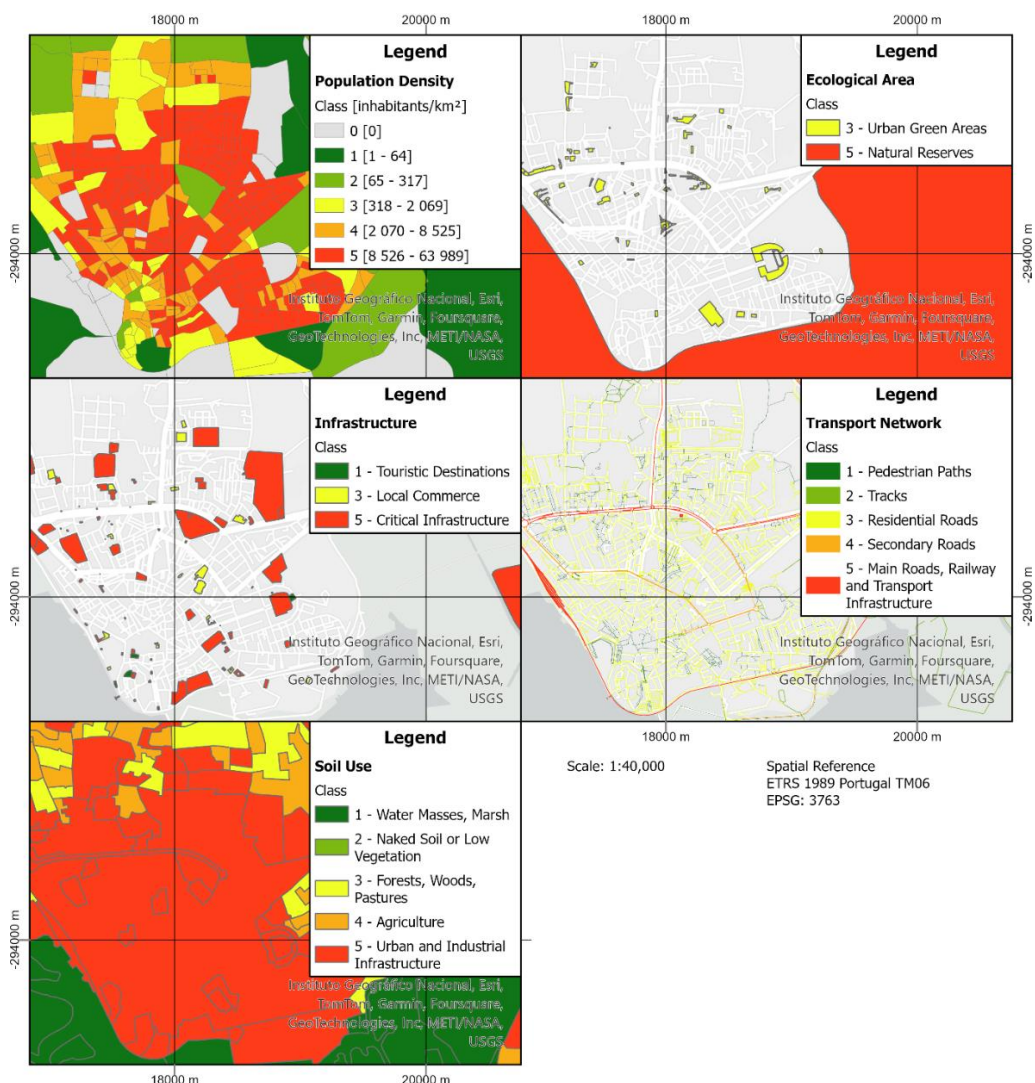


Figure 3.18 - Classification for each Socioeconomic Variable (Faro). Top Left: Population Density. Top Right: Ecological Area. Middle Left: Infrastructure. Middle Right: Transport Network. Bottom Left: Soil Use. The city is classified as an urban area with high population density. There is also a high density of roads and some critical infrastructure. The city is surrounded by the Ria Formosa nature reserve.

### 3.5.1.6 Socioeconomic Susceptibility Index

Creating the Socioeconomic Susceptibility Index (SSI) involves the combination of the five parameters considered into a single value, ranging from 1 to 5. As not all the variables have the same

importance in this index, there is usually a need to employ a methodology to define the weight given to each parameter.

As this project had the objective of incorporating the methodology of Antunes et al. (2019a) for the SSI and damage, the weight distribution of the parameters in this dissertation will use the same results obtained in that project. This classification was done through surveying a focus group of specialists and non-specialists, each asked to evaluate the importance of each parameter related to the others. The weights are then obtained through the application of the AHP method (Saaty, 1988), with higher contribution given to the specialist survey results.

The weights given to each variable can be seen on Table 3.12, and the final formula used to calculate the SSI is shown on equation 3.2.

*Table 3.12 - Weights of each parameter for the SSI, according to the results of Antunes et al. (2019a).*

Variable	Weight
Population Density (PD)	40.5%
Infrastructure (I)	18.7%
Transport Network (TN)	9.8%
Soil Use (SU)	22.0%
Ecological Area (EA)	9.0%

$$SCVI = \frac{PD \times 40.5\% + I \times 18.7\% + TN \times 9.8\% + SU \times 22.0\% + EA \times 9.0\%}{100\%} \quad (3.2)$$

Each layer of information was first converted from vectorial to raster file, followed by using equation (3.2) in the raster calculation toolbox. This result was then rounded to the unit and converted into the susceptibility class. The SSI can be seen in Figure 3.19.

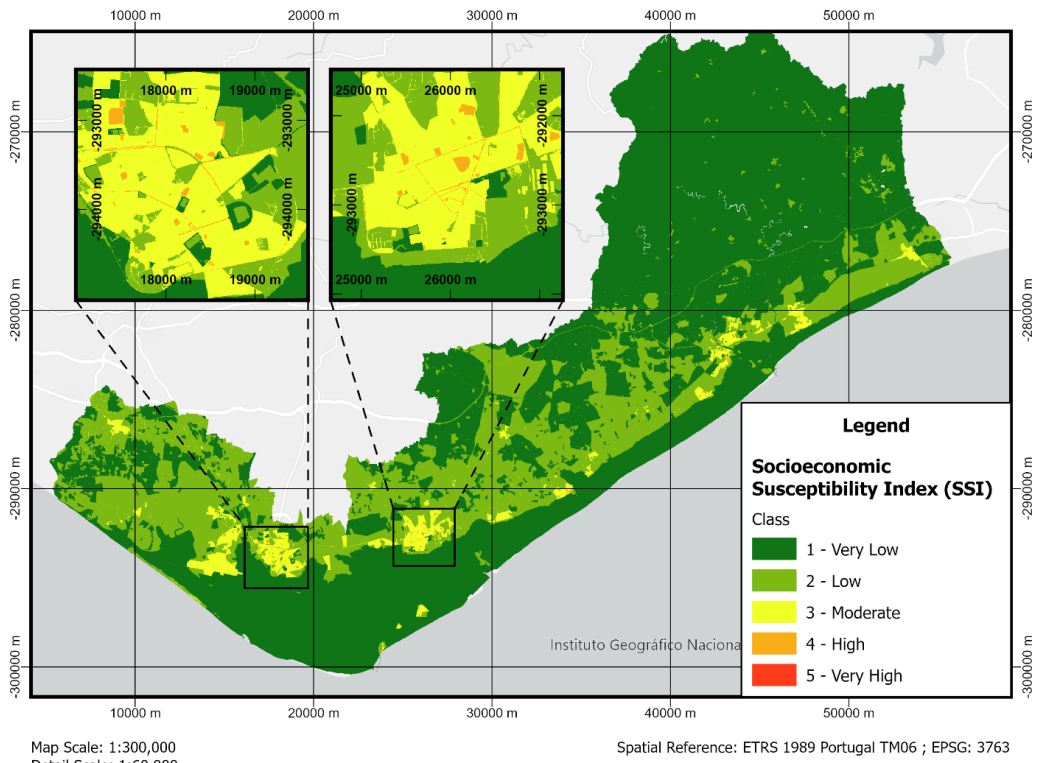


*Figure 3.19 - The Socioeconomic Susceptibility Index (SSI). Top Left: City of Faro and surroundings. Top Right: City of Olhão and surroundings Bottom: Overview of the study area. With most of the region of the Ria Formosa being unpopulated, this area presents a Very Low SSI. In the population centres the SSI reaches the Moderate, High and Very High classes.*

### 3.5.2 Socioeconomic Damage Index (SDI)

Measuring exposure and potential socioeconomic damage to an area is usually done through a deterministic approach, unlike vulnerability. Calculating the value of a building or land is a complex process that involves a large quantity of information that is hard to obtain, and, at the same time, is always relative to the period when it was calculated due to the volatility of the housing markets.

A new methodology reliant on public access data was introduced by Antunes et al. (2019a) that allows for an estimation of potential damage in a BGRI, based on the CIMI (*Código do Imposto Municipal sobre os Imóveis*) which is a reference tax formula approved by the Portuguese Law Decree n.<sup>o</sup> 287/2003 (*Decreto-Lei n.<sup>o</sup> 287/2003*). The full workflow for this chapter can be seen in Figure 3.20.

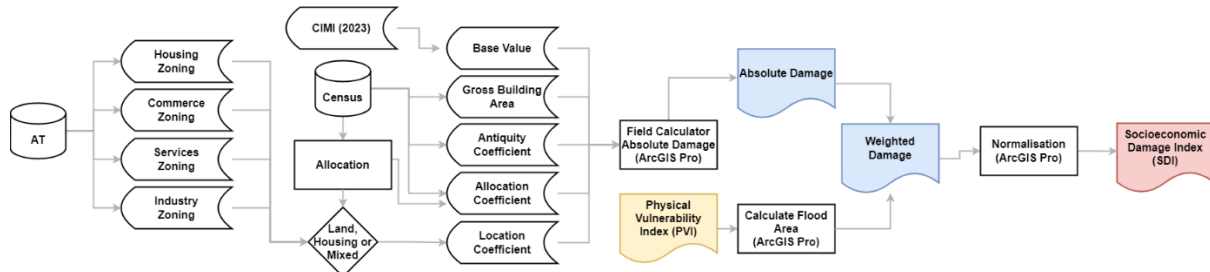


Figure 3.20 - Workflow for chapter 3.5.2. The objective of this chapter was the determination of the Socioeconomic Damage Index (SDI). Initially the Absolute Damage was calculated, based on data obtained from CIMI, Census 2021 and AT. The PVI was used to weigh this damage in a realistic flood scenario, and this was then normalised to reach the SDI.

While the CIMI established a general evaluation formula for the tax asset value of urban buildings, there was a need to adapt this formula into a simplified version that could be calculated with open data, but still allowed for the calculation of damage with sufficient accuracy. The maximum damage ( $D_M$ ) can then be calculated using the following expression:

$$D_M = B \times A \times C_A \times C_L \times C_Q \quad (3.3)$$

Where  $B$  is the base value of constructed buildings per square meter,  $A$  is the gross built up area,  $C_A$  is the allocation coefficient,  $C_L$  is the location coefficient and  $C_Q$  is the antiquity coefficient. Each of these parameters is obtained through the data available from the Portuguese Census 2021 or by a tabled value published in a Law Decree.

Before obtaining these parameters, an auxiliary variable needs to be determined, named “Allocation”. This variable will determine the formulas and constant values applied to each type of statistical unit depending on its use. This parameter is determined with data from the Census 2021 and classifies each unit in one of three categories: “land”, “housing” or “mixed”, as explained in Table 3.13.

Table 3.13 - Classification of the allocation variable based on a comparison between the number of buildings and the number of residential buildings present in a BGRI.

Allocation	Formula
Land	Number of Buildings = 0
Housing	Number of Buildings = Number of Residential Buildings
Mixed	Number of Buildings > Number of Residential Buildings

The base value of constructed buildings,  $B$ , is obtained from the CIMI, most recently updated in 2023. According to this document, the average construction value by square meter is 532.00 €/m<sup>2</sup>, with the addition of the price per square meter of the terrain where it's built, fixed at 25% of the construction value.  $B$  is a constant value, with different values for different allocations, shown in Table 3.14.

Table 3.14 - Base value per allocation type, with the respective formula to determine this value.

Allocation	Value	Formula	
Land	133.00 €	532.00 € x 25%	(3.4)
Housing, Mixed	665.00 €	532.00 € + 532.00 € x 25%	(3.5)

The gross built up area, A, is given by equation 3-4 for housing and mixed allocation, and by equation 3-5 for land:

$$A_{H,M} = \text{Average Net Inhabitable Area} \times \text{Number of Apartments} \quad (3.6)$$

$$A_L = \text{Average Net Inhabitable Area} \quad (3.7)$$

Where both the variables are obtained from the Census 2021. The average net inhabitable value will be a constant throughout all the statistical units and is currently considered 112.4 m<sup>2</sup>.

The allocation coefficient, C<sub>A</sub>, was established in Article 41, Law Decree 287/2003, with values shown on Table 3.15.

Table 3.15 - Allocation coefficients based on use type.

Use	Coefficient
Commerce	1.20
Services	1.10
Housing	1.00

Depending on the use defined by the allocation variable, C<sub>A</sub> was calculated with the expressions on Table 3.16.

Table 3.16 - Allocation coefficient based on the BGRI allocation with the expression used to calculate it.

Allocation	Value	Expression
Housing	1.00	$C_{A(H)} = C_{A(Housing)} = 1.00$ (3.8)
Mixed	1.10	$C_{A(M)} = \frac{C_{A(Housing)} + C_{A(Commerce)} + C_{A(Services)}}{3} = 1.10$ (3.9)
Land <sup>1</sup>	1.10	$C_{A(L)} = C_{A(M)} = 1.10$ (3.10)

<sup>1</sup>Note: there is no defined coefficient in the Portuguese law for land, so the mixed usage allocation coefficient was used.

The location coefficient, C<sub>L</sub>, was defined for each municipality by Ordinance 420-A/2015 (*Portaria n.º 420-A/2015*) and can vary with the type of land use (housing, commerce, industry or services). It is available for public consultation on the website of the Portuguese Tax Authority (*AT – Autoridade Tributária*), with the information in the form of a map. Unfortunately, this data is only available for visualisation and is unable to be downloaded.

This data was then manually digitised in ArcGIS Pro for each land use. Due to the extensive area of study and the long process of digitizing the information, the data was only digitized for the areas covered by the PVI, as any other areas will be null in the final product. As such, the final maximum damage calculation is not complete for the area of study, but it is complete for the RCP 8.5 2100 scenario being considered in this case study. This is the only parameter in the study not easily available and further studies using this methodology could benefit from collaboration with the AT for a smoother access to the data. The location coefficients obtained are shown in Figure 3.21.

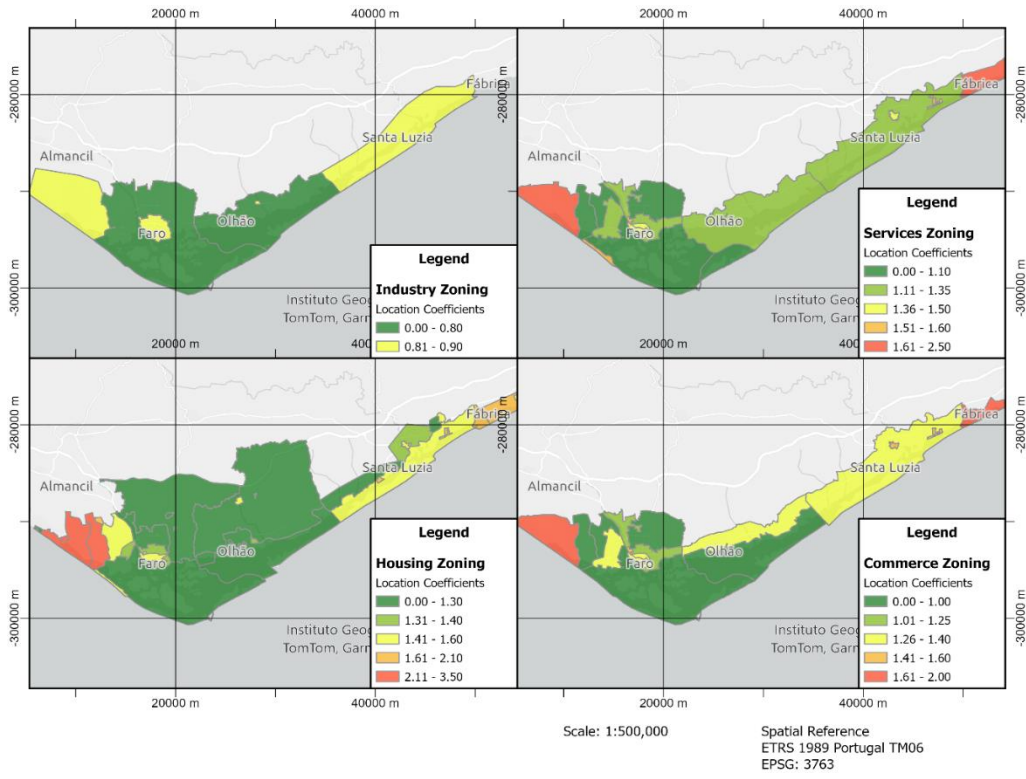


Figure 3.21 - Zoning coefficients available on the AT website, for the Ria Formosa region.

After digitizing the information, the location coefficients for each type of allocation were calculated as shown on Table 3.17.

Table 3.17 - Location coefficients by type of allocation, with the expression used to calculate them.

Allocation	Location Coefficient
Housing	$C_{L(H)} = C_{L(\text{Housing Zoning})}$ (3.11)
Mixed	$C_{L(M)} = \frac{C_{L(\text{Housing Zoning})} + C_{L(\text{Services Zoning})} + C_{L(\text{Commerce Zoning})}}{3}$ (3.12)
Land	$C_{L(L)} = \frac{C_{L(\text{Services Zoning})} + C_{L(\text{Industry Zoning})}}{2}$ (3.13)

The antiquity coefficient ( $C_Q$ ) guideline is a tabled value from the CIMI and has values in the range of 0.40 to 1.00. This coefficient corresponds to the number of years since the date of construction of a building, and can be seen in Table 3.18:

Table 3.18 - Antiquity coefficient by building age according to the CIMI.

Age (years)	Antiquity Coefficient ( $C_Q$ )
Less than 2	1.00
2 to 8	0.90
9 to 15	0.85
16 to 25	0.80
26 to 40	0.75
41 to 50	0.65
51 to 60	0.55
Over 61	0.40

There is a slight divergence with the methodology used by Antunes et al. (2019a) at this point, as that project was done with data from the Census 2011. The variables available for building ages have since been condensed into wider classes, effectively eliminating some of the data granularity. As such, it

would not make sense to use the ages of the most recent constructions as indicators for each statistical unit, as that interval was too large.

The  $C_Q$  was then calculated using an amended table of values, corresponding to  $C_Q$  guideline of the average age of each class present in the Census 2021, shown in Table 3.19.

*Table 3.19 - Antiquity coefficient adapted to the census 2021 data.*

Census 2021 Class	Age	Average Age	$C_Q$ Average Age
Built before 1945 (nB <sub>45</sub> )	76+	76.0	0.40
Built between 1946 – 1980 (nB <sub>80</sub> )	75-41	58.0	0.55
Built between 1981 – 2000 (nB <sub>00</sub> )	40-21	30.5	0.75
Built between 2001 – 2010 (nB <sub>10</sub> )	20-11	15.5	0.85
Built between 2011 – 2021 (nB <sub>21</sub> )	11-0	5.5	0.90

To obtain  $C_Q$  for each statistical unit with “housing” or “mixed” allocation, this value was then weighted by the number of buildings in each age class, divided by the total number of buildings.

$$C_Q = \frac{nB_{45} \times 0.4 + nB_{80} \times 0.55 + nB_{00} \times 0.75 + nB_{10} \times 0.85 + nB_{21} \times 0.9}{\text{Total number of buildings}} \quad (3.14)$$

In the case of “land” statistical units, there are no buildings so the expression above does not work. However, considering that the antiquity coefficient measures the devaluation of property as it ages, it was established that a  $C_Q$  of 1.00 would be used for the “land” statistical units.

Once all parameters had been obtained, equation 3.3 was used to calculate the maximum socioeconomic damage for each statistical unit, shown in Figure 3.22.

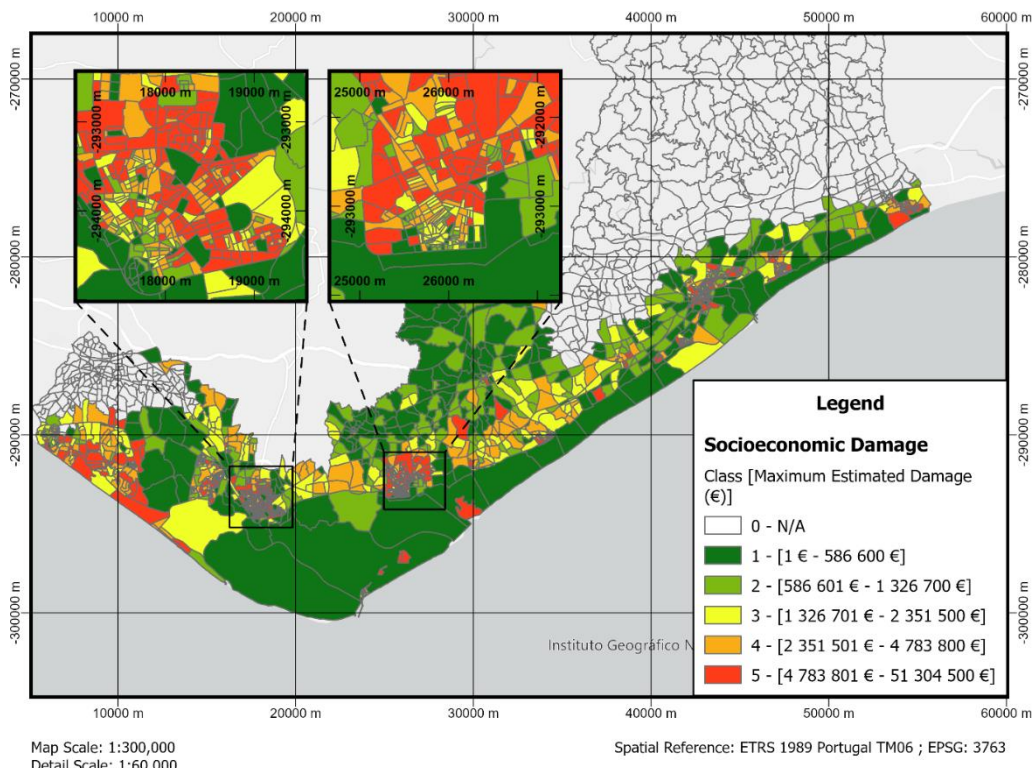


*Figure 3.22 - Maximum Socioeconomic Damage. Top Left: City of Faro and Surroundings. Top Right: City of Olhão and Surroundings. Bottom: Overview of the Area of Study. Areas with the highest levels of damage are found in the urban centres.*

This maximum socioeconomic damage value corresponds to the total damage that would be caused to buildings in a statistical unit, however, this assumes that the whole statistical unit would be affected by

the hazard. As the PVI was calculated in chapter 3.4.3, it is possible to combine these two outputs to obtain a weighted socioeconomic damage, considering only the areas vulnerable to flooding.

The PVI considers five levels of vulnerability, ranked from 1 to 5, with 5 being the most vulnerable and 1 being the least vulnerable. The weighted damage needs to be calculated considering a larger loss in areas subject to a level 5 of vulnerability, as these areas are likely to be flooded more frequently than areas with a lower level of vulnerability. The hazard in this case is extreme flooding, meaning that the damage to the buildings will also not be total, as the return period of the hazard is long. To account for this, the weighted damage was calculated with equation 3.15.

$$D_W = D_A \times \left( \frac{A_{n1}(\%)}{5} + \frac{A_{n2}(\%)}{4} + \frac{A_{n3}(\%)}{3} + \frac{A_{n4}(\%)}{2} + \frac{A_{n5}(\%)}{1} \right) \quad (3.15)$$

Where  $A_{nn}(\%)$  corresponds to the percentage of area in each statistical unit that is vulnerable to the  $n$  level of the PVI. After calculating the weighted damage, the values were then normalised from 1 to 5 using a quintile distribution, creating the Socioeconomic Damage Index (SDI) and allowing the data to be compatible with the rest of the normalised data from the SVI. The weighted damage map can be seen in Figure 3.23.

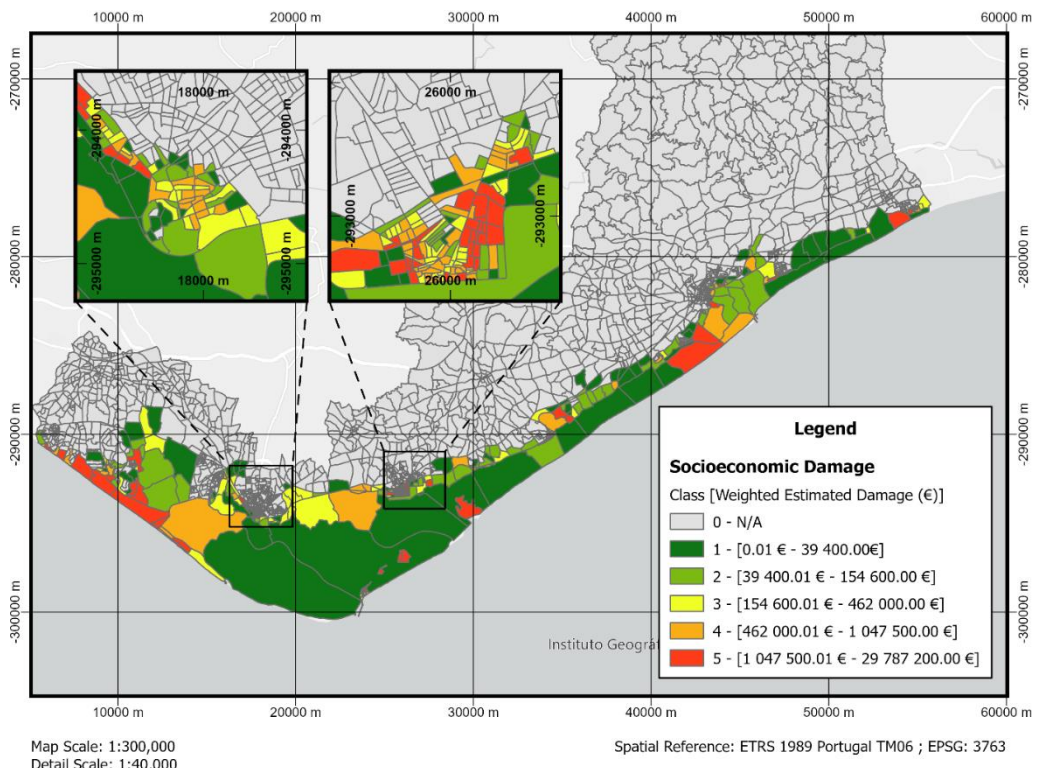


Figure 3.23 - Weighted Socioeconomic Damage. Top Left: City of Faro and surroundings. Top Right: City of Olhão and surroundings. Bottom: Overview of the study area. Using the PVI to weigh the data shows the areas which will be most damaged by SLR. Olhão in particular has a high concentration of BGRIs in class 4 and 5 damage estimations.

### 3.5.3 Socioeconomic Vulnerability Index (SVI)

The socioeconomic coastal vulnerability index (SVI) results from the combination of the SSI and the SDI, as seen in the workflow on Figure 3.24.

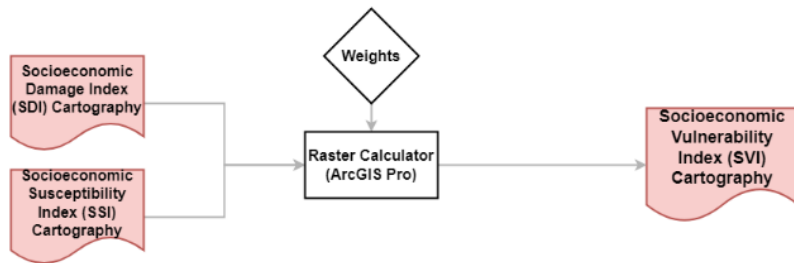


Figure 3.24 - Workflow for chapter 3.5.3. The objective of this chapter was the creation of the Socioeconomic Vulnerability Index (SVI), by combining the SSI and SDI obtained in chapters 3.5.1 and 3.5.2, respectively.

For this combined index, a weighted average approach was used, in line with the methodology applied by Antunes (2019a), where the SDI was given a weight of 60% and the SSI was given a weight of 40%.

$$SVI = \frac{60\% \times SDI + 40\% \times SSI}{100\%} \quad (3.16)$$

The results of equation (3.16) are rounded to the unit and used as classes for the SVI map, which can be seen on Figure 3.25. As with the previous indices, most of the areas under the “high” classification are in the urban areas of the main cities around the Ria Formosa, as well as the Faro Airport, with some small stretches being under the “extreme” classification.

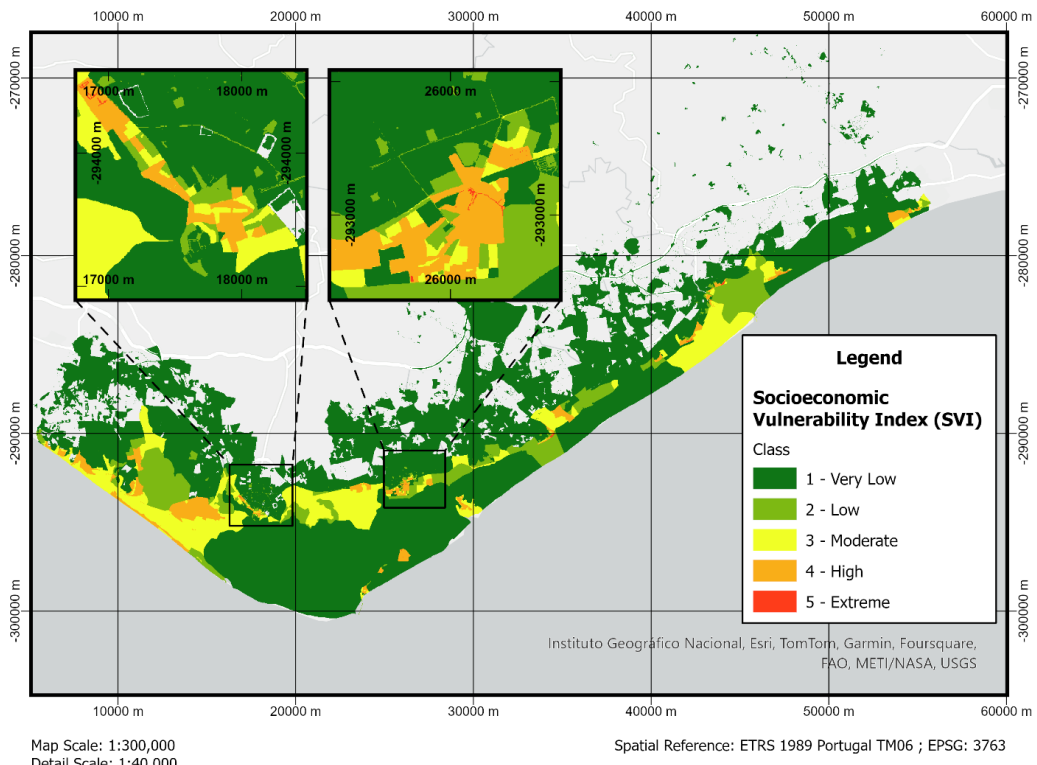


Figure 3.25 - The Socioeconomic Vulnerability Index (SVI). Top Left: City of Faro and surroundings. Top Right: City of Olhão and surroundings Bottom: Overview of the study area.

## 3.6 Environmental Vulnerability

### 3.6.1 Environmental Susceptibility Index (ESI)

As discussed in chapter 3.1, the Ria Formosa is a natural reserve, mainly featuring a saltmarsh environment protected by barrier islands.

Evaluating environmental vulnerability firstly depends on the ability to classify the area in the different types of intertidal ecosystems. A full workflow of the methodology followed in this chapter can be seen in Figure 3.26.

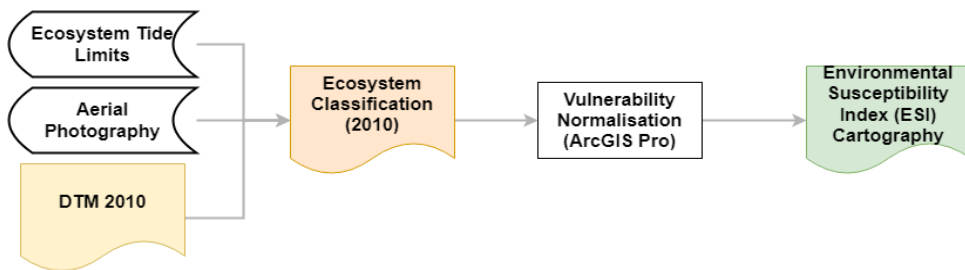


Figure 3.26 - Methodology for Chapter 3.6.1. The objective of this chapter was to obtain the Environmental Susceptibility Index (ESI). This was accomplished by using the ecosystem tide limits. Aerial photography and the DTM 2010 to identify the ecosystems and classify them according to their susceptibility to SLR.

Following the methodology applied by Ferreira (2022), intertidal mudflats, low saltmarsh and high saltmarsh areas can be classified using the elevation of each area and associating it to tide levels, the same process done in chapter 3.4.2 to determinate the accretion rates, following the data in Table 3.5. The ecosystems are delimited with the following criteria:

- Subtidal: Below the lowest low tide;
- Intertidal Mudflats: between the lowest lot tide to the neap tide high tide;
- Low Saltmarsh: between the neap tide high tide and the average high tide;
- High Saltmarsh: between the average high tide and the maximum high tide.

The scenario for 2100 is added of +0.884 m to simulate the sea level rise. Table 3.20 shows the height limits considered for each environment.

Table 3.20 - Ecosystem Boundaries. First column: Tide height (CD), Second column: Tide elevation (MSL), Third column: Tide elevation in 2100 (MSL)

2010			2010			2100		
Ecosystem	Min	Max		Min	Max		Min	Max
Tidal Flats	0.25	2.76	- 2 m (CD)	-1.75	0.76	+0.884 m (SLR)	-0.87	1.65
Low Saltmarsh	2.76	3.14		0.76	1.14		1.65	2.02
High Saltmarsh	3.14	3.92		1.14	1.92		2.02	2.80

Identifying the dunes and beaches (sand barriers) was done manually using the DTM and aerial photography data, with the difference for 2100 coming from differences in the submersed and emersed areas in the DTMs for 2010 and 2100.

Considerations were made with regards to urban and agricultural areas in the Ria and in the surrounding area. In the 2010 scenario these areas are not classified as part of the ecological area but for 2100 multiple paths could be considered: there could be no efforts to protect any of these areas and allow the ecosystem to expand inward or all the urban and agricultural areas could be preserved, compressing the ecosystem. Currently there is a large push from governmental and environmental agencies to abandon the urban areas on the barrier islands (*Despacho n.º 3841/2017, Decreto-Lei n.º 31/2014*), more vulnerable to erosion and previously damaged in storms. The most likely scenario for 2100 could then be a protection of the inland urban and agricultural areas while allowing the barrier islands to evolve without intervention.

Figure 3.27 shows the ecosystem classification of the Ria Formosa in 2010.

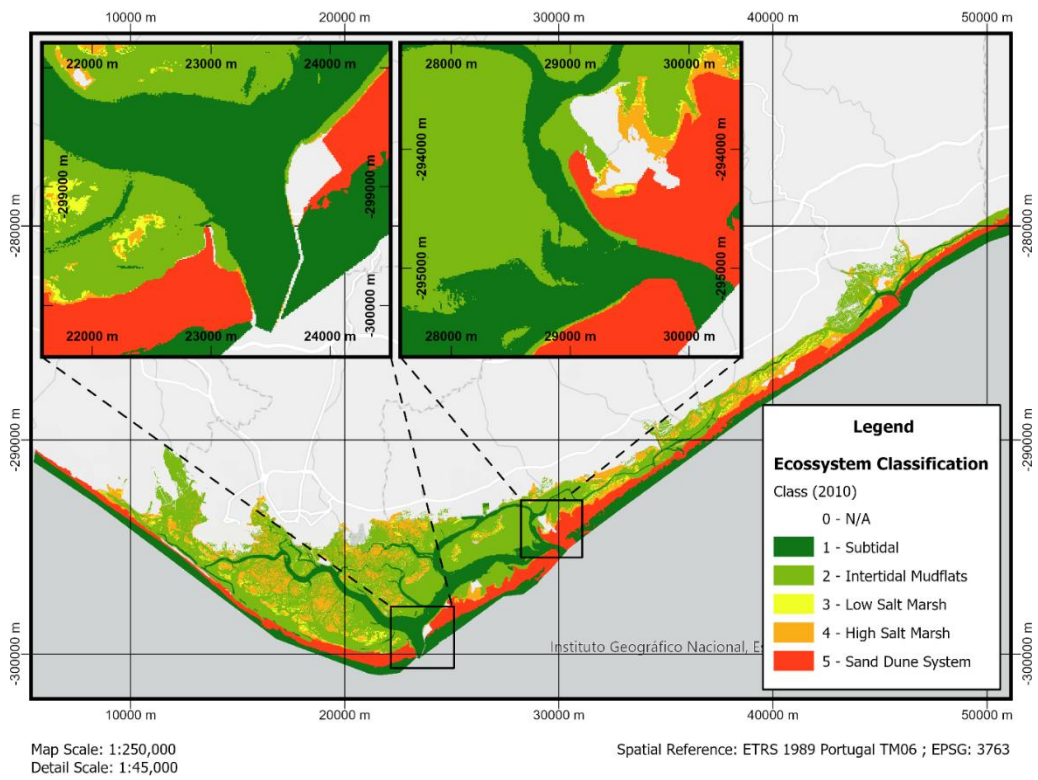


Figure 3.27 - Ria Formosa Ecosystem Classification for 2010. Top Left: Faro-Olhão inlet and the Ilha do Farol urban area. Top Right: Armona inlet and the Armona island urban area. Bottom: Overview of the study area.

The susceptibility of each environment was classified based on their ability to withstand and recover from extreme weather events, as well as their adaptability to long-term steady SLR. It was found that the highest susceptibility is exhibited by the dunes, as they serve as the main protection mechanism for the lagoon, responsible for dissipating most of the wave energy and thus being the most prone to damage during these events. Conversely, the subtidal and intertidal areas are the most adaptable to SLR, resulting in a lower susceptibility. The low and high saltmarsh areas are projected to experience a pressure level falling between that of the dunes and the tidal flats. With these considerations, the classification shown in Table 3.21 was implemented.

Table 3.21 - Susceptibility classification per ecosystem according to their ability to withstand extreme weather events.

Area	Susceptibility Class
Sand Dune System	5
High Saltmarsh	3
Low Saltmarsh	3
Tidal Flats	1
Submersed	1

The ESI classification for the region can be seen in Figure 3.28.

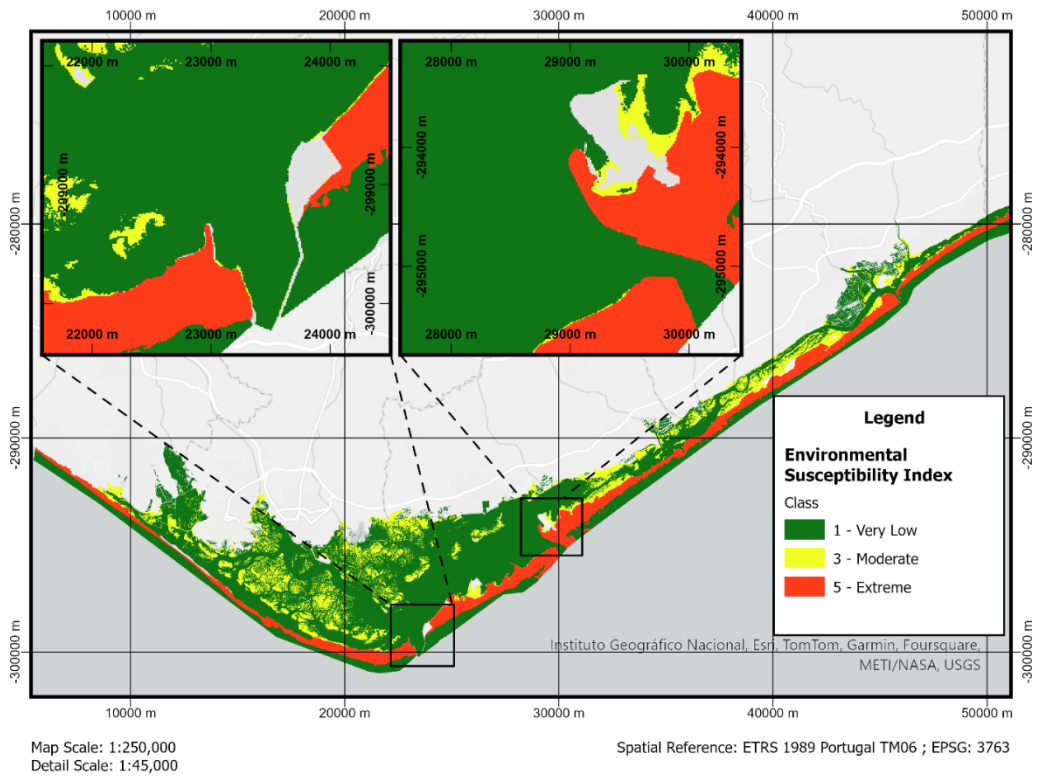


Figure 3.28 - Environmental Susceptibility Index (ESI). Top Left: Faro-Olhão inlet and the Ilha do Farol urban area. Top Right: Armona inlet and the Armona island urban area. Bottom: Overview of the study area.

### 3.6.2 Environmental Damage Index (EDI)

Calculating the value of an ecosystem is a much more subjective task than calculating the value of properties or land. Attributing a monetary value to the Ria Formosa is not only a matter of quantifying the size of the land but also to consider all the services and benefits such a system can provide. Such a project would be beyond the scope of this dissertation and require a much more in depth economic and ecological analysis.

While quantifying the amount of damage caused to the lagoon by sea level rise is extremely hard, it is, however, possible to compare the different ecosystems and assess the differences in the services they provide. The workflow followed in this chapter can be seen in Figure 3.29.

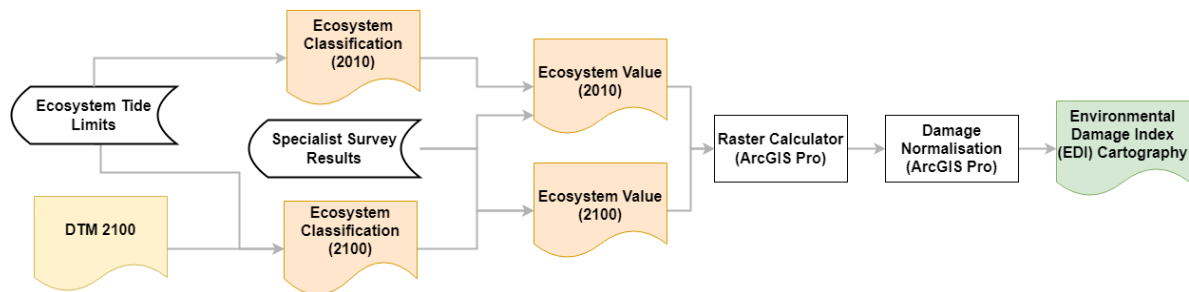


Figure 3.29 - Workflow for chapter 3.6.2. The objective of this chapter was the calculation of the Environmental Damage Index (EDI). This was achieved using the results of a survey of experts and the ecosystem mapping done in chapter 3.6.1.

Focusing on comparing ecosystem services does allow for a certain valuation of the ecosystems, which can then be calculated for both the 2010 DTM and the 2100 DTM, with damage resulting from the difference between them.

To accomplish this valuation, a survey was conducted among experts who have knowledge in both ecosystem services and saltmarsh environments. The survey was conducted between July and

September 2023 and had six respondents from investigators associated with the University of Lisbon and the University of Algarve, in the areas of environmental biology, marine biology, ecology and oceanography. A full overview of the survey results can be found in annex B.

As this is the first study of its type it was established that each expert's input would have the same weight and each ecosystem service would be given the same importance. Further studies using a similar methodology could opt for using a more complex statistical methodology such as an AHP analysis to attribute weights to each parameter to further approximate to a more realistic scenario.

The survey asked each expert to rank from 1 to 5 the importance of each of the ecosystems of the Ria Formosa: sand dune system, high saltmarsh, low saltmarsh, intertidal mudflats and subtidal area, in the context of each ecosystem service: support, provisioning, regulation and cultural. The results were first aggregated by ecosystem service using a geometric average and then averaged once again by ecosystem with a second geometric average. The geometric average was the method chosen as it presented the largest distribution of the results. The value attributed by specialists to each area is shown on Table 3.22.

*Table 3.22 - Value attributed by the experts' survey to each ecosystem using a geometric x geometric averaging method.*

Ecosystem	GG
Sand Dune System	3.46
High Saltmarsh	3.42
Low Saltmarsh	3.80
Intertidal Mudflats	4.26
Subtidal Area	4.22

This data can then be used to reclassify the raster on Figure 3.27 so that each pixel of an ecosystem is assigned the value agreed upon by the study. For ease of processing, the values of each section were multiplied by 100, which will not impact the final result as it will be normalised. The value reclassification can be seen in Figure 3.30:

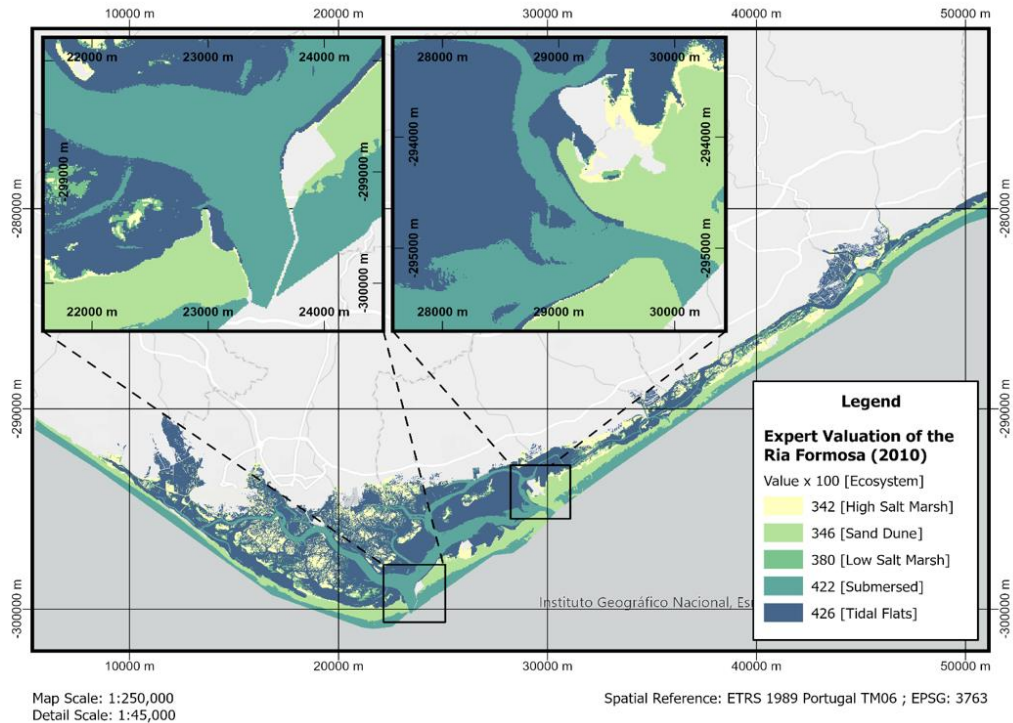


*Figure 3.30 - Mapping of the expert valuation of ecosystems. Top Left: Faro-Olhão inlet and the Ilha do Farol urban area. Top Right: Armona inlet and the Armona island urban area. Bottom: Overview of the study area.*

Calculating the comparative damage to each area is then done by reclassifying the 2100 DTM in the same manner and then subtracting the 2010 valuation from the 2010 valuation. Finally, this result is then normalised into an index (shown in Figure 3.31), classified in accordance with Table 3.23:

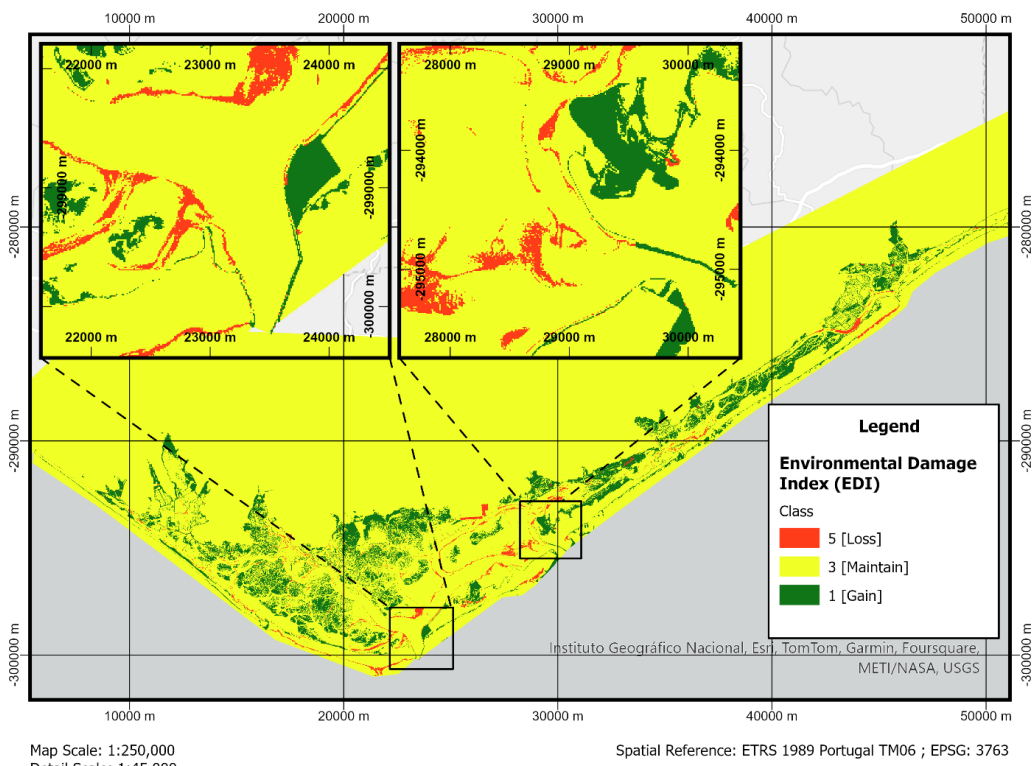


*Figure 3.31 - Environmental Damage Index (EDI) of the Area of Study. Top Left: Faro-Olhão inlet and the Ilha do Farol urban area. Top Right: Armona inlet and the Armona island urban area. Bottom: Overview of the study area. The loss areas mostly correspond to areas where the intertidal mudflats became subtidal.*

Table 3.23 - Normalisation of damage values into classes.

Class	Damage Value	Description
1	< 0	Gain
3	= 0	Maintain
5	> 0	Loss

### 3.6.3 Environmental Vulnerability Index (EVI)

The Environmental Vulnerability Index (EVI) results from the junction of the ESI and the EDI. These indices are combined through a weighted average, as shown in the workflow on Figure 3.32.

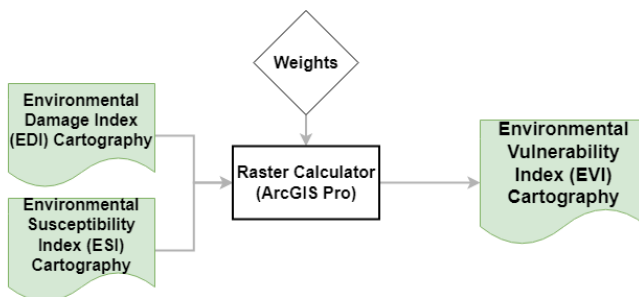


Figure 3.32 - Workflow for chapter 3.6.3. The Environmental Vulnerability Index (EVI) resulted from the combination of the ESI and EDI calculated in chapters 3.6.1 and 3.6.2, respectively.

An argument could be made for using either a 50-50% split or a 60-40% split, similar to what was used in the SCVI, however, as the environmental indices only exhibit classes 1,3 and 5, the results of both approaches would be the same. In any case, since there is a small sample of surveys and no other literature, it would be most prudent to use a 50-50% split until more information can be obtained.

Unlike the ESI and EDI, the EVI will maintain 5 classes in order to be compatible with the socioeconomic and physical vulnerability indices. The EVI for the Ria Formosa is shown in Figure 3.33.

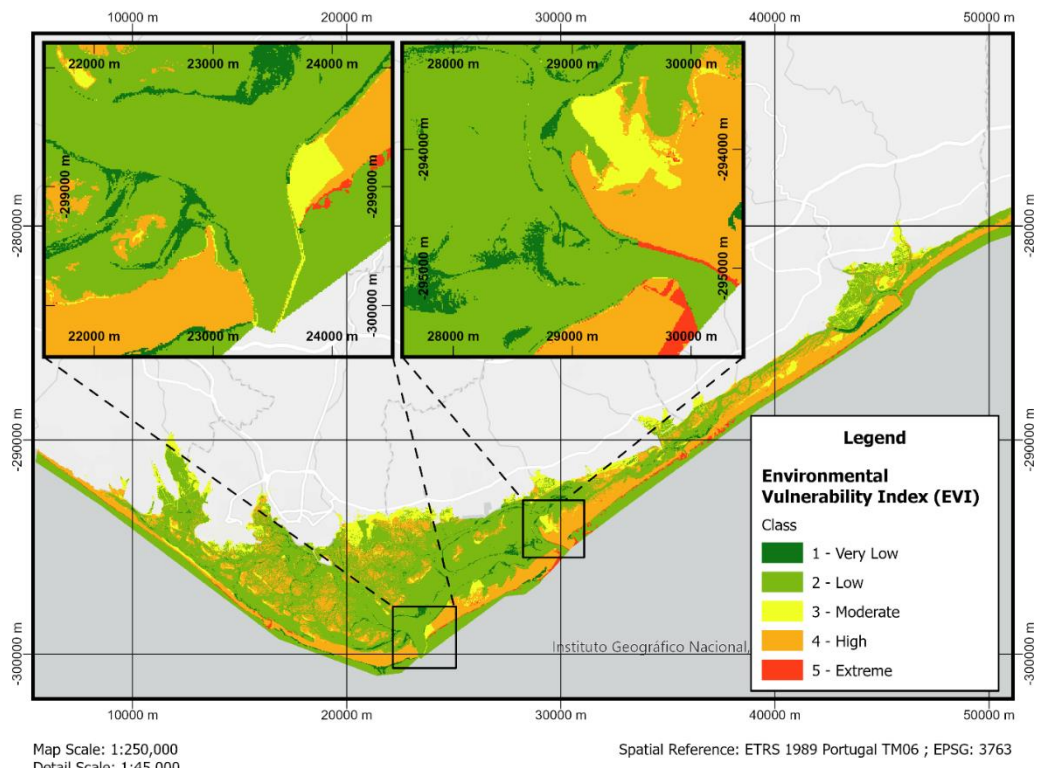


Figure 3.33 - The Environmental Vulnerability Index (EVI). Top Left: Faro-Olhão inlet and the Ilha do Farol urban area. Top Right: Armona inlet and the Armona island urban area. Bottom: Overview of the study area.

### 3.7 Composed Indices and Parameter Sensitivity Analysis

Classically, and as recommended for coastal risk assessment by Rocha et al. (2023) the formulation of the combination of indices to represent risk results from the multiplication of all indices:

$$Risk = Hazard \times Physical\ Susceptibility \times Vulnerability \quad (3.15)$$

Usually, this is normalised by using a geometric or weighted arithmetic average approach.

As indices have evolved, authors (e.g. Antunes et al. (2019a); Bagdanavičiūtė et al. (2019); Calil et al. (2017); Rocha et al. (2020); Satta et al.(2017)), have started to experiment with other approaches to combine these indices together. A weighted average seems to be a popular approach due to the fact that it can more easily be adjusted to give higher importance to certain factors that authors might consider more important.

While the two methods are valid approaches, geometric averages tend to minimise the result of the combination of two indices, while weighted averages tend to maximise the result. When performing sequences of combining indices, the geometric average becomes more disadvantageous as some of the granularity of the data is lost and the result becomes smoother. Figure 3.34 below shows the difference of results between both approaches, as well the result of a 60-40 weighted average.

Geometric Average						50-50 Weighted Average						60-40 Weighted Average					
	1	2	3	4	5		1	2	3	4	5		1	2	3	4	5
1	1	1	2	2	2	1	1	2	2	3	3	1	1	1	2	2	3
2	1	2	2	3	3	2	2	2	3	3	4	2	2	2	2	3	3
3	2	2	3	3	4	3	2	3	3	4	4	3	2	3	3	3	4
4	2	3	3	4	4	4	3	3	4	4	5	4	3	3	4	4	4
5	2	3	4	4	5	5	3	4	4	5	5	5	3	4	4	5	5

Figure 3.34 - Comparison of aggregation methodology, results of joining two different indices.

In this dissertation, as there are multiple steps necessary to reach the final indices, the weighted average was the predominantly used method, following the work done by Antunes et al. (2019a).

### 3.8 Coastal Risk

#### 3.8.1 Socioeconomic Risk Index (SRI)

The Socioeconomic Risk Index (SRI) results from the combination of the SVI and the PVI and is shown in Figure 3.35. This map represents the risk to populations and economic activity in the region.

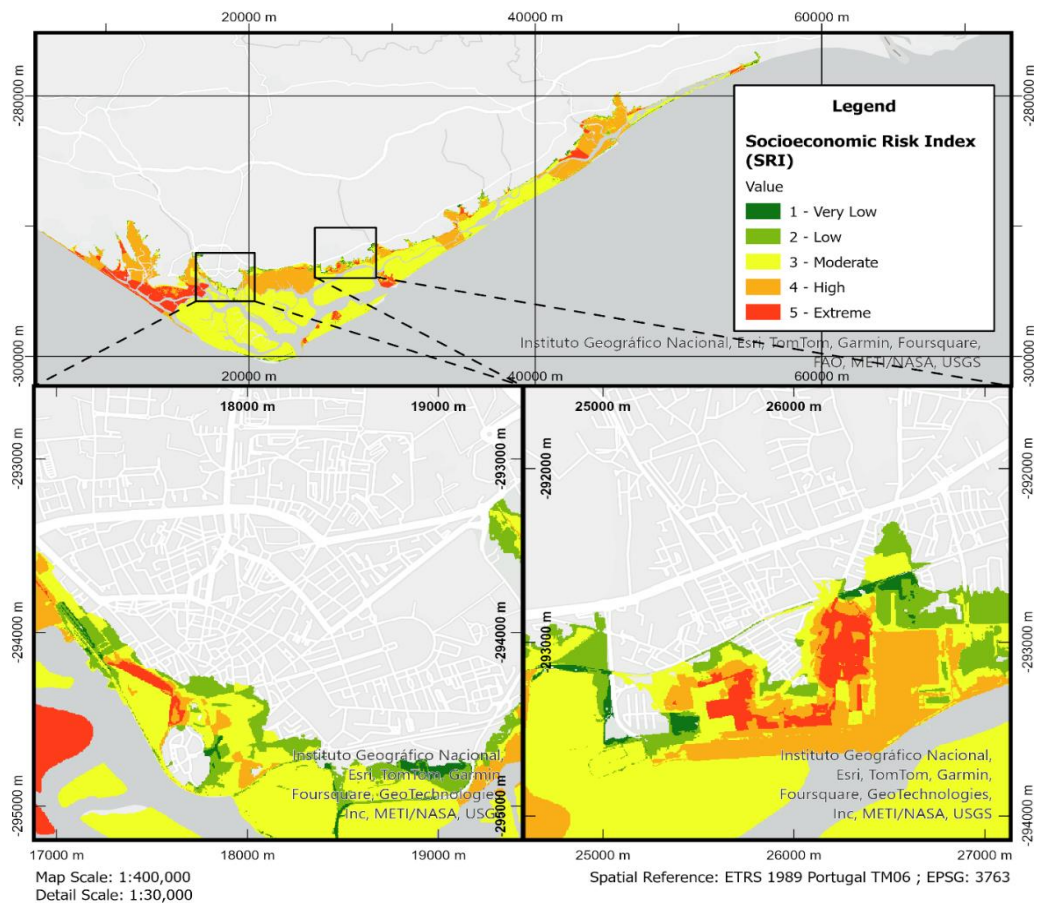
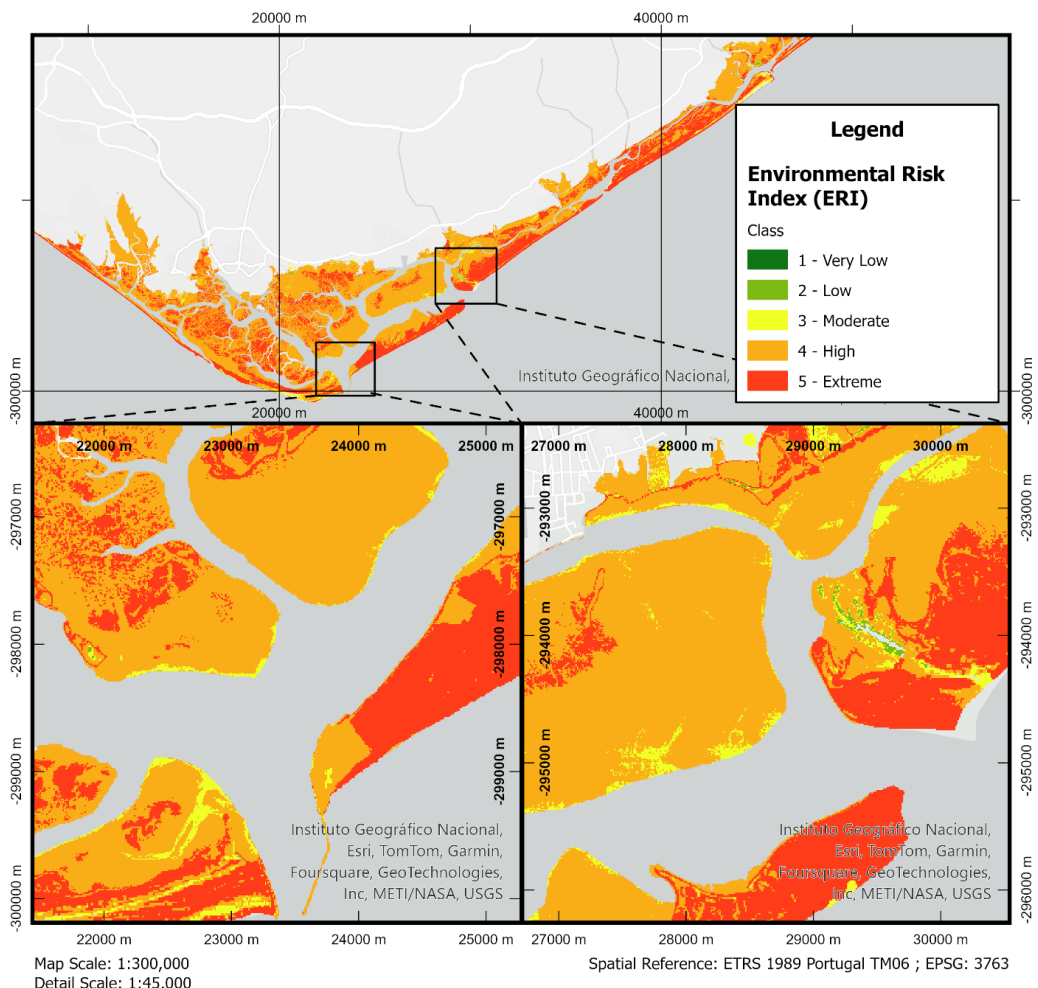


Figure 3.35 - The Socioeconomic Risk Index (SRI). Top: Overview of the study area. Bottom Left: City of Faro and surroundings. Bottom Right: City of Olhão and surroundings. Most of the high and extreme socioeconomic risk is concentrated in the urban areas, notably the inhabited regions of the barrier islands.

### 3.8.2 Environmental Risk Index (ERI)

Equivalently to the SRI, the Environmental Risk Index (ERI) results from the combination of the EVI and the PVI and is shown in Figure 3.36. This map represents the risk to ecosystems in the region.



*Figure 3.36 – The Environmental Risk Index (ERI). Top Left: Faro-Olhão inlet and the Ilha do Farol urban area. Top Right: Armona inlet and the Armona island urban area. Bottom: Overview of the study area. The whole wetland area is mostly at a high or extreme environmental risk.*

### 3.8.3 Multi-parametric Vulnerability Index (MVI)

Creating a multi-parametric coastal risk index (MCRI) implies a two-step process, where first the vulnerability indices for the socioeconomic (SVI) and environmental (EVI) parameters must be aggregated, creating a multi-parametric vulnerability index (MVI) which then can be combined with the PVI.

There are multiple possibilities to combine the EVI and SVI, which all have their advantages and disadvantages.

The first possibility considered consists of mapping the area in a way that where the EVI exists, the EVI is used, otherwise the SVI is used. This ensures that for the natural park the index used reflects the environmental parameters, while maintaining the SVI for the surrounding area. The main concern with this approach is the intricate balance between urban and natural areas in the Ria Formosa – there are urban areas inserted in the protected area (Ilha do Farol, Praia de Faro) where the vulnerability would diminish because only the ecological index would be used in those regions. Concurrently, the natural area was given a socioeconomic value in the SSI, which would be completely disregarded if this approach was used.

A second possibility is, once again, the use of a weighted average between the EVI and SVI. While most of the other indices that used a weighted average had a 50-50% contribution, in this case the contribution of the EVI would have to be much larger than that of the SVI for the areas where the EVI is present. This does solve the issue of the socioeconomic contribution of the natural reserve and

mitigates the problem with the urban areas on the barrier islands, but it's hard to find the ideal balance between the weights of the indices.

The last possibility considered was the use of a maximum function, where the maximum value between the EVI and the SVI in the areas where both exist would be used. In this case, the issue of the urban areas is completely resolved but the use of the ecological part of the SSI still depends on whether the SVI class exceeds that of the EVI.

Figure 3.37 shows a comparison between the three methods, where the weighted method used a distribution of 80% EVI and 20% SVI in the areas where both exist.

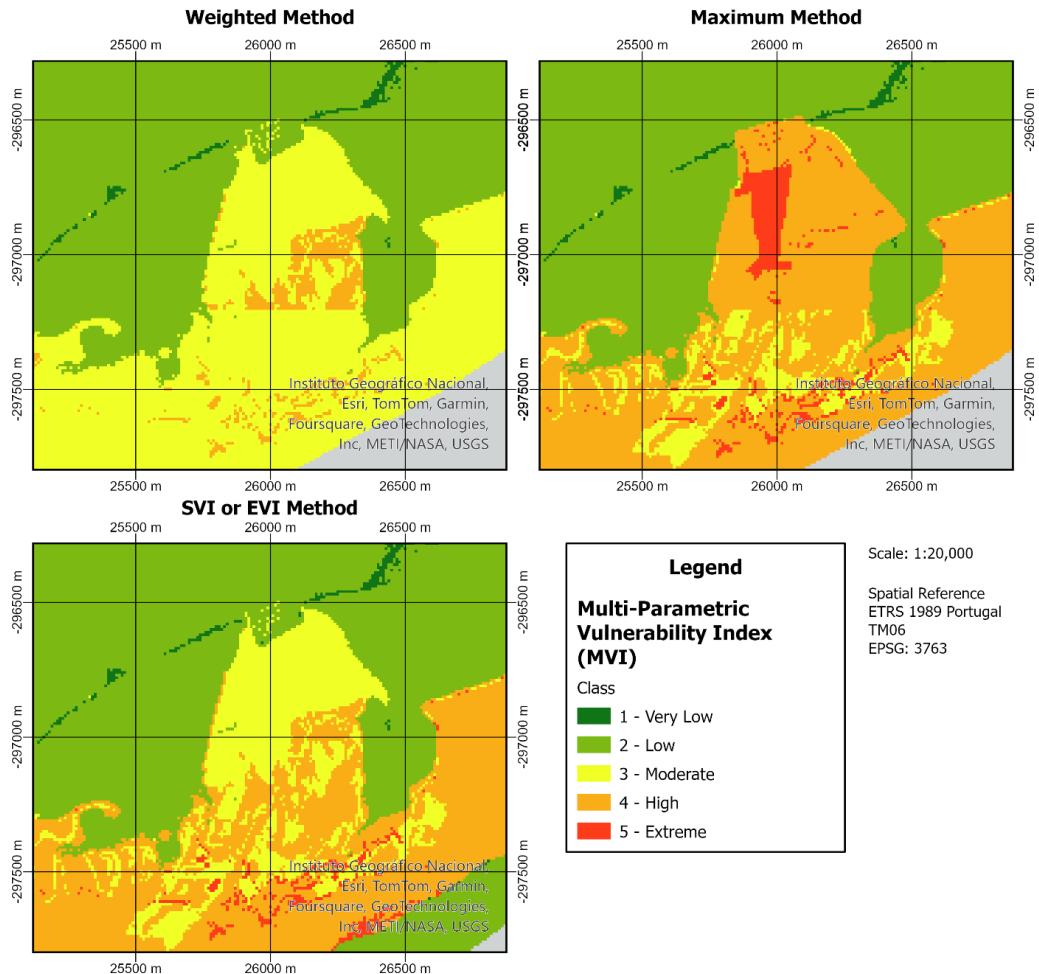


Figure 3.37 - Comparison between the results of MVI methodologies applied to the urban area of Culatra Island.

Choosing a method over another is subjective and highly dependent of the area of study. Regions with different configurations may not have the same complications and as such could use a methodology more in line with the other indices, however, in the case of the Ria Formosa, special attention needs to be paid to the complexity of the barrier island system. Analysing Figure 3.37, it is clear that the maximum method is the only one that reflects the increased socioeconomic vulnerability of the urban area while maintaining a similar environmental vulnerability for the area surrounding it. Taking this into account, the maximum function was chosen to calculate the MVI.

### 3.8.4 Multi-parametric Coastal Risk Index (MCRI)

After calculating the MVI, it can then be used, together with the PVI, to calculate the Multi-parametric Coastal Risk Index (MCRI), using a 50-50% weighted average. The result can be seen in Figure 3.38.

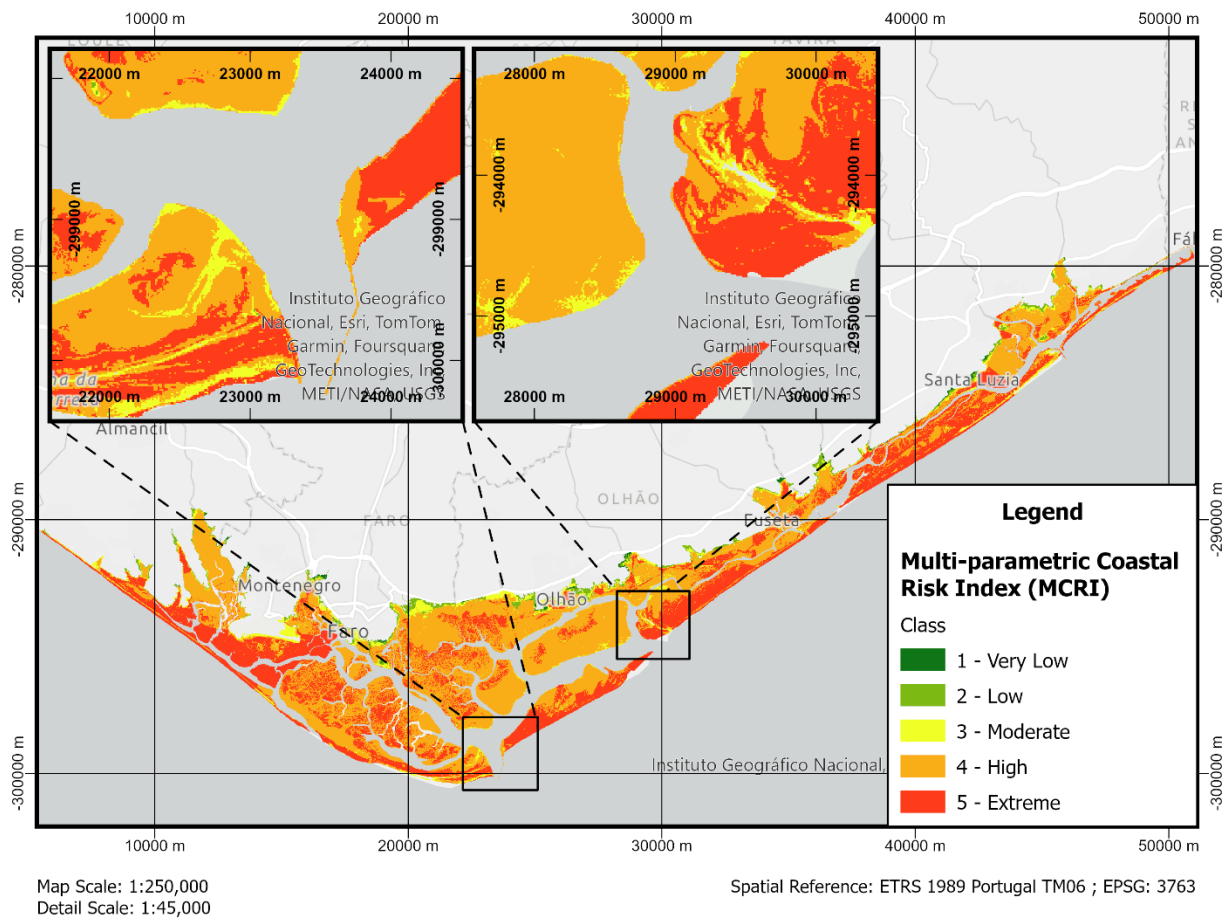


Figure 3.38 - Multi-parametric Coastal Risk Index (MCRI). Top Left: Faro-Olhão inlet and the Ilha do Farol urban area. Top Right: Armona inlet and the Armona island urban area. Bottom: Overview of the study area.

Other versions of the MCRI, using the other variants of the MVI previously discussed are available in annex C.

## 4. Results and Discussion

### 4.1. Physical Vulnerability

The study of the physical vulnerability of the region has shown a weakening of the sand dune system due to increased erosion on the ocean side and SLR. On the lagoon side there is also a notable retreat of the shoreline. Figure 4.1 shows the difference in the shoreline in 2010 and 2100.

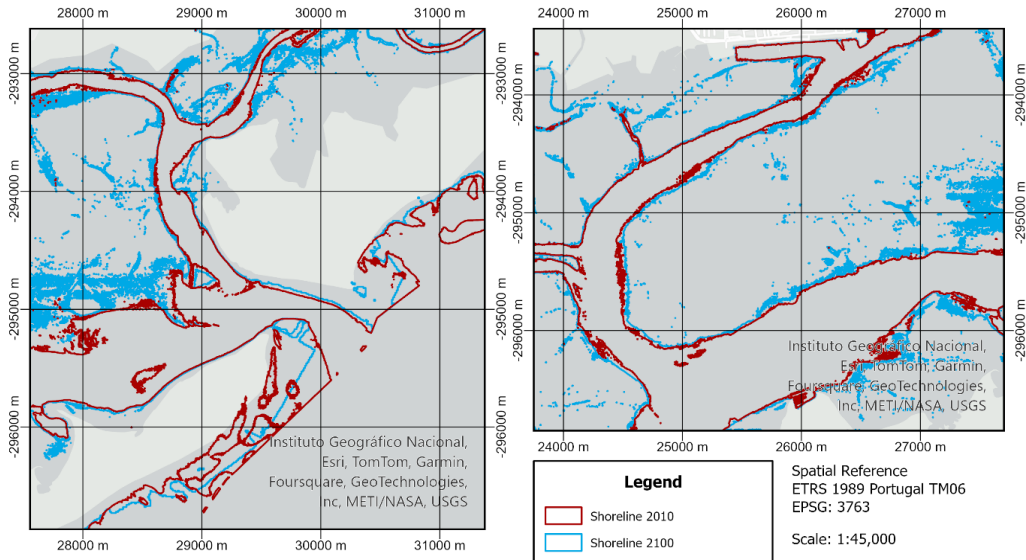


Figure 4.1 - Shoreline difference between 2010 and 2100. Left: Armona Inlet. Right: Lagoon area, south of Olhão.

Considering the total area used in the study, in 2010 there were 257.92 km<sup>2</sup> of land completely or partially above water, which has diminished to 252.34 km<sup>2</sup> by 2100. This represents an increase of over 5 km<sup>2</sup> in the subtidal area. On the ocean front of the barrier island system, in most cases, the shoreline is retreating between 20 m and 70 m, with some exceptions in areas of high sedimentation like the Barreta Island, where the shoreline is advancing. The opposite is true for areas with high sedimentary deficit, such as the east end of the Culatra Island, seen on the left of Figure 4.1, where the shoreline retreat reaches 260 m.

The total stretch of coastline analysed amounts measures a length of 96.96 km, divided in segments of 10 m. The overall land migration observed resulted in a retreat of 140.39 km over 90 years, resulting in a coastline retreat rate of approximately 0.16 m/yr, marking a 0.05 m/yr increase comparatively to the data obtained from Lira et al. (2016). Considering the difficulties with the algorithm encountered in chapter 3.4.2, it is possible this coastline retreat will be even larger than the rate obtained in this project. The distribution of the coastline retreat in these segments can be seen in Figure 4.2.

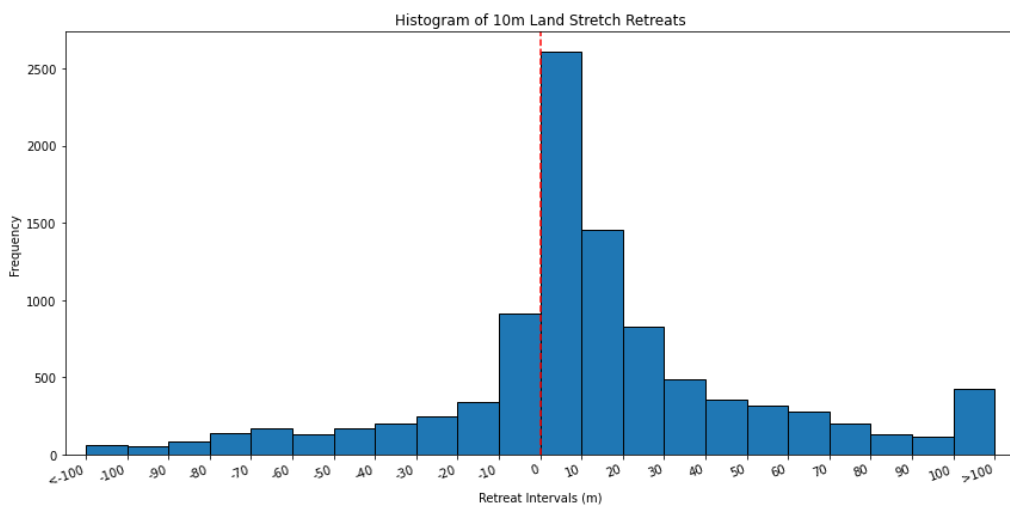


Figure 4.2 - Coastline Retreat by 10 m Segment. Negative Values Represent Shoreline Advance while Positive Values Represent Shoreline Retreat.

These results are reflected in the PVI, which shows most of the barrier islands and lagoon on very high or extreme vulnerability levels: most of the intertidal and inland area is at much lower height than the barrier islands.

With the levels of erosion estimated in this project, the barrier system will be severely damaged and offer less protection over time, putting at risk both the ecosystem and the urban centres that depend on its existence. From the coastline stretches considered in the PVI analysis, shown in figure 3.11, three main areas where the barrier system will be severely weakened are the area around the Ancão Inlet, both on the Ancão Peninsula and Barreta Island, the east side of the Fuzeta Inlet, affecting mainly Tavira Island, and the eastern half of Cabanas Island until the Lacém Inlet. These stretches will probably be completely below the maximum swash by 2100.

## 4.2. Socioeconomic Vulnerability

Using the data from the Census 2021 and the PVI it's possible to infer the number of buildings and residents exposed to the hazard, as well as quantify the percentages of areas that can be impacted. These demographic statistics are evaluated at the statistical unit level and can then be aggregated to the civil parish or municipality level.

Figure 4.3 shows a summary of these demographic exposure statistics, as well as the weighted damage, at a civil parish level. Table 4.1 explores the same information but with a higher level of detail, accounting for the different levels of PVI.

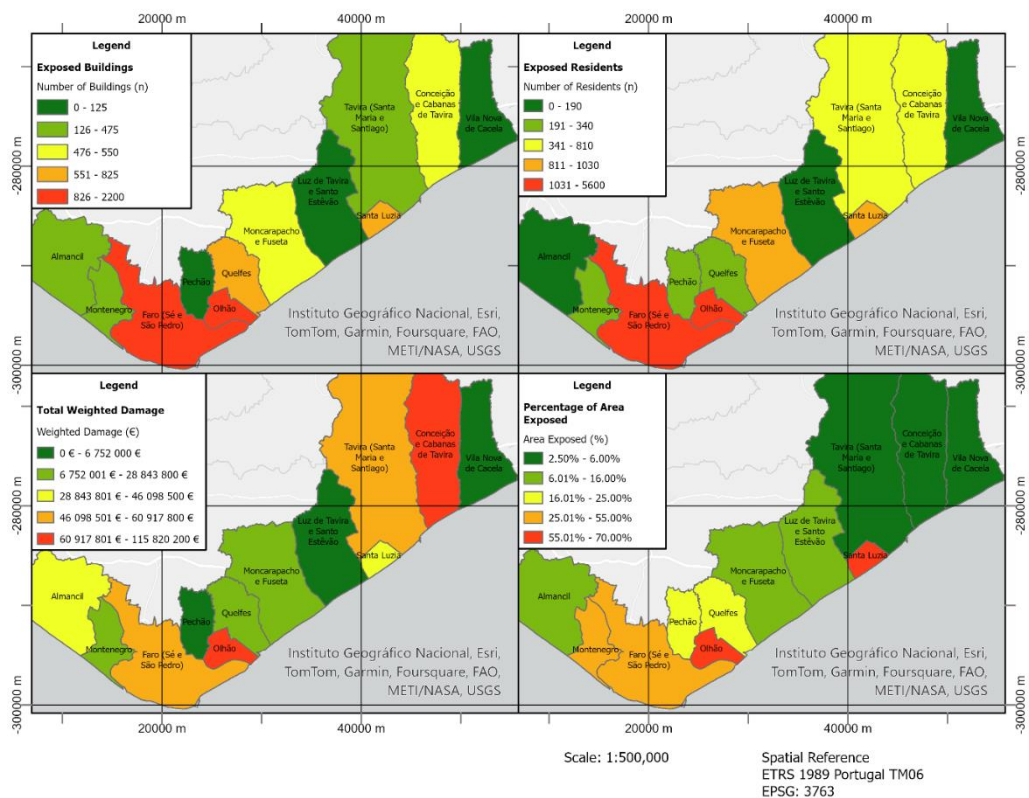


Figure 4.3 - Demographic Vulnerability Statistics. Classes have been divided by quintiles. Olhão is the only civil parish with the highest level of vulnerability on every category.

The area of study includes large population centres and is heavily dependent on economic activities that are directly linked to the Ria Formosa lagoon, such as tourism, fish farming and bivalve aquaculture. The high vulnerability of the population and the high damage it is exposed to will only continue to worsen considering the weakening of the barrier island system alluded to on chapter 4.1.

Olhão is the civil parish where the impact of SLR is most critical, with 5550 residents and 2192 buildings affected, resulting in an estimated weighted damage of over 115 million euro. With 69% of

*Table 4.1 - Exposure demographic statistics of the Ria Formosa's civil parishes to the extreme flooding scenarios of RCP 8.5 2100. Olhão is the most affected civil parish in this scenario. Conceição e Cabanas de Tavira has the second highest weighted damage even though there is a low number of residents due to a high density of hotels near the beach. Faro is the second most affected civil parish in terms of buildings and residents at risk.*

Variable	Residents (n)						Buildings (n)						Flooded Area (Km <sup>2</sup> )						Flooded Area (%)	Weighted Damage (€)
	1	2	3	4	5	Total	1	2	3	4	5	Total	1	2	3	4	5	Total		
PVI Class	1	2	3	4	5	Total	1	2	3	4	5	Total	1	2	3	4	5	Total	-	-
Almancil	12	6	5	10	155	187	58	21	14	34	170	296	0.45	0.26	0.23	0.55	7.77	9.26	14.87%	34,843,025.86
Montenegro	59	16	10	20	148	253	34	16	13	27	229	318	0.56	0.28	0.18	0.78	5.98	7.77	36.67%	20,469,389.23
Olhão	1862	656	536	1124	1371	5550	538	307	269	512	567	2192	0.25	0.15	0.11	0.32	7.63	8.46	69.09%	115,820,189.72
Pechão	78	77	64	19	43	280	34	34	28	8	20	123	0.25	0.22	0.19	0.34	3.76	4.76	24.06%	3,404,412.57
Quelfes	157	39	19	35	86	337	132	103	64	203	321	824	0.42	0.35	0.20	0.67	4.62	6.26	22.19%	25,714,745.12
Santa Luzia	64	75	105	135	464	843	36	28	41	89	382	575	0.23	0.16	0.10	0.29	4.45	5.23	61.48%	46,098,444.50
Conceição e Cabanas de Tavira	109	66	49	101	205	530	100	59	49	104	205	518	0.13	0.10	0.08	0.22	1.20	1.74	2.50%	98,708,648.44
Faro (Sé e São Pedro)	1334	625	296	427	673	3355	374	256	146	311	507	1594	1.28	0.98	0.70	1.93	35.80	40.69	54.44%	60,917,768.54
Luz de Tavira e Santo Estêvão	24	10	5	7	11	57	23	10	5	6	11	56	0.22	0.14	0.10	0.26	5.06	5.78	9.65%	1,579,219.68
Moncarapacho e Fuseta	173	183	122	352	192	1023	102	114	63	161	110	549	0.45	0.32	0.23	0.60	9.20	10.80	15.29%	28,843,719.78
Tavira (Santa Maria e Santiago)	67	50	82	93	512	803	30	18	24	46	356	473	0.35	0.24	0.20	0.73	6.01	7.53	5.09%	48,052,719.64
Vila Nova de Cacela	19	7	4	6	7	43	33	13	11	11	6	74	0.22	0.14	0.08	0.24	0.75	1.43	3.10%	6,751,962.38
Total	3959	1812	1300	2332	3872	13260	1496	979	730	1515	2888	7593	5.81	5.34	5.40	10.94	97.23	109.71	17.67%	491,204,245.46

its area vulnerable to flooding, Olhão tops the socioeconomic vulnerability list on each of the variables considered.

Another analysis that can be derived from this socioeconomic study is the vulnerability of infrastructures in the region. Figure 4.4 shows some of the transport infrastructure vulnerable to SLR detected in the Ria Formosa, using data available on open platforms such as OSM.

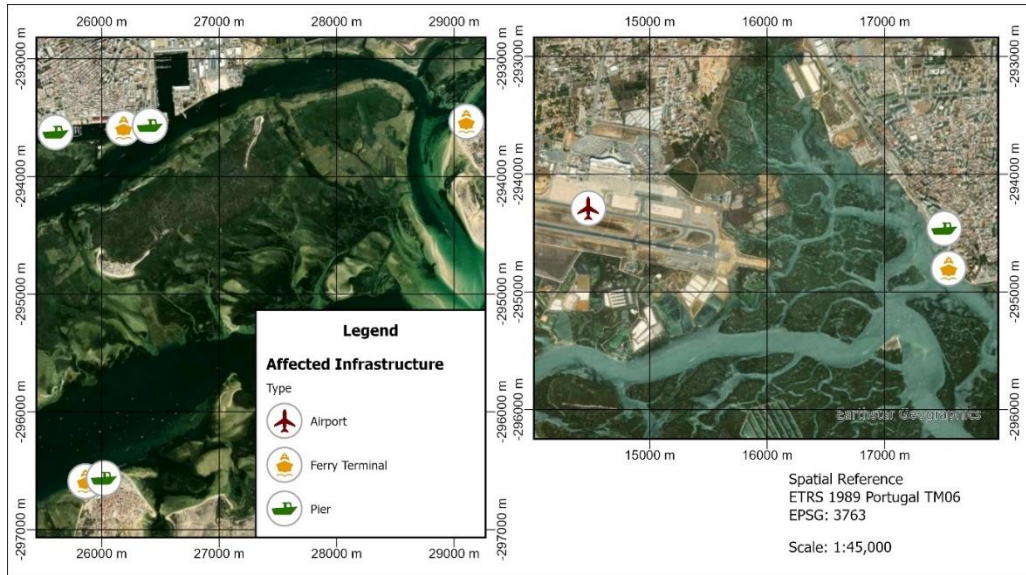


*Figure 4.4 - Infrastructure affected by the RCP 8.5 SLR scenario. The Faro airport is the largest infrastructure at risk in this scenario, but many other ferry terminals and piers used mostly for fishing or recreation can also be damaged.*

Several navigational infrastructures are in vulnerable areas, which in an extreme flooding scenario could turn evacuation scenarios even more difficult, especially when it comes to the population resident in the barrier islands which is one of the many reasons why it's so important to relocate those urban areas.

### 4.3. Environmental Vulnerability

The data obtained in the environmental vulnerability study enables an estimation of the areas currently occupied by each habitat and how they will evolve until 2100, shown in Table 4.2.

*Table 4.2 - Evolution of ecosystem areas between 2010 and 2100. 1) Inland urban and agricultural area protected; 2) No protections. 3) Urban and agricultural area protected including on the Barrier Island System.*

Habitat / Area	2010 (km <sup>2</sup> )	2100 <sup>1</sup> (km <sup>2</sup> )	Change <sup>1</sup> (km <sup>2</sup> )	2100 <sup>2</sup> (km <sup>2</sup> )	Change <sup>2</sup> (km <sup>2</sup> )	2100 <sup>3</sup> (km <sup>2</sup> )	Change <sup>3</sup> (km <sup>2</sup> )
Dune System	21.47	21.13	-0.34	21.13	-0.34	20.40	-1.07
High Saltmarsh	17.52	8.34	-9.18	9.98	-7.54	7.11	-10.41
Low Saltmarsh	5.24	6.34	+1.1	6.43	+1.19	6.15	+0.95
Tidal Flats	63.97	79.71	+15.74	79.93	+15.96	78.07	+14.1
Subtidal	32.91	36.47	+3.56	36.66	+3.75	36.46	+3.55

The values in Table 4.2 show that the habitat which will be most affected by SLR will be the high saltmarsh, with loss of over half of its area, followed by the sand dune system. The other habitats in the Ria Formosa will occupy a larger area in 2100 than they do in 2010, as area that once belonged to high saltmarsh becomes low saltmarsh or intertidal mudflat. The abandonment of urban areas in the barrier islands, present in both scenario one and two, mitigates the loss of the sand dune system. In scenario two, where the lagoon would be allowed to expand inward without any protection to

agriculture or urban areas, the loss of high saltmarsh is slightly mitigated. Scenario 3, which includes protections to the urban areas in the barrier islands, shows much larger losses than the two previous scenarios, as there is no space for the ecosystem to expand. The reasons why gains are larger than losses is due to the areas that currently don't belong to any of the ecosystems nor to urban or agricultural classes potentially becoming part of the lagoon, as well as the addition of the area previously occupied by the urban settlements in the barrier islands.

These results reflect the highly susceptibility of the region to SLR, however, the data obtained from the survey results suggests that the SLR could have a positive environmental impact for the region, as intertidal flats and subtidal areas were classified as having the most value under the ecosystem services theory.

This approach to calculate damage has its limitations. Assigning a value to a pixel of a certain category does not distinguish between differences that may occur even inside the same habitat: a part of the sand dune system in 2010 will either remain a part of the sand dune system or be submersed in 2100 – but even if the sand dune remains it may still have become damaged, lost volume or height and overall do a poorer job of protecting the lagoon. Another issue that this approach does not consider is the increased loss in value caused by the disappearance or extreme loss of particular habitats. In the terms of damage calculation, a pixel of high saltmarsh becoming intertidal mudflat would result in a gain according to the classification resultant from the specialist study, however, as more and more high saltmarsh is lost, species that thrive in the high saltmarsh become increasingly pressured, possibly damaging the biodiversity and ecological equilibrium of the whole system.

Another issue is that this environmental classification seems to be very subjective, and this study was conducted on a small population. Perhaps the inclusion of more researchers in more fields would produce a more standardised result. The findings in this dissertation do not match the findings of similar studies such as Inge et al. (2013), where the classification was done on some similar habitats in estuaries. This study was not used as it did not encompass all the habitats of the Ria Formosa and it did not distinguish between high and low saltmarsh. However, some key differences in evaluation, shown in Table 4.3, indicate that in that project the comparative ecosystem services value given to marshes is higher than that of tidal flats or subtidal areas, unlike the results obtained in this study.

*Table 4.3 - Comparison between the results obtained in this dissertation and the results of Inge et al. (2013)*

Habitat	Overall Specialist Score	Normalisation	Inge et al. (2013)	Normalisation
Low Saltmarsh	3.80	3	3.23	1
Intertidal Flat	4.25	1	3.18	2
Subtidal	4.22	2	3.08	3

Results in areas where the SLR is turning saltmarsh into intertidal mudflats show up as gains according to the rating given in this project but would show up as losses following the classification proposed by Inge et al. (2013). Figure 4.5 shows the damage comparison (disregarding the dune system) in the area north of the Faro-Olhão inlet. The area classified as “loss” in the Inge et al. (2013) model is four times larger than the area of the same classification following the EDI methodology presented in this dissertation.

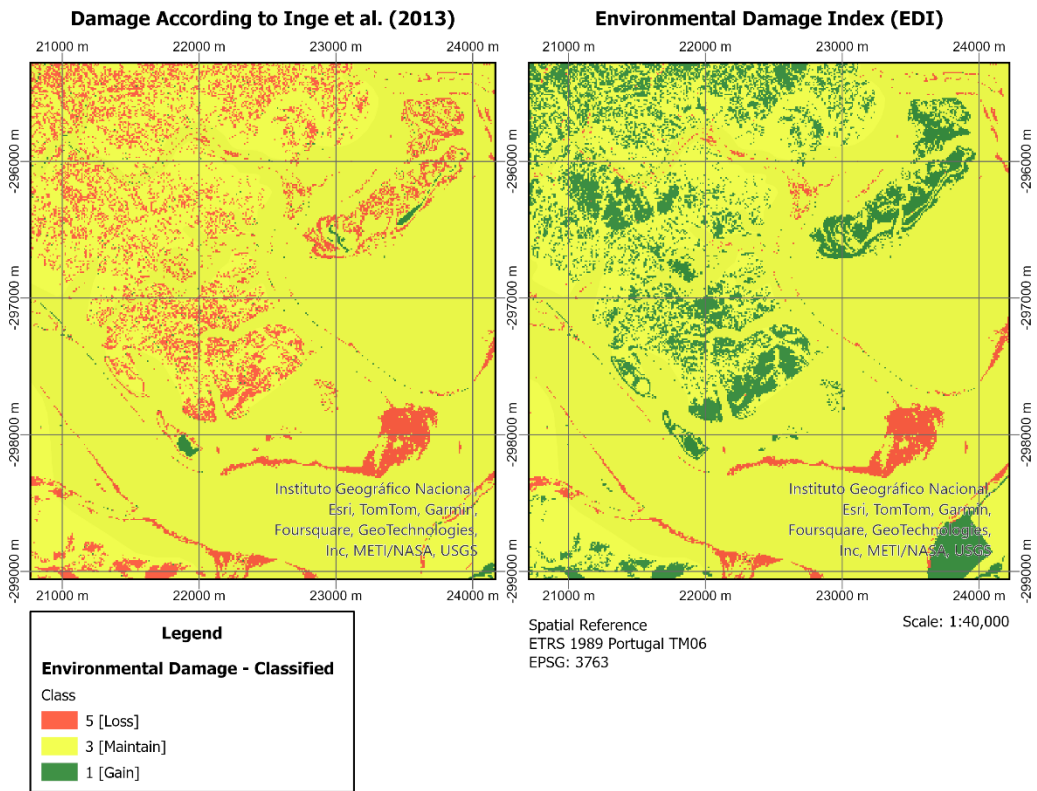


*Figure 4.5 - Comparison between the classified damage to the ecosystem obtained by applying the methodology of Inge et al. (2013) and the methodology for the EDI presented in this dissertation.*

The need arises for a more comprehensive study of the Portuguese coastal ecosystems and the value they produce, so that an actual monetary value can be given to these areas, turning the data more compatible with the socioeconomic data and to have a definitive guide for studies of this kind that reflects the national reality. Having a robust methodology and a centralised database would facilitate the inclusion of environmental variables in risk assessments, not only for SLR but also other hazards that may cause harm to ecosystems, such as forest fires or heat waves.

#### 4.4 Multi-parametric Coastal Risk

The inclusion of environmental vulnerability in the coastal risk assessment allowed for a more realistic approach to the mapping of the SLR risk in this region.

Figure 4.6 demonstrates the differences between the results obtained by Antunes et al. (2019a) and the results obtained by the MCRI developed in this dissertation for the civil parish of Almancil. Unfortunately, the SLR models used are not exactly the same, with the MOD.FC\_2 shown on the left being a scenario with higher SLR than the RCP 8.5 shown on the right. Regardless of this factor, the inclusion of the EVI allowed for the whole area of the natural reserve to be characterised in regards to risk, which, in this area, is mostly on high or extreme levels. This is important information for coastal protection and adaptation measures. The slight changes in methodology, mainly from the use of erosion/accretion algorithms (local/regional study scale) instead of deriving physical vulnerability from the intersection of information layers of the physical parameters (national study scale), has shown that the coastal area is in fact at higher risk than the results obtained by Antunes et al. (2019a).

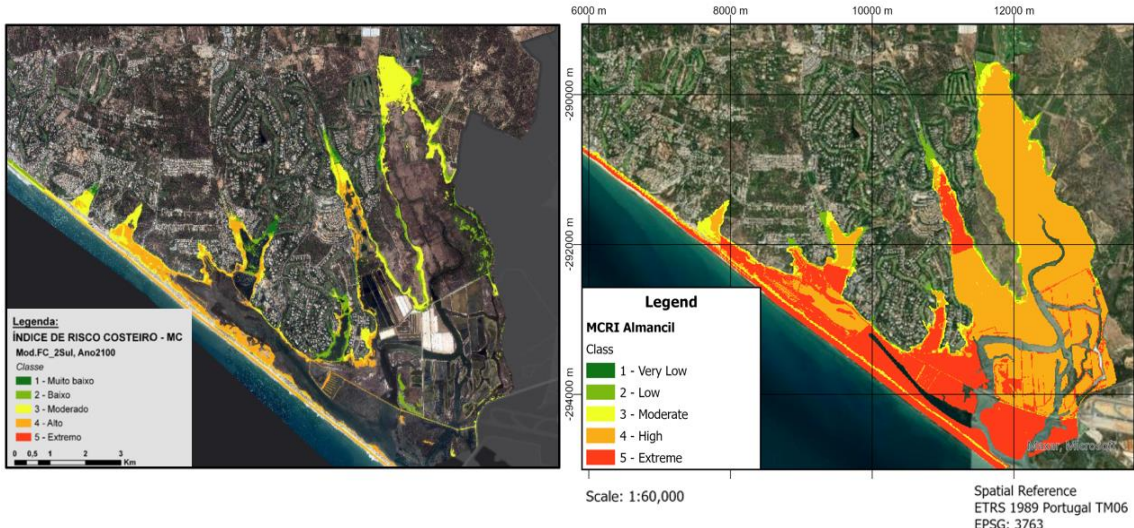


*Figure 4.6 - Comparison of results obtained for Almancil Civil Parish. Left: Coastal Risk Index (Antunes et al., 2019a), SLR Model: MOD.FC\_2; Right: Multi-parametric Coastal Risk Index SLR Model: RCP 8.5. The figure on the left shows that the inclusion of the EVI allows for a more thorough classification of risk.*

The barrier island system, in particular, is an area of critical importance to the preservation of the lagoon system and the protection of populations. With the introduction of the EVI, this area, mostly included in classes 3 and 4 in the SRI, moves to a higher risk class in the MCRI. The methodology applied for the MVI allowed for the higher socioeconomic risk areas in the barrier islands to retain their risk level.

The Multi-parametric Coastal Risk cartography is then a contribution for a broader assessment, an indicator of multiple coastal vulnerabilities. It can support decision-making not only for adaptation but also to increase the resilience of the coastal system as a whole.

## 5. Conclusions

### 5.1 Conclusions

The results obtained in this dissertation show that the methodological approach proposed in chapter 3 allows for the characterisation of risk in a region using physical, socioeconomic and environmental parameters.

The main objectives of the study were the creation of a DTM of the coastal areas for future scenarios of SLR; the creation of a socioeconomic vulnerability map; the creation of an environmental vulnerability map for the intertidal ecosystems; the development of a new methodological approach to calculate risk based on multiple vulnerability parameters and the creation of a multiparametric risk assessment map of the Ria Formosa. These objectives were all achieved and have allowed for the following conclusions:

- The methodology for creating a future scenario DTM is very dependent on a few factors, chief among them the existence of good quality ground data. One of the largest challenges of this project was the validation of the DTM without any field work and with very few data points from the national high precision geodesic levelling network. Additionally, the existent validation data is located in the urbanised areas, whereas the lagoon and barrier islands, subject to the highest rate of change, lack this type of validation data. One other factor that needs to be accounted for is the existence of erosion/accretion rate studies for the area in

question – while there are some studies regarding erosion rates on the Portuguese coast, and these were used as a guideline in this project, they don't present the same level of detail as the DTM, adding to the uncertainty of calculating the future scenario. On the other hand, there is a distinct lack of studies relating to accretion that present concrete rates, with only one data source being used here, as well as how accretion varies with height and/or submersion time.

- While the data necessary for the study of the socioeconomic vulnerability exists and is free to access, there were some hurdles to obtain it and to harmonise each source to make it compatible with all others. Data sources like soil use and population density are available from national geospatial databases, while more detailed information like the location of infrastructures or transport networks must be downloaded from open-source databases, where the information is at times incomplete or hard to align temporally with the national data sources. However, the hardest challenge of the socioeconomic vulnerability assessment was the formulation of the damage calculation and the acquisition of the data necessary for it, which involved manual digitalisation of the data.
- The approach to determining the vulnerability of ecosystems to SLR is a completely new methodology developed for this dissertation. It adequately characterises and classifies the habitats present in the Ria Formosa and adds the environmental layer to the socioeconomic information. The methodology does still require some further development, as evidenced by chapters 4.3 and 5.2.
- Creating risk and vulnerability indices is a task which has evolved over the years, using different aggregation methods, different parameters and applied to different spatial resolutions. Many choices were made during the project that reflect the context of the study area and of past projects (Antunes et al., 2019a; Antunes et al., 2024a), as evidenced by the analysis conducted in chapter 3.7.
- The results obtained combine the environmental and socioeconomic risk to a region, for a specific time frame and a specific scenario of SLR. This makes the maps useful as decision tools to plan mitigation and adaptation measures. However, they need to be followed up with models of other scenarios and updated at constant intervals to ensure a higher certainty in the results.

The physical vulnerability cartography obtained shows that the increase in the erosion rate facilitated by the SLR will cause the destruction of part of the sand dune system by 2100, also weakening other parts of the dunes, causing the area to become increasingly more vulnerable. There are areas with rates of accretion that are sufficiently high to still accumulate sand despite the SLR predicted by the RCP 8.5 scenario considered in this project, but should the sea level continue to rise at an accelerated rate past 2100, these areas will also enter a sedimentary deficit.

The socioeconomic vulnerability cartography reflects an alarming scenario for the region: currently there are approximately 110 km<sup>2</sup> vulnerable to flooding, corresponding to 17% of the total area of study. The most affected civil parishes, in terms of percentage of vulnerable area, are Olhão (69%), Santa Luzia (61%) and Faro (54%). Olhão and Faro are particularly relevant, as they include the two largest population centres in the region. In terms of demographics, the SLR will affect an estimated population of over 13 000 people, with approximately 7 600 buildings vulnerable to flooding.

The environmental vulnerability cartography has a slight difference to the previous two, and that is how the evolution of the area can be shaped by decisions to allow the ecosystem to expand inward or to protect the urban and agricultural areas that surround the Ria Formosa, as well as the decisions to relocate the population resident in the barrier islands. Assuming a scenario where the barrier islands are uninhabited, but the lagoon is not allowed to migrate inward, the ecosystem that suffers the largest

loss of area is the high saltmarsh, being reduced to less than half its current extension today. The intertidal flat area will increase the most, with gains of around 25%.

Finally, the multi-parametric coastal risk cartography allows for a more comprehensive view of the three, acknowledging not only the contribution of the economy of the region but also the importance of the ecosystem to the population.

## 5.2 Future Recommendations

This project proposes a new and more encompassing approach to identify areas of high risk along the coast that are particularly vulnerable to SLR. The methodology is still at its early stages and, as such, it is important to continue to develop it and apply it in further projects. Some recommendations for future studies include:

- Using higher quality ground data and field validation of the DTM, particularly in the zones with higher change rates, not only to obtain more precise results but also to validate the erosion rates of the Ria Formosa barrier island system.
- Studies of the accretion rates in the lagoon so that any future DTM can represent a more likely scenario. This can involve calculating sedimentation gains on multiple areas of the Ria Formosa and creating a differential surface for sedimentation, similar to what was done for the height corrections in the tidal plane.
- Simulating different protection measures in the region and evaluating the resulting scenarios.
- Creating a standardized methodology to evaluate potential damage to extreme flooding caused by SLR versus cost to mitigate damage, adapt and/or protect the coast, as a decision tool for policy makers. This methodology should aim to include both socioeconomic and environmental damage.
- A more thorough study of ecosystem services and the value they provide to populations, based on a more comprehensive survey of specialists. This was unfortunately not possible in this project due to only six researchers agreeing to undertake the survey and the limited time frame to complete the project.
- Adapting the methodology to other types of coastal ecosystems such as mangroves and other wetland types.

## Bibliography

- Allen, J. R. L. (2000). Morphodynamics of Holocene saltmarshes: A review sketch from the Atlantic and Southern North Sea coasts of Europe. *Quaternary Science Reviews*, 19(12), 1155–1231. [https://doi.org/10.1016/S0277-3791\(99\)00034-7](https://doi.org/10.1016/S0277-3791(99)00034-7)
- Almeida, C. M. R., Mucha, A. P., & Teresa Vasconcelos, M. (2011). Role of different saltmarsh plants on metal retention in an urban estuary (Lima estuary, NW Portugal). *Estuarine, Coastal and Shelf Science*, 91(2), 243–249. <https://doi.org/10.1016/j.ecss.2010.10.037>
- Anderson, T. R., Fletcher, C. H., Barbee, M. M., Frazer, L. N., & Romine, B. M. (2015). Doubling of coastal erosion under rising sea level by mid-century in Hawaii. *Natural Hazards*, 78(1), 75–103. <https://doi.org/10.1007/s11069-015-1698-6>
- Andrade, C. (1990). *O Ambiente de barreira da Ria Formosa, Algarve – Portugal* [Tese de Doutoramento]. Universidade de Lisboa.
- Andrade, C., Freitas, M. C., Moreno, J., & Craveiro, S. C. (2004). Stratigraphical evidence of Late Holocene barrier breaching and extreme storms in lagoonal sediments of Ria Formosa, Algarve, Portugal. *Marine Geology*, 210(1), 339–362. <https://doi.org/10.1016/j.margeo.2004.05.016>
- Andrade, C., Pires, H., Taborda, R., & Freiras, M. C. (2006). *Zonas Costeiras, in: Santos, F.D., Miranda, P. (Eds.), Alterações Climáticas Em Portugal. Cenários, Impactos e Medidas de Adaptação – SIAM II*. Gradiva. [https://www.cimac.pt/wp-content/uploads/2020/07/PIAAC-AC\\_Bibliografia\\_Projeto\\_SIAMI2\\_2006.pdf](https://www.cimac.pt/wp-content/uploads/2020/07/PIAAC-AC_Bibliografia_Projeto_SIAMI2_2006.pdf)
- Aníbal, J., Gomes, A., Mendes, I., & Moura, D. (2019). *Ria Formosa: Challenges of a coastal lagoon in a changing environment*. Universidade do Algarve Editora. <https://sapientia.ualg.pt/handle/10400.1/12475>
- Anthony, A., Atwood, J., August, P., Byron, C., Cobb, S., Foster, C., Fry, C., Gold, A., Hagos, K., Heffner, L., Kellogg, D. Q., Lellis-Dibble, K., Opaluch, J. J., Oviatt, C., Pfeiffer-Herbert, A., Rohr, N., Smith, L., Smythe, T., Swift, J., & Vinhateiro, N. (2009). Coastal Lagoons and Climate Change: Ecological and Social Ramifications in U.S. Atlantic and Gulf Coast Ecosystems. *Ecology and Society*, 14(1). <https://www.jstor.org/stable/26268055>

- Antunes, C. (2007). *Previsão de Marés dos Portos Principais de Portugal*.  
[http://webpages.fc.ul.pt/~cmantunes/hidrografia/hidro\\_mares.html](http://webpages.fc.ul.pt/~cmantunes/hidrografia/hidro_mares.html)
- Antunes, C. (2011). Monitoring sea level change at Cascais tide gauge. *Journal of Coastal Research*, 870–874.
- Antunes, C. (2012). *Implicação da subida do NMM na necessidade de revisão dos sistemas de referência verticais*.
- Antunes, C. (2014). *Eventos Extremos e a variação do Nível do mar*. Actas das 3.as Jornadas de Engenharia Hidrográfica. <https://www.hidrografico.pt/jornada/4>
- Antunes, C. (2017). *Metodologia de Aplicação da Regra de Recuo da Linha de Costa à Modelação do MDT - Regra de Bruun modificada*. not published.
- Antunes, C. (2019). *Assessment of Sea Level Rise at West Coast of Portugal Mainland and Its Projection for the 21st Century*. <https://doi.org/10.20944/preprints201902.0113.v1>
- Antunes, C., Catita, C., & Rocha, C. (2018). *Estudo de Avaliação da Subida do Nível Médio do Mar e Sobrelevação da Maré em Eventos Extremos de Galgamento e Inundação Costeira do Município de Loulé—Cartografia de Inundação e Vulnerabilidade*. not published.
- Antunes, C., Catita, C., & Rocha, C. (2019a). *Estudo de Avaliação da Subida do Nível Médio do Mar e Sobrelevação da Maré em Eventos Extremos de Galgamento e Inundação Costeira do Município de Loulé—Cartografia de Risco*. not published.
- Antunes, C., & Godinho, J. M. (2011). Estudo da análise harmónica da maré aplicada ao marégrafo de Cascais. *Actas da VII Conferência Nacional de Cartografia e Geodesia*.
- Antunes, C., Lemos, G., Bosnic, I., Soares, P. M., Semedo, Á., Costa, P., Lima, D., Rocha, C., Catita, C., Ferreira, V., Santo, M., & Mourão, S. (2024a). *National Roadmap for Adaptation 2100; WP4 – Sectoral Impacts and Modelling; WP4.5/6 – The impact of climate change on the Portuguese coastal areas: From sea level rise to coastal erosion*.  
<https://rna2100.apambiente.pt/pagina/programa-ambiente-alteracoes-climaticas-e-economia-de-baixo-carbono>
- Antunes, C., Mourão, S., Santo, M., Ferreira, V., Rocha, C., & Catita, C. (2023). *Estudo de impacto de inundação e de galgamento costeiro e estuarino do Município de Almada*. not published.

- Antunes, C., Rocha, C., & Catita, C. (2019b). Coastal Flood Assessment due to Sea Level Rise and Extreme Storm Events: A Case Study of the Atlantic Coast of Portugal's Mainland. *Geosciences*, 9(5), Article 5. <https://doi.org/10.3390/geosciences9050239>
- Antunes, C., & Taborda, R. (2009). Sea Level at Cascais Tide Gauge: Data, Analysis and Results. *Journal of Coastal Research Journal of Coastal Research SI Journal of Coastal Research SI*, 56, 218–222.
- ATEAM. (2004). *Final report 2004, Section 5 and 6 and Annex 1 to 6: Detailed report, related to overall project duration*. [https://www.pik-potsdam.de/ateam/ateam\\_final\\_report\\_sections\\_5\\_to\\_6.pdf](https://www.pik-potsdam.de/ateam/ateam_final_report_sections_5_to_6.pdf)
- Bagdanavičiūtė, I., Kelpšaitė-Rimkienė, L., Galinienė, J., & Soomere, T. (2019). Index based multi-criteria approach to coastal risk assesment. *Journal of Coastal Conservation*, 23(4), 785–800. <https://doi.org/10.1007/s11852-018-0638-5>
- Barbier, E. B. (2007). Valuing ecosystem services as productive inputs. *Economic Policy*, 22(49), 178–229. <https://doi.org/10.1111/j.1468-0327.2007.00174.x>
- Barros, J. L., Tavares, A. O., Santos, P. P., & Freire, P. (2022). *Enhancing a Coastal Territorial Vulnerability Index: Anticipating the Impacts of Coastal Flooding with a Local Scale Approach*. <https://www.tandfonline.com/doi/epdf/10.1080/08920753.2022.2107858?needAccess=true>
- Basheer, K. K., Mahendra, R. S., & Pandey, A. C. (2016). Coastal Vulnerability Assessment for Eastern Coast of India, Andhra Pradesh by Using Geo-Spatial Technique. *Geoinformatics & Geostatistics: An Overview*, 2016. <https://doi.org/10.4172/2327-4581.1000146>
- Beck, M. W., Losada, I. J., Menéndez, P., Reguero, B. G., Díaz-Simal, P., & Fernández, F. (2018). The global flood protection savings provided by coral reefs. *Nature Communications*, 9(1), Article 1. <https://doi.org/10.1038/s41467-018-04568-z>
- Behera, R., Kar, A., Das, M. R., & Panda, P. P. (2019). GIS-based vulnerability mapping of the coastal stretch from Puri to Konark in Odisha using analytical hierarchy process. *Natural Hazards*, 96(2), 731–751. <https://doi.org/10.1007/s11069-018-03566-0>

- Bera, R., & Maiti, R. (2021). An assessment of coastal vulnerability using geospatial techniques. *Environmental Earth Sciences*, 80(8), 306. <https://doi.org/10.1007/s12665-021-09616-4>
- Bernardo, P., Bastos, R., & Dias, J. (2002). Historic Roots for Barrier Island Occupation in the Ria Formosa. *Littoral 2002, The Changing Coast. EUROCOAST / EUCC, Porto – Portugal Ed. EUROCOAST – Portugal, ISBN: 9728558090.*
- Bird, E. C. F. (1996). Coastal Erosion and Rising Sea-Level. In J. D. Milliman & B. U. Haq (Eds.), *Sea-Level Rise and Coastal Subsidence: Causes, Consequences, and Strategies* (pp. 87–103). Springer Netherlands. [https://doi.org/10.1007/978-94-015-8719-8\\_5](https://doi.org/10.1007/978-94-015-8719-8_5)
- Blumberg, A. F., & Bruno, M. S. (Eds.). (2018). Water Level Changes. In *The Urban Ocean: The Interaction of Cities with Water* (pp. 52–71). Cambridge University Press.  
<https://doi.org/10.1017/9781108123839.007>
- Boorman, L. A. (1995). Sea-level Rise and the Future of the British Coast. *Coastal Zone Topics : Process, Ecology and Management.*  
[https://scholar.google.com/scholar\\_lookup?&title=Sea%20level%20rise%20and%20the%20future%20of%20the%20British%20coast&journal=Coastal%20Zone%20Topics%3A%20Process%2C%20Ecology%20and%20Management&volume=1&pages=10-13&publication\\_year=1995&author=Boorman%2CL.A.#d=gs\\_cit&t=1701627480851&u=%2Fscholar%3Fq%3Dinfo%3ARZbmAiX0wLkJ%3Ascholar.google.com%2F%26output%3Dcite%26scirp%3D0%26hl%3Den](https://scholar.google.com/scholar_lookup?&title=Sea%20level%20rise%20and%20the%20future%20of%20the%20British%20coast&journal=Coastal%20Zone%20Topics%3A%20Process%2C%20Ecology%20and%20Management&volume=1&pages=10-13&publication_year=1995&author=Boorman%2CL.A.#d=gs_cit&t=1701627480851&u=%2Fscholar%3Fq%3Dinfo%3ARZbmAiX0wLkJ%3Ascholar.google.com%2F%26output%3Dcite%26scirp%3D0%26hl%3Den)
- Boorman, L. A. (1999). Saltmarshes – present functioning and future change. *Mangroves and Saltmarshes*, 3(4), 227–241. <https://doi.org/10.1023/A:1009998812838>
- Boruff, B. J., Emrich, C., & Cutter, S. L. (2005). Erosion Hazard Vulnerability of US Coastal Counties. *Journal of Coastal Research*, 2005(215), 932–942. <https://doi.org/10.2112/04-0172.1>
- Bouhmadouche, M., & Hemdane, Y. (2016). Erosion of a sandy coast: Continuous follow-up of the coastal groynes of protection in Boumerdes (Algeria). *Environmental Earth Sciences*, 75(10), 866. <https://doi.org/10.1007/s12665-016-5665-7>

- Bowen, A. J., Inman, D. L., & Simmons, V. P. (1968). Wave ‘set-down’ and set-Up. *Journal of Geophysical Research (1896-1977)*, 73(8), 2569–2577.  
<https://doi.org/10.1029/JB073i008p02569>
- Bricker-Urso, S., Nixon, S. W., Cochran, J. K., Hirschberg, D. J., & Hunt, C. (1989). Accretion rates and sediment accumulation in Rhode Island saltmarshes. *Estuaries*, 12(4), 300–317.  
<https://doi.org/10.2307/1351908>
- Brito, A. C., Newton, A., Tett, P., & Fernandes, T. F. (2012). How will shallow coastal lagoons respond to climate change? A modelling investigation. *Estuarine, Coastal and Shelf Science*, 112, 98–104. <https://doi.org/10.1016/j.ecss.2011.09.002>
- Bruun, P. (1962). Sea-Level Rise as a Cause of Shore Erosion. *Journal of the Waterways and Harbors Division*, 88(1), 117–130. <https://doi.org/10.1061/JWHEAU.0000252>
- Bunse, L., Rendon, O., & Luque, S. (2015). What can deliberative approaches bring to the monetary valuation of ecosystem services? A literature review. *Ecosystem Services*, 14, 88–97.  
<https://doi.org/10.1016/j.ecoser.2015.05.004>
- Cabaço, S., Alexandre, A., & Santos, R. (2005). Population-level effects of clam harvesting on the seagrass *Zostera noltii*. *Marine Ecology Progress Series*, 298, 123–129.  
<https://doi.org/10.3354/meps298123>
- Cabral, J. (1995). *Neotectónica em Portugal Continental* (Vol. 31). Ministério da Indústria e Energia, Secretaria de Estado da Indústria, Instituto Geológico e Mineiro.  
<https://docbase.lneg.pt/docs/Memorias/31.pdf>
- Calil, J., Reguero, B. G., Zamora, A. R., Losada, I. J., & Méndez, F. J. (2017). Comparative Coastal Risk Index (CCRI): A multidisciplinary risk index for Latin America and the Caribbean. *PLOS ONE*, 12(11), e0187011. <https://doi.org/10.1371/journal.pone.0187011>
- Cardona, O.-D., Van Aalst, M. K., Birkmann, J., Fordham, M., McGregor, G., Perez, R., Pulwarty, R. S., Schipper, E. L. F., Sinh, B. T., Décamps, H., Keim, M., Davis, I., Ebi, K. L., Lavell, A., Mechler, R., Murray, V., Pelling, M., Pohl, J., Smith, A.-O., & Thomalla, F. (2012). Determinants of Risk: Exposure and Vulnerability. In C. B. Field, V. Barros, T. F. Stocker, & Q. Dahe (Eds.), *Managing the Risks of Extreme Events and Disasters to Advance Climate*

*Change Adaptation* (1st ed., pp. 65–108). Cambridge University Press.

<https://doi.org/10.1017/CBO9781139177245.005>

Cardoso, R. M., Lima, D. C. A., & Soares, P. M. M. (2023). How persistent and hazardous will extreme temperature events become in a warming Portugal? *Weather and Climate Extremes*, 41, 100600. <https://doi.org/10.1016/j.wace.2023.100600>

Cassar, L. F., & Stevens, D. T. (2002). *Coastal sand dunes under siege: A guide to conservation for environmental managers*. International Environment Institute, Foundation for International Studies.

Ceia, F. (2007). *Vulnerabilidade das Ilhas-Barreira e dinâmica da Ria Formosa na óptica da gestão* [masterThesis]. <https://sapientia.ualg.pt/handle/10400.1/671>

Ceia, F. R., Patrício, J., Marques, J. C., & Dias, J. A. (2010). Coastal vulnerability in barrier islands: The high risk areas of the Ria Formosa (Portugal) system. *Ocean & Coastal Management*, 53(8), 478–486. <https://doi.org/10.1016/j.ocecoaman.2010.06.004>

Chaplin-Kramer, R., Sharp, R. P., Weil, C., Bennett, E. M., Pascual, U., Arkema, K. K., Brauman, K. A., Bryant, B. P., Guerry, A. D., Haddad, N. M., Hamann, M., Hamel, P., Johnson, J. A., Mandle, L., Pereira, H. M., Polasky, S., Ruckelshaus, M., Shaw, M. R., Silver, J. M., ... Daily, G. C. (2019). Global modeling of nature's contributions to people. *Science*, 366(6462), 255–258. <https://doi.org/10.1126/science.aaw3372>

Chmura, G. L. (2009). Coastal Zone and Estuaries. *Coastal Zones and Estuaries. Encyclopedia of Life Support Systems*.

Christiansen, T., Wiberg, P. L., & Milligan, T. G. (2000). Flow and Sediment Transport on a Tidal Saltmarsh Surface. *Estuarine, Coastal and Shelf Science*, 50(3), 315–331. <https://doi.org/10.1006/ecss.2000.0548>

Christie, M., Fazey, I., Cooper, R., Hyde, T., & Kenter, J. O. (2012). An evaluation of monetary and non-monetary techniques for assessing the importance of biodiversity and ecosystem services to people in countries with developing economies. *Ecological Economics*, 83, 67–78. <https://doi.org/10.1016/j.ecolecon.2012.08.012>

- Christie, M., Hanley, N., Warren, J., Murphy, K., Wright, R., & Hyde, T. (2006). Valuing the diversity of biodiversity. *Ecological Economics*, 58(2), 304–317.  
<https://doi.org/10.1016/j.ecolecon.2005.07.034>
- Church, J. A., & White, N. J. (2011). Sea-Level Rise from the Late 19th to the Early 21st Century. *Surveys in Geophysics*, 32(4), 585–602. <https://doi.org/10.1007/s10712-011-9119-1>
- Coburn, A., Sspence, R. J. S., & Pomonis, A. (1994). *Vulnerability and Risk Assessment*.
- Coelho, C. D. B. (2005). *Riscos de exposição de frentes urbanas para diferentes intervenções de defesa costeira* [doctoralThesis, Universidade de Aveiro]. <https://ria.ua.pt/handle/10773/2405>
- Conser, C., & Connor, E. F. (2009). Assessing the residual effects of *Carpobrotus edulis* invasion, implications for restoration. *Biological Invasions*, 11(2), 349–358.  
<https://doi.org/10.1007/s10530-008-9252-z>
- Cooper, A., & Jackson, D. (2021). Dune gardening? A critical view of the contemporary coastal dune management paradigm. *Area*, 53(2), 345–352. <https://doi.org/10.1111/area.12692>
- Costa, M. de S. (2017). *Desenvolvimento de uma metodologia de avaliação de risco costeiro face aos cenários de alterações climáticas: Aplicação ao Estuário do Tejo e à Ria de Aveiro* [masterThesis]. <https://repositorio.ul.pt/handle/10451/31432>
- Costa, M., Silva, R., & Vitorino, J. (2001, October 17). *Contribuição para o Estudo do Clima de Agitação Marítima na Costa Portuguesa* (in Portuguese).
- Cunha, J. C. S. T. (2019). *Contribuição da barra da Armona para as trocas de matéria entre o setor oeste da Ria Formosa e o Oceano*.  
[https://sapientia.ualg.pt/bitstream/10400.1/15036/1/MACStese\\_joaocarloscunha.pdf](https://sapientia.ualg.pt/bitstream/10400.1/15036/1/MACStese_joaocarloscunha.pdf)
- Daily, G. C., Polasky, S., Goldstein, J., Kareiva, P. M., Mooney, H. A., Pejchar, L., Ricketts, T. H., Salzman, J., & Shallenberger, R. (2009). Ecosystem services in decision making: Time to deliver. *Frontiers in Ecology and the Environment*, 7(1), 21–28.  
<https://doi.org/10.1890/080025>
- Davis, R. A., & Dalrymple, R. W. (Eds.). (2012). *Principles of Tidal Sedimentology*. Springer Netherlands. <https://doi.org/10.1007/978-94-007-0123-6>

- Davy, A. (2009). Life on the edge: Saltmarshes ancient and modern. Presidential Address delivered to the Society on 18 November 2008. *Transactions of the Norfolk & Norwich Naturalists' Society*, 41, 1–10.
- De Serio, F., Armenio, E., Mossa, M., & Petrillo, A. F. (2018). How to Define Priorities in Coastal Vulnerability Assessment. *Geosciences*, 8(11), Article 11.  
<https://doi.org/10.3390/geosciences8110415>
- Dean, B., Collins, I., Divoky, D., Hatheway, D., & Scheffner, N. (2005). *Wave setup: FEMA coastal flood hazard analysis and mapping guidelines*. [https://www.fema.gov/sites/default/files/2020-03/frm\\_p1wave1.pdf](https://www.fema.gov/sites/default/files/2020-03/frm_p1wave1.pdf)
- Delauney, B. (1934). *Sur la sphère vide. A la mémoire de Georges Voronoï*.
- Delgado-Fernandez, I., Davidson-Arnott, R. G. D., & Hesp, P. A. (2019). Is ‘re-mobilisation’ nature restoration or nature destruction? A commentary. *Journal of Coastal Conservation*, 23(6), 1093–1103. <https://doi.org/10.1007/s11852-019-00716-9>
- Devoy, R. J. N. (1992). Questions of Coastal Protection and the Human Response to Sea-level Rise in Ireland and Britain. *Irish Geography*, 25(1), 1–22.  
<https://doi.org/10.1080/00750779209478736>
- Dias, J. (1988). Aspectos Geológicos do Litoral Algarvio. *Geonovas (ISSN: 0870-7375)*, Lisboa, Portugal., 10, 113–128.
- Dias, J. A., Ferreira, Ó., & Moura, D. (2004). *O sistema de ilhas-barreira da Ria Formosa. 3ºSimpósio Interdisciplinar sobre Processos Estuarinos*. 18.
- Dias, J. A., & Taborda, R. (1992). Tidal Gauge Data in Deducing Secular Trends of Relative Sea Level and Crustal Movements in Portugal. *Journal of Coastal Research*, 8(3), Article 3.  
<https://journals.flvc.org/jcr/article/view/78897>
- Dias, J., & Taborda, R. (1988). Evolução Recente do Nível Médio do Mar em Portugal. *Anais Do Instituto Hidrográfico (ISSN: 0870-3884)*, Lisboa, Portugal., 9, 83–97.
- Dilley, R. S., & Rasid, H. (1990). Human Response to Coastal Erosion: Thunder Bay, Lake Superior. *Journal of Coastal Research*, 6(4), 779–788.

- Direktorate-General for Environment (European Commission), Mézard, N., Sundseth, K., & Wegefelt, S. (2008). *Natura 2000 :protecting Europe's biodiversity*. Publications Office of the European Union. <https://data.europa.eu/doi/10.2779/45963>
- Doctor, J. N., Bleichrodt, H., Miyamoto, J., Temkin, N. R., & Dikmen, S. (2004). A new and more robust test of QALYs. *Journal of Health Economics*, 23(2), 353–367.  
<https://doi.org/10.1016/j.jhealeco.2003.11.004>
- Doody, J. P. (2012). *Sand Dune Conservation, Management and Restoration*. Springer Science & Business Media.
- Dunford, R. W., Ginn, T. C., & Desvouges, W. H. (2004). The use of habitat equivalency analysis in natural resource damage assessments. *Ecological Economics*, 48(1), 49–70.  
<https://doi.org/10.1016/j.ecolecon.2003.07.011>
- Duvat, V. K. E. (2019). A global assessment of atoll island planform changes over the past decades. *WIREs Climate Change*, 10(1), e557. <https://doi.org/10.1002/wcc.557>
- Everard, M., Jones, L., & Watts, B. (2010). Have we neglected the societal importance of sand dunes? An ecosystem services perspective. *Aquatic Conservation: Marine and Freshwater Ecosystems*, 20(4), 476–487. <https://doi.org/10.1002/aqc.1114>
- Falcão, M., Fonseca, L., Serpa, D., Matias, D., Joaquim, S., Duarte, P., Pereira, A., Martins, C., & Guerreiro, M. J. (2003). *Development of an Information Technology Tool for the Management of European Southern Lagoons under the influence of river-basin runoff*.  
<https://web.fe.up.pt/~amcp/papers/DITTY%20-%20Synthesis%20Report%20-%20Ria%20Formosa%20%28PT%29.pdf>
- Farber, S. C., Costanza, R., & Wilson, M. A. (2002). Economic and ecological concepts for valuing ecosystem services. *Ecological Economics*, 41(3), 375–392. [https://doi.org/10.1016/S0921-8009\(02\)00088-5](https://doi.org/10.1016/S0921-8009(02)00088-5)
- Feagin, R. A., Sherman, D. J., & Grant, W. E. (2005). Coastal erosion, global sea-level rise, and the loss of sand dune plant habitats. *Frontiers in Ecology and the Environment*, 3(7), 359–364.  
[https://doi.org/10.1890/1540-9295\(2005\)003\[0359:CEGSRA\]2.0.CO;2](https://doi.org/10.1890/1540-9295(2005)003[0359:CEGSRA]2.0.CO;2)

- Ferreira, J. C., Cardona, F. S., Jóia Santos, C., & Tenedório, J. A. (2021). Hazards, Vulnerability, and Risk Analysis on Wave Overtopping and Coastal Flooding in Low-Lying Coastal Areas: The Case of Costa da Caparica, Portugal. *Water*, 13(2), Article 2.  
<https://doi.org/10.3390/w13020237>
- Ferreira, Ó., Dias, J. A., & Taborda, R. (2008). Implications of Sea-Level Rise for Continental Portugal. *Journal of Coastal Research*, 24(2), 317–324.
- Ferreira, Ó., Matias, A., & Pacheco, A. (2016). The East Coast of Algarve: A Barrier Island Dominated Coast. *Thalassas: An International Journal of Marine Sciences*, 32(2), 75–85.  
<https://doi.org/10.1007/s41208-016-0010-1>
- Ferreira, V. A. C. (2022). *Avaliação da Vulnerabilidade dos Ecossistemas Intermareais e Avifauna do Estuário do Tejo devido à Subida do Nível Médio do Mar* [masterThesis].  
<https://repositorio.ul.pt/handle/10451/59258>
- Figueiredo, P. M., Cabral, J., & Rockwell, T. K. (2013). Recognition of Pleistocene marine terraces in the southwest of Portugal (Iberian Peninsula): Evidences of regional Quaternary uplift. *Annals of Geophysics*, 56(6), Article 6. <https://doi.org/10.4401/ag-6276>
- Freire, P. (1999). *Evolução Morfo-Sedimentar de Margens Estuarinas (Estuário do Tejo, Portugal)* [doctoralThesis, \*\*\*\*\*]. <http://repositorio.lnec.pt:8080/xmlui/handle/123456789/8729>
- Furlan, E., Pozza, P. D., Michetti, M., Torresan, S., Critto, A., & Marcomini, A. (2021). Development of a Multi-Dimensional Coastal Vulnerability Index: Assessing vulnerability to inundation scenarios in the Italian coast. *Science of The Total Environment*, 772, 144650.  
<https://doi.org/10.1016/j.scitotenv.2020.144650>
- Gamito, S. (2008). Three main stressors acting on the Ria Formosa lagoonal system (Southern Portugal): Physical stress, organic matter pollution and the land–ocean gradient. *Estuarine, Coastal and Shelf Science*, 77(4), 710–720. <https://doi.org/10.1016/j.ecss.2007.11.013>
- Gaodi, X., Lin, Z., Chunxia, L., Yu, X., & Wenhua, L. (2010). Applying Value Transfer Method for Eco-Service Valuation in China. *Journal of Resources and Ecology*, 1(1), 51–59.  
<https://doi.org/10.3969/j.issn.1674-764x.2010.01.007>

- Gareau, B. J. (2007). Ecological Values amid Local Interests: Natural Resource Conservation, Social Differentiation, and Human Survival in Honduras\*. *Rural Sociology*, 72(2), 244–268.  
<https://doi.org/10.1526/003601107781169992>
- Ghoussein, Y., Mhawej, M., Jaffal, A., Fadel, A., El Hourany, R., & Faour, G. (2018). Vulnerability assessment of the South-Lebanese coast: A GIS-based approach. *Ocean & Coastal Management*, 158, 56–63. <https://doi.org/10.1016/j.ocecoaman.2018.03.028>
- Giuliani, S., & Bellucci, L. G. (2019). Chapter 4 - Saltmarshes: Their Role in Our Society and Threats Posed to Their Existence. In C. Sheppard (Ed.), *World Seas: An Environmental Evaluation (Second Edition)* (pp. 79–101). Academic Press. <https://doi.org/10.1016/B978-0-12-805052-1.00004-8>
- Gonçalves, P. R. dos S. (2016). *Os sapais em Portugal continental. Levantamento e evolução das suas envolventes desde 1990 a 2012* [masterThesis, ISA/UL].  
<https://www.repository.utl.pt/handle/10400.5/13849>
- Gornitz, V. M., Daniels, R. C., White, T. W., & Birdwell, K. R. (1994). The Development of a Coastal Risk Assessment Database: Vulnerability to Sea-Level Rise in the U.S. Southeast. *Journal of Coastal Research*, 327–338.
- Guimarães, M. H. M. E., Cunha, A. H., Nzinga, R. L., & Marques, J. F. (2012). The distribution of seagrass (*Zostera noltii*) in the Ria Formosa lagoon system and the implications of clam farming on its conservation. *Journal for Nature Conservation*, 20(1), 30–40.  
<https://doi.org/10.1016/j.jnc.2011.07.005>
- Hamm, L., Capobianco, M., Dette, H. H., Lechuga, A., Spanhoff, R., & Stive, M. J. F. (2002). A summary of European experience with shore nourishment. *Coastal Engineering*, 47(2), 237–264. [https://doi.org/10.1016/S0378-3839\(02\)00127-8](https://doi.org/10.1016/S0378-3839(02)00127-8)
- Hardisty, J. (1994). *Beach and nearshore sediment transport, Sediment transport and depositional processes*.
- Hayashi, M. (2012). A Quick Method for Assessing Economic Damage Caused by Natural Disasters: An Epidemiological Approach. *International Advances in Economic Research*, 18(4), 417–427. <https://doi.org/10.1007/s11294-012-9367-y>

- Häyhä, T., & Franzese, P. P. (2014). Ecosystem services assessment: A review under an ecological-economic and systems perspective. *Ecological Modelling*, 289, 124–132.  
<https://doi.org/10.1016/j.ecolmodel.2014.07.002>
- Hegde, A. V., & Reju, V. R. (2007). Development of Coastal Vulnerability Index for Mangalore Coast, India. *Journal of Coastal Research*, 23(5 (235)), 1106–1111. <https://doi.org/10.2112/04-0259.1>
- Heslenfeld, P., Jungerius, P. D., & Klijn, J. A. (2004). European Coastal Dunes: Ecological Values, Threats, Opportunities and Policy Development. In M. L. Martínez & N. P. Psuty (Eds.), *Coastal Dunes: Ecology and Conservation* (pp. 335–351). Springer.  
[https://doi.org/10.1007/978-3-540-74002-5\\_20](https://doi.org/10.1007/978-3-540-74002-5_20)
- Hesp, P. A. (2004). Coastal Dunes in the Tropics and Temperate Regions: Location, Formation, Morphology and Vegetation Processes. In M. L. Martínez & N. P. Psuty (Eds.), *Coastal Dunes: Ecology and Conservation* (pp. 29–49). Springer. [https://doi.org/10.1007/978-3-540-74002-5\\_3](https://doi.org/10.1007/978-3-540-74002-5_3)
- Hinkel, J., Lincke, D., Vafeidis, A. T., Perrette, M., Nicholls, R. J., Tol, R. S. J., Marzeion, B., Fettweis, X., Ionescu, C., & Levermann, A. (2014). Coastal flood damage and adaptation costs under 21st century sea-level rise. *Proceedings of the National Academy of Sciences*, 111(9), 3292–3297. <https://doi.org/10.1073/pnas.1222469111>
- Höhle, J., & Höhle, M. (2009). Accuracy assessment of digital elevation models by means of robust statistical methods. *ISPRS Journal of Photogrammetry and Remote Sensing*, 64(4), 398–406.  
<https://doi.org/10.1016/j.isprsjprs.2009.02.003>
- Inácio, M. F. P. de O. (2017). *Evolução morfosedimentar do sapal da Caldeira de Tróia em contexto de subida do nível médio do mar* [masterThesis]. <https://repositorio.ul.pt/handle/10451/31656>
- Inácio, M., Freitas, M. C., Cunha, A. G., Antunes, C., Leira, M., Lopes, V., Andrade, C., & Silva, T. A. (2022). Simplified Marsh Response Model (SMRM): A Methodological Approach to Quantify the Evolution of Saltmarshes in a Sea-Level Rise Context. *Remote Sensing*, 14(14), Article 14. <https://doi.org/10.3390/rs14143400>
- Inge, L., Steven, B., & Leo, D. N. (2013). *Manual for the valuation of ecosystem services in estuaries*.

Instituto Hidrográfico. (2023). *Tabela de Marés*. [https://loja.hidrografico.pt/sdm\\_downloads/tabela-mares-vol-i-2023/](https://loja.hidrografico.pt/sdm_downloads/tabela-mares-vol-i-2023/)

Instituto Nacional de Estatística. (2019). *Anuário Estatístico da Região Algarve: 2018*.

Instituto Nacional de Estatística (Ed.). (2022). *Censos 2021. XVI Recenseamento Geral da População. VI Recenseamento Geral da Habitação: Resultados definitivos*.

IPCC. (2021). Climate Change 2021: The Physical Science Basis. Contribution of Working Group I to the Sixth Assessment Report of the Intergovernmental Panel on Climate Change [Masson-Delmotte, V., P. Zhai, A. Pirani, S.L. Connors, C. Péan, S. Berger, N. Caud, Y. Chen, L. Goldfarb, M.I. Gomis, M. Huang, K. Leitzell, E. Lonnoy, J.B.R. Matthews, T.K. Maycock, T. Waterfield, O. Yelekçi, R. Yu, and B. Zhou (eds.)]. *Cambridge University Press, Cambridge, United Kingdom and New York, NY, USA*, 2391. <https://doi.org/10.1017/9781009157896>.

IPCC. (2022). Climate Change 2022: Impacts, Adaptation and Vulnerability. Contribution of Working Group II to the Sixth Assessment Report of the Intergovernmental Panel on Climate Change [H.-O. Pörtner, D.C. Roberts, M. Tignor, E.S. Poloczanska, K. Mintenbeck, A. Alegría, M. Craig, S. Langsdorf, S. Löschke, V. Möller, A. Okem, B. Rama (eds.)]. *Cambridge University Press. Cambridge University Press, Cambridge, UK and New York, NY, USA*, 3056.

<https://doi.org/10.1017/9781009325844>

IPCC. (2023). *IPCC, 2023: Climate Change 2023: Synthesis Report. Contribution of Working Groups I, II and III to the Sixth Assessment Report of the Intergovernmental Panel on Climate Change* [Core Writing Team, H. Lee and J. Romero (eds.)]. *IPCC, Geneva, Switzerland*. (First). Intergovernmental Panel on Climate Change (IPCC).

<https://doi.org/10.59327/IPCC/AR6-9789291691647>

Islam, Md. A., Mitra, D., Dewan, A., & Akhter, S. H. (2016). Coastal multi-hazard vulnerability assessment along the Ganges deltaic coast of Bangladesh—A geospatial approach. *Ocean & Coastal Management*, 127, 1–15. <https://doi.org/10.1016/j.ocecoaman.2016.03.012>

Jevrejeva, S., Grinsted, A., & Moore, J. C. (2014). Upper limit for sea level projections by 2100. *Environmental Research Letters*, 9(10), 104008. <https://doi.org/10.1088/1748-9326/9/10/104008>

- Jiménez, J. A., Valdemoro, H. I., Bosom, E., Sánchez-Arcilla, A., & Nicholls, R. J. (2017). Impacts of sea-level rise-induced erosion on the Catalan coast. *Regional Environmental Change*, 17(2), 593–603. <https://doi.org/10.1007/s10113-016-1052-x>
- Jones, M. L. M., Sowerby, A., Williams, D. L., & Jones, R. E. (2008). Factors controlling soil development in sand dunes: Evidence from a coastal dune soil chronosequence. *Plant and Soil*, 307(1), 219–234. <https://doi.org/10.1007/s11104-008-9601-9>
- Kantamaneni, K., Phillips, M., Thomas, T., & Jenkins, R. (2018). Assessing coastal vulnerability: Development of a combined physical and economic index. *Ocean & Coastal Management*, 158, 164–175. <https://doi.org/10.1016/j.ocecoaman.2018.03.039>
- Kenyon, W., Hanley, N., & Nevin, C. (2001). Citizens' juries: An aid to environmental valuation? *Environment and Planning C: Government and Policy*, 19(4), 557–566. Scopus. <https://doi.org/10.1068/c4s>
- Kerambrun, P. (1986). Coastal lagoons along the Southern Mediterranean coast (Algeria, Egypt, Libya, Morocco, Tunisia): Description and bibliography. *Unesco Reports in Marine Science*.
- King, M., & Faasili, U. (1999). Community-based management of subsistence fisheries in Samoa. *Fisheries Management and Ecology*, 6(2), 133–144. <https://doi.org/10.1046/j.1365-2400.1999.00136.x>
- Klein, R. J. T., & Nicholls, R. J. (1999). Assessment of Coastal Vulnerability to Climate Change. *Ambio*, 28(2), 182–187.
- Kombiadou, K., Matias, A., Carrasco, R., Ferreira, O., Costas, S., & Vieira, G. (2018). Towards assessing the resilience of complex coastal systems: Examples from Ria Formosa (South Portugal). *Journal of Coastal Research -Special Issue, SI 85*, 646–650. <https://doi.org/10.2112/si85-130.1>
- Kubal, C., Haase, D., Meyer, V., & Scheuer, S. (2009). Integrated urban flood risk assessment – adapting a multicriteria approach to a city. *Natural Hazards and Earth System Sciences*, 9(6), 1881–1895. <https://doi.org/10.5194/nhess-9-1881-2009>
- Kutiel, P. (2001). Conservation and management of the mediterranean coastal sand dunes in Israel. *Journal of Coastal Conservation*, 7(2), 183–192. <https://doi.org/10.1007/BF02742480>

- Laffoley, D., Baxter, J. M., Day, J. C., Wenzel, L., Bueno, P., & Zischka, K. (2019). Chapter 29—Marine Protected Areas. In C. Sheppard (Ed.), *World Seas: An Environmental Evaluation (Second Edition)* (pp. 549–569). Academic Press. <https://doi.org/10.1016/B978-0-12-805052-1.00027-9>
- Laffoley, D., & Grimsditch, G. D. (2009). *The Management of Natural Coastal Carbon Sinks*. IUCN.
- Leatherman, S. P., Zhang, K., & Douglas, B. C. (2000). Sea level rise shown to drive coastal erosion. *Eos, Transactions American Geophysical Union*, 81(6), 55–57.  
<https://doi.org/10.1029/00EO00034>
- Lee, H. W., & Park, S. S. (2013). A hydrodynamic modeling study to estimate the flushing rate in a large coastal embayment. *Journal of Environmental Management*, 115, 278–286.  
<https://doi.org/10.1016/j.jenvman.2012.10.055>
- Lele, S., Springate-Baginski, O., Lakerveld, R., Deb, D., & Dash, P. (2013). Ecosystem Services: Origins, Contributions, Pitfalls, and Alternatives. *Conservation and Society*, 11(4), 343.  
<https://doi.org/10.4103/0972-4923.125752>
- Li, X., Zhou, Y., Tian, B., Kuang, R., & Wang, L. (2015). GIS-based methodology for erosion risk assessment of the muddy coast in the Yangtze Delta. *Ocean & Coastal Management*, 108, 97–108. <https://doi.org/10.1016/j.ocecoaman.2014.09.028>
- Li, Z., Zhu, C., & Gold, C. (2005). *Digital Terrain Modeling: Principles and Methodology*. CRC Press.
- Lira, C. P., Silva, A. N., Taborda, R., & Freire de Andrade, C. (2016). Coastline evolution of Portuguese low-lying sandy coast in the last 50 years: An integrated approach. *Earth System Science Data*, 8(1), 265–278. <https://doi.org/10.5194/essd-8-265-2016>
- Lloret, J., Marín, A., & Marín-Guirao, L. (2008). Is coastal lagoon eutrophication likely to be aggravated by global climate change? *Estuarine, Coastal and Shelf Science*, 78(2), 403–412.  
<https://doi.org/10.1016/j.ecss.2008.01.003>
- Luisetti, T., Jackson, E. L., & Turner, R. K. (2013). Valuing the European ‘coastal blue carbon’ storage benefit. *Marine Pollution Bulletin*, 71(1), 101–106.  
<https://doi.org/10.1016/j.marpolbul.2013.03.029>

- Ma, Z., Ysebaert, T., van der Wal, D., & Herman, P. M. J. (2018). Conditional effects of tides and waves on short-term marsh sedimentation dynamics. *Earth Surface Processes and Landforms*, 43(10), 2243–2255. <https://doi.org/10.1002/esp.4357>
- Magnan, A. K., Pörtner, H.-O., Duvat, V. K. E., Garschagen, M., Guinder, V. A., Zommers, Z., Hoegh-Guldberg, O., & Gattuso, J.-P. (2021). Estimating the global risk of anthropogenic climate change. *Nature Climate Change*, 11(10), Article 10. <https://doi.org/10.1038/s41558-021-01156-w>
- Mahapatra, M., Ratheesh, R., & Rajawat, A. S. (2014). Shoreline Change Analysis along the Coast of South Gujarat, India, Using Digital Shoreline Analysis System. *Journal of the Indian Society of Remote Sensing*, 42(4), 869–876. <https://doi.org/10.1007/s12524-013-0334-8>
- Mani Murali, R., Ankita, M., Amrita, S., & Vethamony, P. (2013). Coastal vulnerability assessment of Puducherry coast, India, using the analytical hierarchical process. *Natural Hazards and Earth System Sciences*, 13(12), 3291–3311. <https://doi.org/10.5194/nhess-13-3291-2013>
- Mani Murali, R., Vethamony, P., Saran, A. K., & Jayakumar, S. (2006). Change detection studies in coastal zone features of Goa, India by remote sensing. *Current Science*, 91(6), 816–820.
- Martins, H., & Veloso-Gomes, F. (2011). *Alimentação artificial de praias em ambientes energéticos Intermédios, in: Actas Das 6.as Jornadas de Hidráulica, Recursos Hídricos e Ambiente*. (pp. 29–40). FEUP.
- Martins, V. N., Pires, R., & Cabral, P. (2012). Modelling of coastal vulnerability in the stretch between the beaches of Porto de Mós and Falésia, Algarve (Portugal). *Journal of Coastal Conservation*, 16(4), 503–510. <https://doi.org/10.1007/s11852-012-0191-6>
- McLaughlin, S., Cooper, J., & Andrew, G. (2010). A multi-scale coastal vulnerability index: A tool for coastal managers? *Environmental Hazards*, 9(3), 233–248.  
<https://doi.org/10.3763/ehaz.2010.0052>
- McLaughlin, S., McKenna, J., & Cooper, J. A. G. (2002). Socio-economic data in coastal vulnerability indices: Constraints and opportunities. *Journal of Coastal Research*, 36 (10036), 487–497. <https://doi.org/10.2112/1551-5036-36.sp1.487>

- Mendes, D., & Oliveira, T. C. A. (2021). Deep-water spectral wave steepness offshore mainland Portugal. *Ocean Engineering*, 236, 109548. <https://doi.org/10.1016/j.oceaneng.2021.109548>
- Meyer, V., Scheuer, S., & Haase, D. (2009). A multicriteria approach for flood risk mapping exemplified at the Mulde river, Germany. *Natural Hazards*, 48(1), 17–39. <https://doi.org/10.1007/s11069-008-9244-4>
- Millennium Ecosystem Assessment (Ed.). (2005). *Ecosystems and human well-being: Wetlands and water synthesis: a report of the Millennium Ecosystem Assessment*. World Resources Institute.
- Möller, A., & Ranke, U. (2006). Estimation of the on-farm-costs of soil erosion in Sleman, Indonesia. *Geo-Environment and Landscape Evolution II: Monitoring, Simulation, Management and Remediation*, 1, 43–52. <https://doi.org/10.2495/GEO060061>
- Moreira, M. E. (1987). Estudo fitogeográfico do ecossistema de sapal do estuário do Sado. *Finisterra*, 22(44), Article 44. <https://doi.org/10.18055/Finis2000>
- Moskalski, S. M., & Sommerfield, C. K. (2012). Suspended sediment deposition and trapping efficiency in a Delaware saltmarsh. *Geomorphology*, 139–140, 195–204. <https://doi.org/10.1016/j.geomorph.2011.10.018>
- Nave, S., & Rebêlo, L. (2021). Coastline evolution of the Portuguese south eastern coast: A high-resolution approach in a 65 years' time-window. *Journal of Coastal Conservation*, 25(1), 1–22. <https://doi.org/10.1007/s11852-020-00791-3>
- NEMUS, G. e R. A., Lda. (2005). *Concepção do projeto de um pequeno porto de pesca em Santa Luzia* (Estudo de Impacte Ambiental-Aditamento; p. 51). Ministério das obras públicas transportes e habitação.
- Newton, A., Brito, A. C., Icely, J. D., Derolez, V., Clara, I., Angus, S., Schernewski, G., Inácio, M., Lillebø, A. I., Sousa, A. I., Béjaoui, B., Solidoro, C., Tosic, M., Cañedo-Argüelles, M., Yamamuro, M., Reizopoulou, S., Tseng, H.-C., Canu, D., Roselli, L., ... Khokhlov, V. (2018). Assessing, quantifying and valuing the ecosystem services of coastal lagoons. *Journal for Nature Conservation*, 44, 50–65. <https://doi.org/10.1016/j.jnc.2018.02.009>

- Newton, A., & Mudge, S. M. (2003). Temperature and salinity regimes in a shallow, mesotidal lagoon, the Ria Formosa, Portugal. *Estuarine, Coastal and Shelf Science*, 57(1), 73–85.  
[https://doi.org/10.1016/S0272-7714\(02\)00332-3](https://doi.org/10.1016/S0272-7714(02)00332-3)
- Nguyen, T. T. X., Bonetti, J., Rogers, K., & Woodroffe, C. D. (2016). Indicator-based assessment of climate-change impacts on coasts: A review of concepts, methodological approaches and vulnerability indices. *Ocean & Coastal Management*, 123, 18–43.  
<https://doi.org/10.1016/j.ocecoaman.2015.11.022>
- Nicholls, S. (2019). Impacts of environmental disturbances on housing prices: A review of the hedonic pricing literature. *Journal of Environmental Management*, 246, 1–10.  
<https://doi.org/10.1016/j.jenvman.2019.05.144>
- NOAA. (2017). *Global and regional sea level rise scenarios for the United States*.  
[https://tidesandcurrents.noaa.gov/publications/tech rpt83\\_Global\\_and\\_Regional\\_SLR\\_Scenarios\\_for\\_the\\_US\\_final.pdf](https://tidesandcurrents.noaa.gov/publications/tech rpt83_Global_and_Regional_SLR_Scenarios_for_the_US_final.pdf)
- Nunes, P. A. L. D., & van den Bergh, J. C. J. M. (2001). Economic valuation of biodiversity: Sense or nonsense? *Ecological Economics*, 39(2), 203–222. [https://doi.org/10.1016/S0921-8009\(01\)00233-6](https://doi.org/10.1016/S0921-8009(01)00233-6)
- Office of the United Nations Disaster Relief Coordinator. (1980). *Natural disasters and vulnerability analysis: Report of Expert Group Meeting, 9-12 July 1979*. Expert Group Meeting on Vulnerability Analysis (1979 : Geneva). <https://digitallibrary.un.org/record/95986>
- OpenStreetMap contributors. (2017). *Planet dump retrieved from https://planet.osm.org*.
- Pacheco, A., Ferreira, Ó., Williams, J. J., Garel, E., Vila-Concejo, A., & Dias, J. A. (2010). Hydrodynamics and equilibrium of a multiple-inlet system. *Marine Geology*, 274(1), 32–42.  
<https://doi.org/10.1016/j.margeo.2010.03.003>
- Parthasarathy, A., & Natesan, U. (2015). Coastal vulnerability assessment: A case study on erosion and coastal change along Tuticorin, Gulf of Mannar. *Natural Hazards*, 75(2), 1713–1729.  
<https://doi.org/10.1007/s11069-014-1394-y>
- Pearce, D. W. (1993). *Economic Values and the Natural World*. Earthscan.

- Peduzzi, P., Dao, H., & Herold, C. (2002). *Global Risk And Vulnerability Index Trends per Year (GRAVITY) Phase II: Development, analysis and results.*
- [http://mathemouton.free.fr/MCF/Publis\\_HDR\\_applis/ew\\_gravity2.pdf](http://mathemouton.free.fr/MCF/Publis_HDR_applis/ew_gravity2.pdf)
- Pendleton, L., Donato, D. C., Murray, B. C., Crooks, S., Jenkins, W. A., Sifleet, S., Craft, C., Fourqurean, J. W., Kauffman, J. B., Marbà, N., Megonigal, P., Pidgeon, E., Herr, D., Gordon, D., & Baldera, A. (2012). Estimating Global “Blue Carbon” Emissions from Conversion and Degradation of Vegetated Coastal Ecosystems. *PLOS ONE*, 7(9), e43542.
- <https://doi.org/10.1371/journal.pone.0043542>
- Pilkey, O. H., Neal, W. J., Monteiro, J. H., & Dias, J. M. A. (1989). Algarve Barrier Islands: A Noncoastal-Plain System in Portugal. *Journal of Coastal Research*, 5(2), 239–261.
- Pinto, C. A., Silveira, T. M., & Teixeira, S. B. (2018). *Alimentação Artificial de Praias na Faixa Costeira de Portugal Continental: Enquadramento e retrospectiva das intervenções realizadas (1950-2017)*. APA.
- [https://sniambgeoviewer.apambiente.pt/GeoDocs/geoportaldocs/DESTAQUES/2018/Alimento\\_Artificial\\_Praias/Relatorio\\_Tecnico\\_AAP\\_14-02-2018\\_VFinal.pdf](https://sniambgeoviewer.apambiente.pt/GeoDocs/geoportaldocs/DESTAQUES/2018/Alimento_Artificial_Praias/Relatorio_Tecnico_AAP_14-02-2018_VFinal.pdf)
- PROT Algarve. (2004). *Plano Regional de Ordenamento do Território, VOLUME II - Caracterização e Diagnóstico, ANEXO H - Recursos Hídricos, Planeamento e Gestão do Recurso Água*.
- [https://prot.ccdr-alg.pt/Storage/pdfs/Volume\\_II\\_ANEXO\\_H.pdf](https://prot.ccdr-alg.pt/Storage/pdfs/Volume_II_ANEXO_H.pdf)
- Pugh, D. (2004). *Changing Sea Levels: Effects of Tides, Weather and Climate*.
- <https://www.abebooks.com/9780521532181/Changing-Sea-Levels-Effects-Tides-0521532183/plp>
- Rahmstorf, S. (2007). A Semi-Empirical Approach to Projecting Future Sea-Level Rise. *Science (New York, N.Y.)*, 315, 368–370. <https://doi.org/10.1126/science.1135456>
- Ramieri, E., Hartley, A., Barbanti, A., Santos, F. D., Gomes, A., Laihonens, P., Marinova, N., & Santini, M. (2011). *Methods for assessing coastal vulnerability to climate change*.
- Reid, W., Mooney, H., Cropper, A., Capistrano, D., Carpenter, S., & Chopra, K. (2005). *Millennium Ecosystem Assessment. Ecosystems and human well-being: Synthesis*.

Ribeiro, J. L. (2010). *Riscos Costeiros Estratégias de prevenção, mitigação e protecção, no âmbito do planeamento de emergência e do ordenamento do território*. Autoridade nacional de Protecção Civil. [https://protecaocivil.sintra.pt/images/servico-municipal-de-protecao-civil/cadernos\\_tecnicos/CT15%20-%20Riscos%20Costeiros%20-%20Estrat%C3%A9gias%20de%20preven%C3%A7%C3%A3o,%20mitiga%C3%A7%C3%A7%C3%A3o%20e%20protec%C3%A7%C3%A3o%20no%20planeamento%20de%20emerg%C3%A7%C3%A3o%20e%20do%20ordenamento%20do%20territ%C3%B3rio.pdf](https://protecaocivil.sintra.pt/images/servico-municipal-de-protecao-civil/cadernos_tecnicos/CT15%20-%20Riscos%20Costeiros%20-%20Estrat%C3%A9gias%20de%20preven%C3%A7%C3%A3o,%20mitiga%C3%A7%C3%A7%C3%A3o%20e%20protec%C3%A7%C3%A3o%20no%20planeamento%20de%20emerg%C3%A7%C3%A3o%20e%20do%20ordenamento%20do%20territ%C3%B3rio.pdf)

Ribeiro, J., Monteiro, C., Monteiro, P., Bentes, L., Coelho, R., Gonçalves, J., Lino, P., & Erzini, K. (2008). Long-term changes in fish communities of the Ria Formosa coastal lagoon (southern Portugal) based on two studies made 20 years apart. *Estuarine Coastal and Shelf Science*, 76, 57–68. <https://doi.org/10.1016/j.ecss.2007.06.001>

Rocha, C., Antunes, C., & Catita, C. (2020). Coastal Vulnerability Assessment Due to Sea Level Rise: The Case Study of the Atlantic Coast of Mainland Portugal. *Water*, 12(2), Article 2. <https://doi.org/10.3390/w12020360>

Rocha, C., Antunes, C., & Catita, C. (2023). Coastal indices to assess sea-level rise impacts—A brief review of the last decade. *Ocean & Coastal Management*, 237, 106536. <https://doi.org/10.1016/j.ocemarman.2023.106536>

Rocha, C. S. (2016). *Estudo e análise da vulnerabilidade costeira face a cenários de subida do nível do mar e eventos extremos devido ao efeito das alterações climáticas* [masterThesis]. <https://repositorio.ul.pt/handle/10451/26321>

Rolim, J. P. A. (2014). *Modelação hidrodinâmica da sobreelevação do nível do mar de origem meteorológica no Estuário do Tejo* [Instituto Superior Técnico, Universidade de Lisboa]. <http://www.fenixedu.org>

Rosati, J. D. (2005). Concepts in Sediment Budgets. *Journal of Coastal Research*, 21(2), 307–322.

Rosati, J. D., Dean, R. G., & Walton, T. L. (2013). The modified Bruun Rule extended for landward transport. *Marine Geology*, 340, 71–81. <https://doi.org/10.1016/j.margeo.2013.04.018>

- Royo, M. L., Ranasinghe, R., & Jiménez, J. A. (2016). A Rapid, Low-Cost Approach to Coastal Vulnerability Assessment at a National Level. *Journal of Coastal Research*, 32(4), 932–945. <https://doi.org/10.2112/JCOASTRES-D-14-00217.1>
- Saaty, T. L. (1988). What is the Analytic Hierarchy Process? In G. Mitra, H. J. Greenberg, F. A. Lootsma, M. J. Rijckaert, & H. J. Zimmermann (Eds.), *Mathematical Models for Decision Support* (pp. 109–121). Springer. [https://doi.org/10.1007/978-3-642-83555-1\\_5](https://doi.org/10.1007/978-3-642-83555-1_5)
- Salles, P. A. de A. (2001). *Hydrodynamic controls on multiple tidal inlet persistence* [Thesis, Massachusetts Institute of Technology]. <https://dspace.mit.edu/handle/1721.1/84213>
- Salles, P., Voulgaris, G., & Aubrey, D. G. (2005). Contribution of nonlinear mechanisms in the persistence of multiple tidal inlet systems. *Estuarine, Coastal and Shelf Science*, 65(3), 475–491. <https://doi.org/10.1016/j.ecss.2005.06.018>
- Santo, M. M. D. E. (2022). *Desenvolvimento de um método paramétrico semiautomático de recuo do perfil topográfico da costa devido aos efeitos cumulativos de erosão e subida do nível médio do mar* [masterThesis]. <https://repositorio.ul.pt/handle/10451/59163>
- Santos, F. D., Forbes, K., & Moita, R. (Eds.). (2002). *Climate Change in Portugal. Scenarios, Impacts and Adaptation Measures—SIAM Project*. Gradiva. <http://cciam.fc.ul.pt/prj/siam/>
- Santos, F. D., & Miranda, P. (Eds.). (2006). *Alterações Climáticas em Portugal. Cenários, Impactos e Medidas de Adaptação—Projecto SIAM II*. Gradiva.
- Satta, A. (2014). *An Index-based method to assess vulnerabilities and risks of Mediterranean coastal zones to multiple hazards*. Ca’Foscari University of Venice, Italy.
- Satta, A., Puddu, M., Venturini, S., & Giupponi, C. (2017). Assessment of coastal risks to climate change related impacts at the regional scale: The case of the Mediterranean region. *International Journal of Disaster Risk Reduction*, 24, 284–296. <https://doi.org/10.1016/j.ijdrr.2017.06.018>
- Savenije, H. H. G., Toffolon, M., Haas, J., & Veling, E. J. M. (2008). Analytical description of tidal dynamics in convergent estuaries. *Journal of Geophysical Research: Oceans*, 113(C10). <https://doi.org/10.1029/2007JC004408>

- Schuerch, M., Spencer, T., Temmerman, S., Kirwan, M. L., Wolff, C., Lincke, D., McOwen, C. J., Pickering, M. D., Reef, R., Vafeidis, A. T., Hinkel, J., Nicholls, R. J., & Brown, S. (2018). Future response of global coastal wetlands to sea-level rise. *Nature*, 561(7722), Article 7722. <https://doi.org/10.1038/s41586-018-0476-5>
- Serpa, D., Jesus, D., & Falcão, M. (2005). *Ria Formosa Ecosystem: Socio-Economic Approach*.
- Serpelloni, E., Faccenna, C., Spada, G., Dong, D., & Williams, S. D. P. (2013). Vertical GPS ground motion rates in the Euro-Mediterranean region: New evidence of velocity gradients at different spatial scales along the Nubia-Eurasia plate boundary. *Journal of Geophysical Research: Solid Earth*, 118(11), 6003–6024. <https://doi.org/10.1002/2013JB010102>
- Shrestha, R. K., Seidl, A. F., & Moraes, A. S. (2002). Value of recreational fishing in the Brazilian Pantanal: A travel cost analysis using count data models. *Ecological Economics*, 42(1), 289–299. [https://doi.org/10.1016/S0921-8009\(02\)00106-4](https://doi.org/10.1016/S0921-8009(02)00106-4)
- Silva, A. A. A., Freire, E., & Crisóstomo, G. (2008). Variações do nível médio anual do mar em Cascais: Características e tendências. *Estudos Do Quaternário / Quaternary Studies*, 5, Article 5. <https://doi.org/10.30893/eq.v0i5.61>
- Silva, S. F., Martinho, M., Capitão, R., Reis, T., Fortes, C. J., & Ferreira, J. C. (2017). An index-based method for coastal-flood risk assessment in low-lying areas (Costa de Caparica, Portugal). *Ocean & Coastal Management*, 144, 90–104. <https://doi.org/10.1016/j.ocecoaman.2017.04.010>
- Silva, T. A. A. (2013). *Sedimentologia e morfodinâmica de sapais do estuário do Tejo em cenários de alteração climática* [masterThesis]. <https://repositorio.ul.pt/handle/10451/10507>
- Solidoro, C., Cossarini, G., Libralato, S., & Salon, S. (2010). Remarks on the redefinition of system boundaries and model parameterization for downscaling experiments. *Progress in Oceanography*, 84(1–2), 134–137. <https://doi.org/10.1016/j.pocean.2009.09.017>
- Sousa, C. A. M., Cunha, M. E., & Ribeiro, L. (2020). Tracking 130 years of coastal wetland reclamation in Ria Formosa, Portugal: Opportunities for conservation and aquaculture. *Land Use Policy*, 94, 104544. <https://doi.org/10.1016/j.landusepol.2020.104544>

- Sousa, C., Boski, T., & Pereira, L. (2019). Holocene evolution of a barrier island system, Ria Formosa, South Portugal. *The Holocene*, 29(1), 64–76.  
<https://doi.org/10.1177/0959683618804639>
- Sprung, M. (1994). Macrobenthic Secondary Production in the Intertidal Zone of the Ria Formosa—A Lagoon in Southern Portugal. *Estuarine, Coastal and Shelf Science*, 38(6), 539–558.  
<https://doi.org/10.1006/ecss.1994.1037>
- Struhsaker, T. T., Struhsaker, P. J., & Siex, K. S. (2005). Conserving Africa's rain forests: Problems in protected areas and possible solutions. *Biological Conservation*, 123(1), 45–54.  
<https://doi.org/10.1016/j.biocon.2004.10.007>
- Szlagsztein, C., & Sterr, H. (2007). A GIS-based vulnerability assessment of coastal natural hazards, state of Pará, Brazil. *Journal of Coastal Conservation*, 11(1), 53–66.  
<https://doi.org/10.1007/s11852-007-0003-6>
- Taborda, R., & Ribeiro, M. A. (2015). A simple model to estimate the impact of sea-level rise on platform beaches. *Geomorphology*, 234, 204–210.  
<https://doi.org/10.1016/j.geomorph.2015.01.015>
- TEEB (Ed.). (2010). *Mainstreaming the economics of nature: A synthesis of the approach, conclusions and recommendations of TEEB*. UNEP.
- Thatcher, C., Brock, J., & Pendleton, E. (2013). Economic Vulnerability to Sea-Level Rise Along the Northern U.S. Gulf Coast. *Journal of Coastal Research*, 63, 234–243.  
<https://doi.org/10.2307/23486515>
- Titus, J. G. (1986). Greenhouse effect, sea level rise, and coastal zone management. *Coastal Zone Management Journal*, 14(3), 147–171. <https://doi.org/10.1080/08920758609362000>
- Titus, J. G. (1990). Greenhouse effect, sea level rise, and barrier Islands: Case study of long beach Island, New Jersey. *Coastal Management*, 18(1), 65–90.  
<https://doi.org/10.1080/08920759009362101>
- Torresan, S., Critto, A., Dalla Valle, M., Harvey, N., & Marcomini, A. (2008). Assessing coastal vulnerability to climate change: Comparing segmentation at global and regional scales. *Sustainability Science*, 3(1), 45–65. <https://doi.org/10.1007/s11625-008-0045-1>

- Turpie, J. K. (2003). The existence value of biodiversity in South Africa: How interest, experience, knowledge, income and perceived level of threat influence local willingness to pay. *Ecological Economics*, 46(2), 199–216. [https://doi.org/10.1016/S0921-8009\(03\)00122-8](https://doi.org/10.1016/S0921-8009(03)00122-8)
- UNESCO. (1971). *Convention on Wetlands of International Importance especially as Waterfowl Habitat*. [https://www.ramsar.org/sites/default/files/documents/library/current\\_convention\\_text\\_e.pdf](https://www.ramsar.org/sites/default/files/documents/library/current_convention_text_e.pdf)
- UNESCO. (1979). Coastal ecosystems of the southern Mediterranean: Lagoons, deltas and saltmarshes: Report of a meeting of experts, Tunis, 25-27 September 1978. *Unesco Reports in Marine Science*.
- UNISDR, UN. O. for D. R. R. (2004). *Living with risk: A global review of disaster reduction initiatives* (2004 version). United Nations.
- UNISDR, UN. O. for D. R. R. (2009). *UNISDR terminology on disaster risk reduction*. <https://digitallibrary.un.org/record/3967528>
- United Nations. (1992). *Convention on biological diversity*. <https://www.cbd.int/doc/legal/cbd-en.pdf>
- USAID. (2009). *Adapting to Coastal Climate Change: A Guidebook for Development Planners*.
- Vallés, S. M., & Cambrollé, J. (2013). Coastal Dune Hazards. In C. W. Finkl (Ed.), *Coastal Hazards* (pp. 491–510). Springer Netherlands. [https://doi.org/10.1007/978-94-007-5234-4\\_18](https://doi.org/10.1007/978-94-007-5234-4_18)
- Van Coppenolle, R., & Temmerman, S. (2020). Identifying global hotspots where coastal wetland conservation can contribute to nature-based mitigation of coastal flood risks. *Global and Planetary Change*, 187, 103125. <https://doi.org/10.1016/j.gloplacha.2020.103125>
- van der Meulen, F., & Salman, A. H. P. M. (1996). Management of Mediterranean coastal dunes. *Ocean & Coastal Management*, 30(2), 177–195. [https://doi.org/10.1016/0964-5691\(95\)00060-7](https://doi.org/10.1016/0964-5691(95)00060-7)
- Yusuf, A. A., & Francisco, H. (2009). *Climate Change Vulnerability Mapping for Southeast Asia*.
- Zhu, Z.-T., Cai, F., Chen, S.-L., Gu, D.-Q., Feng, A.-P., Cao, C., Qi, H.-S., & Lei, G. (2019). Coastal Vulnerability to Erosion Using a Multi-Criteria Index: A Case Study of the Xiamen Coast. *Sustainability*, 11(1), Article 1. <https://doi.org/10.3390/su11010093>

## Annexes

### A. Classification of Socioeconomic Parameters

#### i. Population Density Reclassification

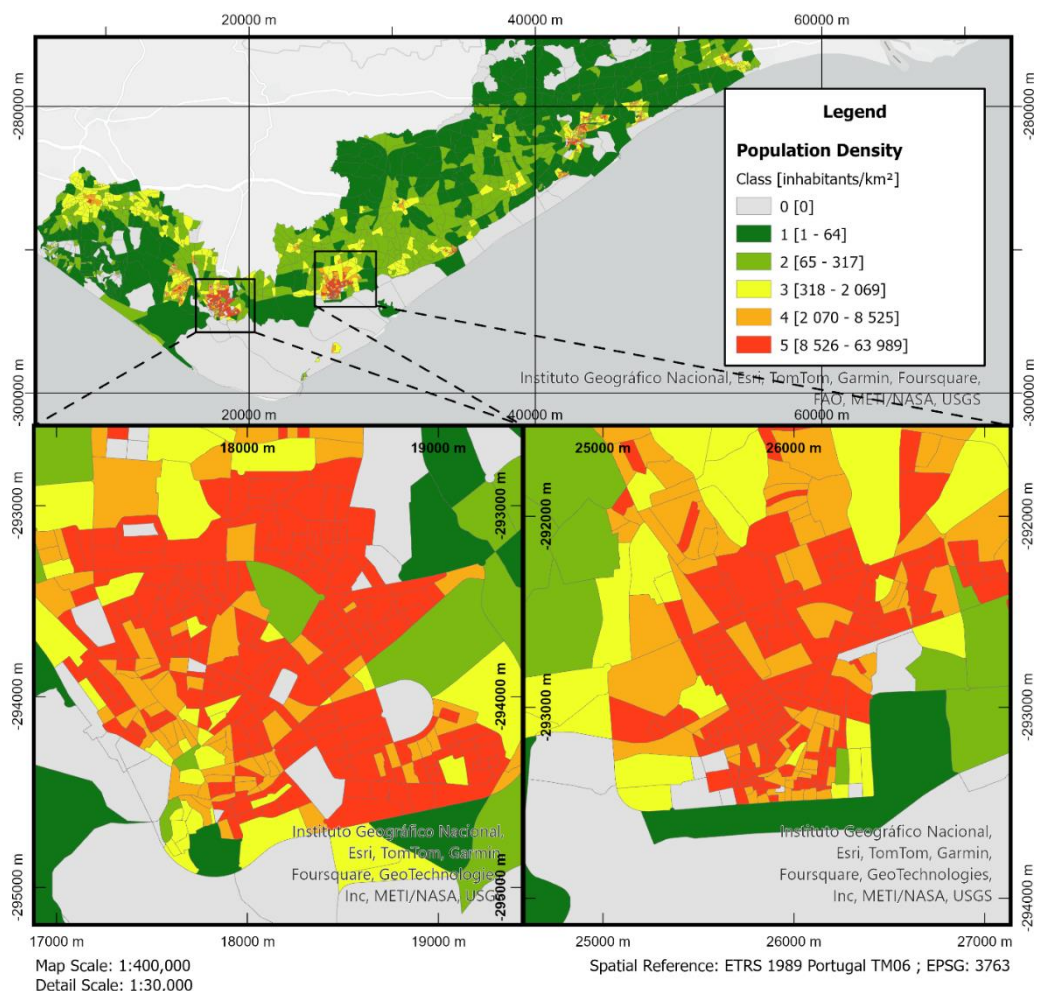


Figure A.1 - Population Density (PD) Classification. Top: Overview of the Area of Study. Bottom Left: City of Faro and Surroundings. Bottom Right: City of Olhão and Surroundings.

ii. Infrastructure Reclassification

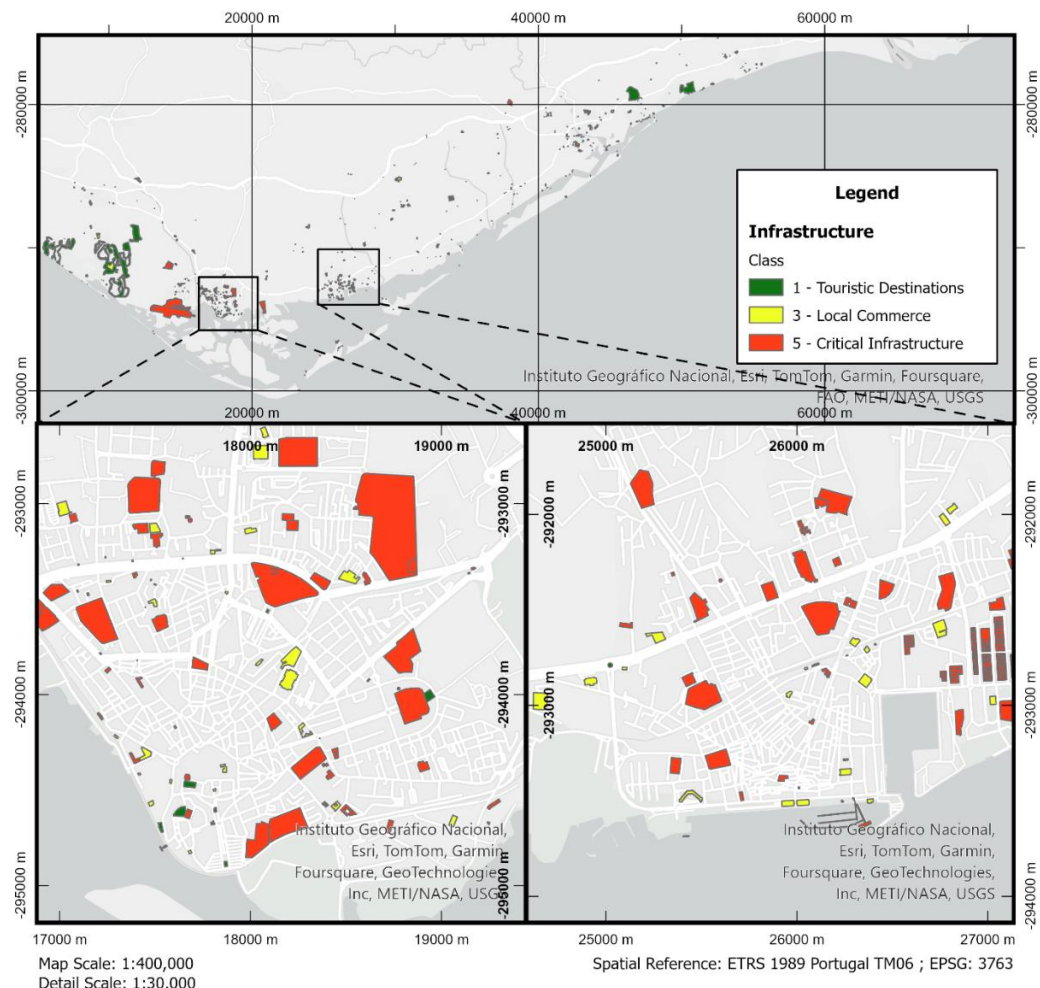
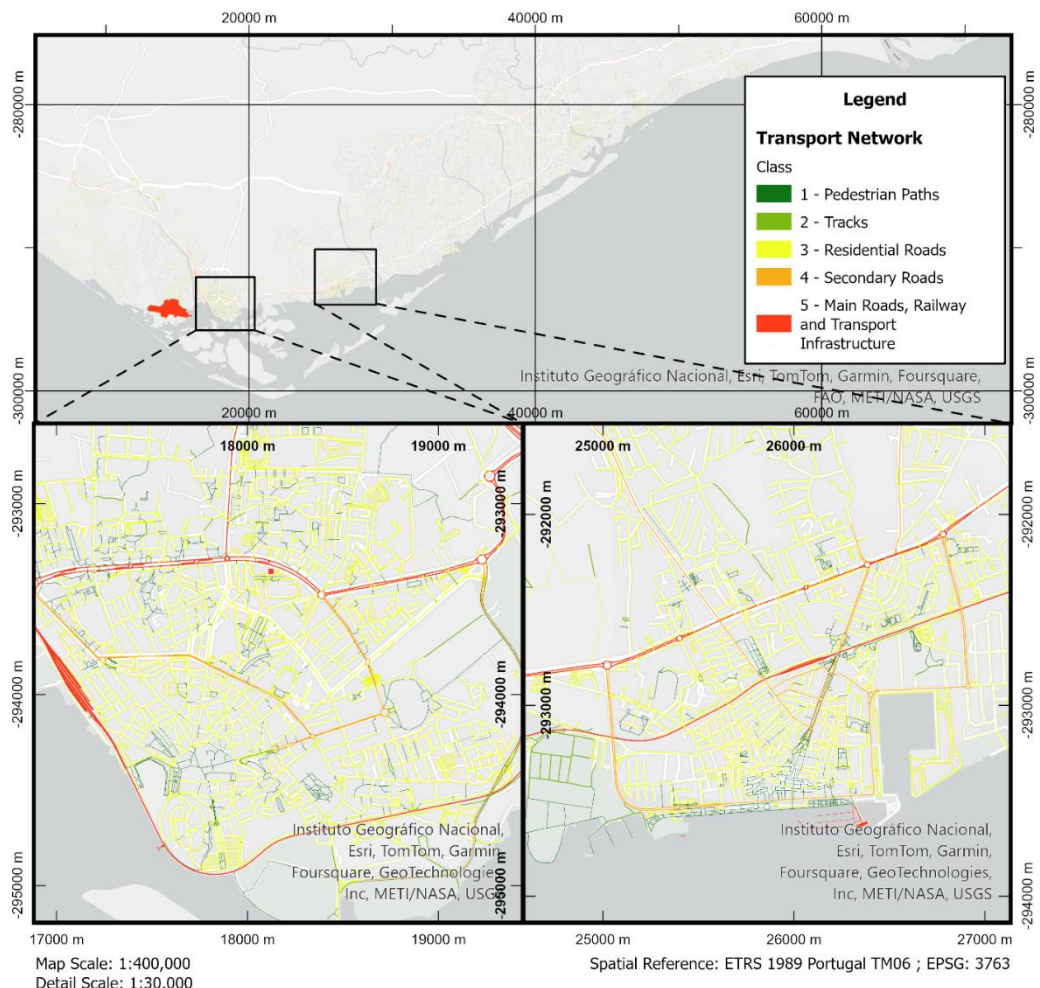


Figure A.2 - Infrastructure (I) Classification. Top: Overview of the Area of Study. Bottom Left: City of Faro and Surroundings. Bottom Right: City of Olhão and Surroundings.

### iii. Transport Network Reclassification



*Figure A.3 - Transport Network (TN) Classification. Top: Overview of the Area of Study. Bottom Left: City of Faro and Surroundings. Bottom Right: City of Olhão and Surroundings.*

iv. Soil Use Reclassification

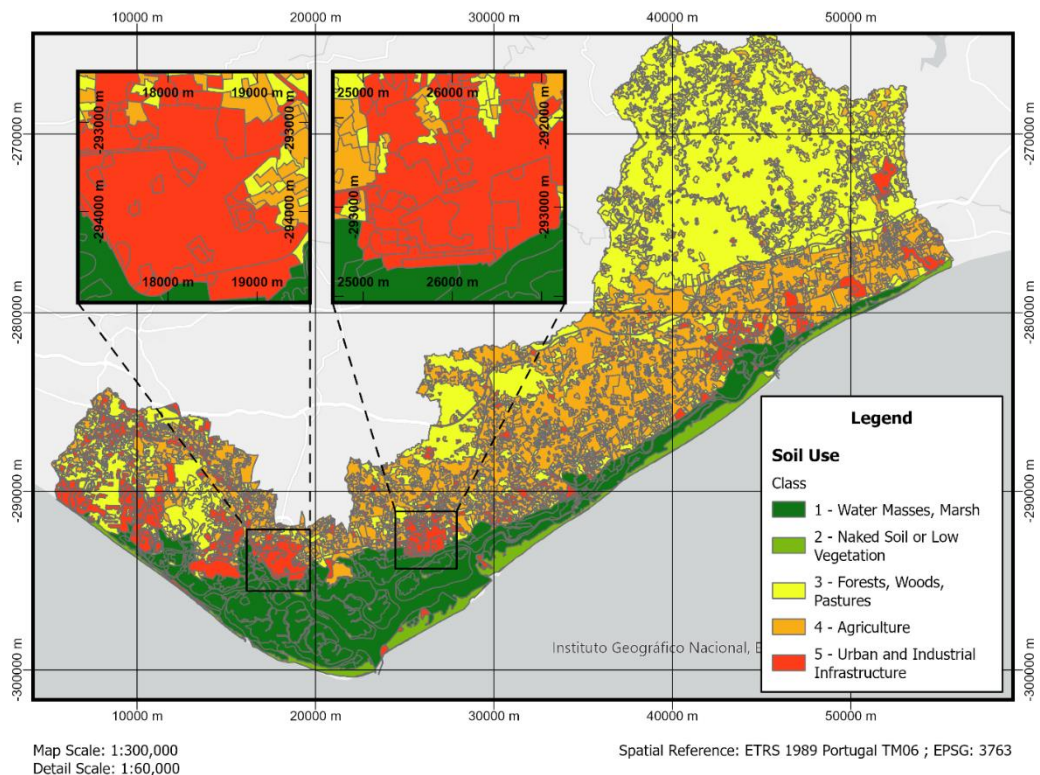


Figure A.4 – Soil Use (SU) Classification. Top Left: City of Faro and Surroundings. Top Right: City of Olhão and Surroundings Bottom: Overview of the Area of Study.

v. Ecological Areas Reclassification

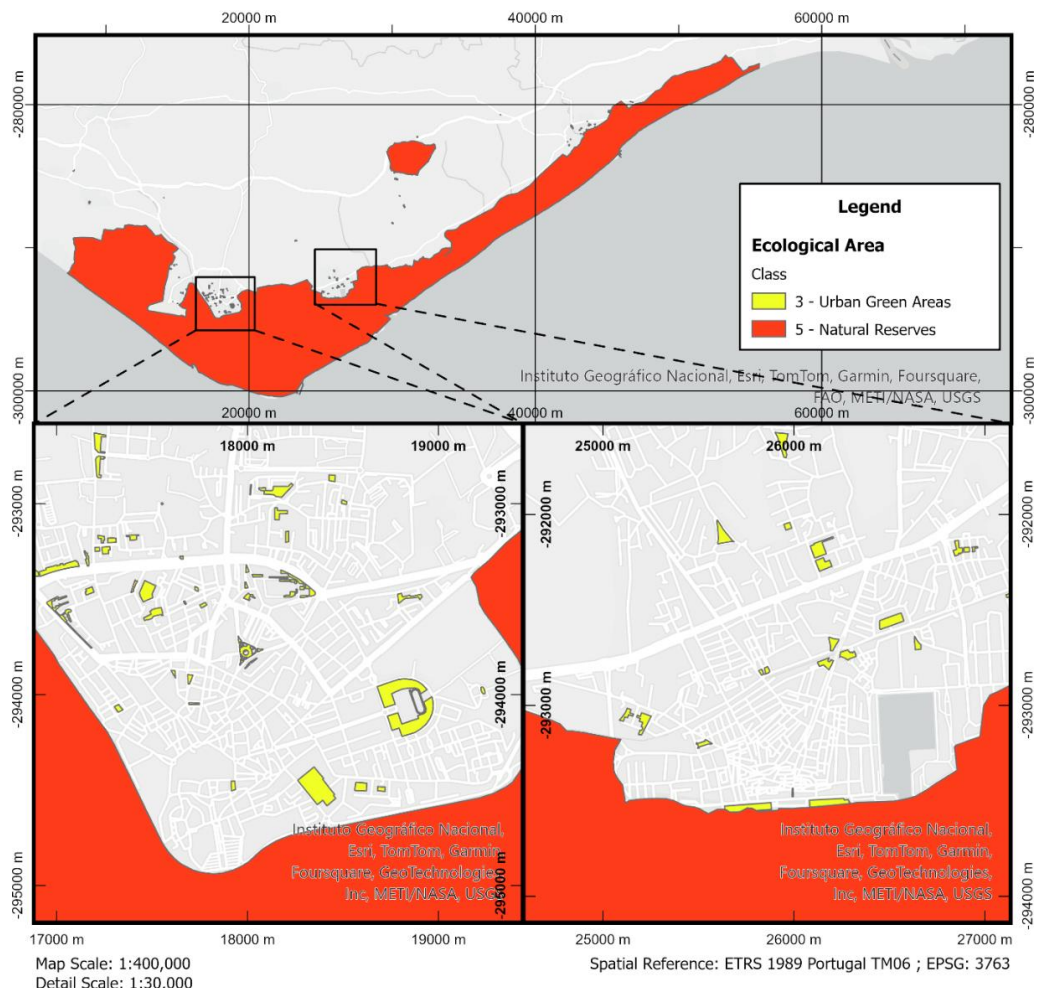


Figure A.5 – Ecological Areas (EA) Classification. Top: Overview of the Area of Study. Bottom Left: City of Faro and Surroundings. Bottom Right: City of Olhão and Surroundings.

## B. Survey Results

### i. Raw Data and Averages per Ecosystem per Service

*Table B.1- Survey Results. Each Expert was Asked to Rank from 1 to 5 the Importance of the Contribution of each Ecosystem to each Ecosystem Service. A - Arithmetic Average; W - Weighted Average; G - Geometric Average*

		E1	E2	E3	E4	E5	E6	Sum	A	W	G
Supporting Services	Dunes	5	5	5	4	5	3	27	4.50	4.48	4.42
	High Saltmarsh	4	5	4	3	5	3	24	4.00	3.92	3.91
	Low Saltmarsh	5	5	5	3	5	3	26	4.33	4.28	4.22
	Intertidal Mudflat	3	5	5	3	5	5	26	4.33	4.28	4.22
	Subtidal Area	2	5	5	5	5	5	27	4.50	4.52	4.29
Provisioning Services	Dunes	3	4	2	2	1	2	14	2.33	2.24	2.14
	High Saltmarsh	5	5	3	2	1	2	18	3.00	2.88	2.59
	Low Saltmarsh	5	5	5	2	5	5	27	4.50	4.40	4.29
	Intertidal Mudflat	5	5	5	5	4	5	29	4.83	4.84	4.82
	Subtidal Area	4	5	5	5	5	5	29	4.83	4.84	4.82
Regulating Services	Dunes	2	4	5	3	4	5	23	3.83	3.84	3.66
	High Saltmarsh	5	5	5	3	4	5	27	4.50	4.44	4.42
	Low Saltmarsh	5	5	5	3	4	5	27	4.50	4.44	4.42
	Intertidal Mudflat	5	5	4	3	4	3	24	4.00	3.92	3.91
	Subtidal Area	4	5	4	3	4	3	23	3.83	3.76	3.77
Cultural Services	Dunes	5	5	5	2	4	5	26	4.33	4.24	4.14
	High Saltmarsh	1	4	5	2	4	5	21	3.50	3.48	3.05
	Low Saltmarsh	1	4	2	2	4	5	18	3.00	2.88	2.62
	Intertidal Mudflat	2	4	5	5	5	5	26	4.33	4.40	4.14
	Subtidal Area	4	3	5	5	3	5	25	4.17	4.28	4.06

Averaged Total	3.75	4.65	4.45	3.25	4.05	4.20	
Expertise Self-Assessment	4	3	5	5	4	4	25
Expert Weight	0.16	0.12	0.20	0.20	0.16	0.16	1.00

### ii. Averages per Ecosystem

*Table B.2 - Survey Results Averaged per Ecosystem. A - Arithmetic Average; W - Weighted Average; G- Geometric Average.  
e.g. AA = Arithmetic x Arithmetic*

Ecosystem	Sum	AA	AW	AG	GA	GW	GG	WA	WG
Dunes	90	3.75	3.70	3.59	3.63	3.58	3.46	3.93	3.78
High Saltmarsh	90	3.75	3.68	3.49	3.71	3.63	3.42	3.98	3.81
Low Saltmarsh	98	4.08	4.00	3.89	4.03	3.94	3.80	4.28	4.14
Intertidal Mudflat	105	4.38	4.36	4.27	4.37	4.35	4.26	4.29	4.19
Subtidal Area	104	4.33	4.35	4.24	4.32	4.33	4.22	4.28	4.17

## C. MCRI – Results with Different MVI Methodologies

### i. MCRI using the EVI or SVI Methodology for MVI

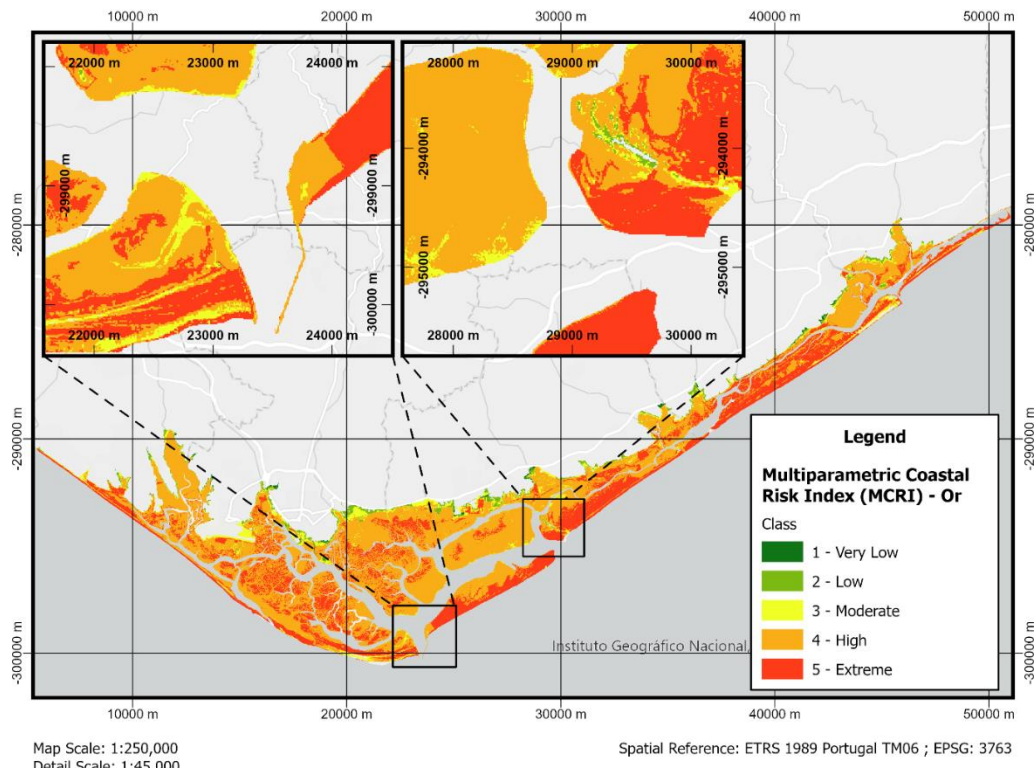


Figure C.1 - Multi-Parametric Coastal Risk Index (MCRI) with “Or” methodology. Top Left: Ecological Area Surrounding the Faro-Olhão Inlet and the Ilha do Farol Urban Area. Top Right: Ecological Area Surrounding the Armona Inlet and the Armona Island Urban Area. Bottom: Overview of the Area of Study.

ii. MCRI using the Weighted Methodology for MVI

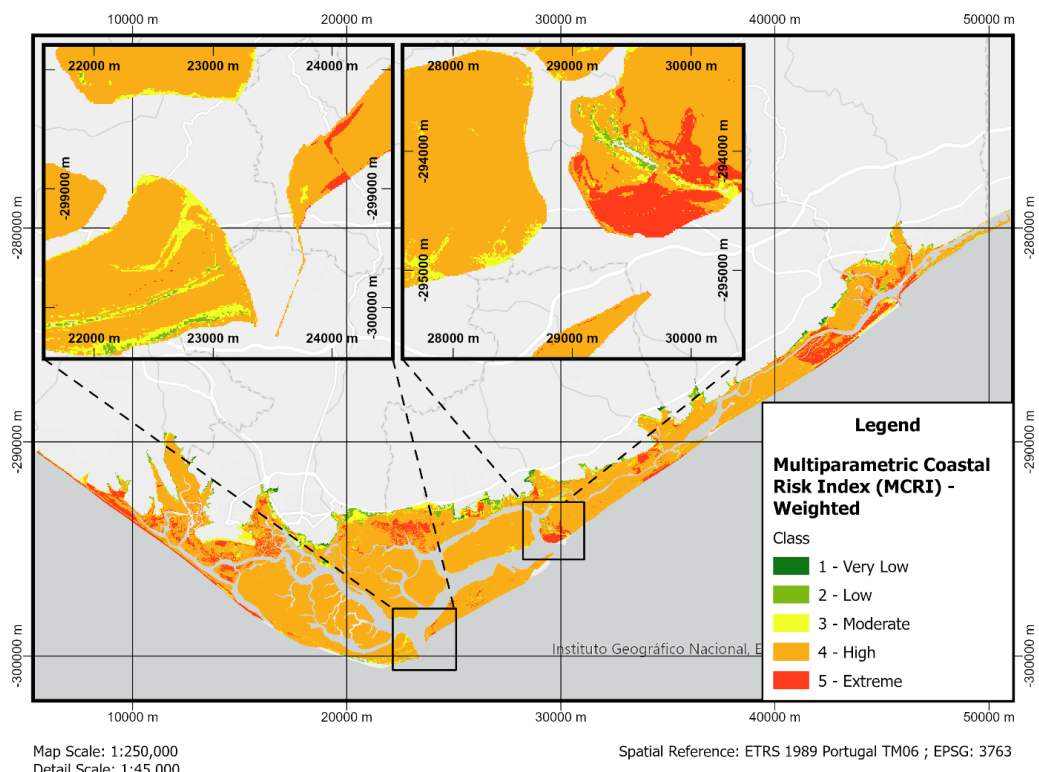


Figure C.2 - Multi-Parametric Coastal Risk Index (MCRI) with “Weighted” methodology (80% EVI, 20% SVI). Top Left: Ecological Area Surrounding the Faro-Olhão Inlet and the Ilha do Farol Urban Area. Top Right: Ecological Area Surrounding the Armona Inlet and the Armona Island Urban Area. Bottom: Overview of the Area of Study.